

# DISSERTATION

Titel der Dissertation

**An evolutionary study on the role of the *PEX11* gene family as a key player in peroxisome proliferation in *A. thaliana*.**

Verfasserin

Mag.rer.nat. Kornelija Pranjić

angestrebter akademischer Grad

Doktorin der Naturwissenschaften (Dr.rer.nat.)

Wien, 2011

Studienkennzahl: A 091 438

Dissertationsgebiet: Botanik

Betreuer: Univ. Doz. Dr. Friedrich Kragler



# Contents

<b>Abstract</b>	9
<b>Zusammenfassung</b>	11
<b>A. Introduction</b>	13
A.1. Peroxisomes	13
A.1.1. Plant peroxisomes	13
A.1.1.1. Metabolic function of peroxisomes in plant cells	14
A.1.1.1.1. Detoxification of reactive oxygen species (ROS)	14
A.1.1.1.2. Lipid Metabolism	15
A.1.1.1.3. Peroxisomal fatty acid $\beta$ -oxidation	16
A.1.1.1.4. Glyoxylate Cycle	16
A.1.1.1.5. Photorespiration and the Glycolate pathway	17
A.1.1.1.6. Photomorphogenesis	19
A.1.1.1.7. Biosynthesis of Hormones	20
(A) Jasmonates	20
(B) Auxin	23
(C) Salicylic acid	24
A.1.1.1.8. Pathogen response	25
A.1.2. Peroxisome Biogenesis	26
A.1.2.1. Peroxisins	26
A.1.2.2. Peroxisome Assembly and Formation	28
(A) <i>The formation of peroxisomal membrane.</i>	28
(B) <i>The import of peroxisome matrix proteins</i>	28
(C) <i>Proliferation</i>	31
A.1.3. Induction and regulation of Peroxisomes Proliferation	33
A.1.4. The PEX11 gene family	35
A.1.4.1. Yeast PEX11	35

A.1.4.2. Human PEX11.....	35
A.1.4.3. Plant PEX11-gene family .....	36
<b>B.Results.....</b>	<b>39</b>
B.1. Expression profiles of the five AtPEX11 members in <i>A. thaliana</i> plants.....	39
B.2. Intracellular distribution of yeast, human and plant PEX11 fusion proteins in epidermal cells of <i>N. benthamiana</i> .....	41
B.3. Plant, yeast and human PEX11 fusion proteins change the appearance of peroxisomes in plant cells. ....	43
B.3.1. Heterologous PEX11 fusion proteins alter the size and number of peroxisomes in plant cells .....	44
B3.2. Over-expressing yeast, human and plant PEX11 fusion proteins lead to cluster formation of peroxisomes.....	45
B.4. Over-expression of the plant AtPEX11D fusion protein leads to the formation of aberrant membrane structures. ....	46
B.4.1. Analysis of the dynamics of aberrant membrane and ER-like structures after over-expressing AtPEX11D. ....	51
B.5. Analysis of transgenic <i>A. thaliana</i> lines expressing PEX11 fusion proteins .....	54
B.5.1. Over-expression of AtPEX11A lead to significant smaller plants with upward curved leafs.....	54
B.5.2. Over expression of ScPEX27 and HsPEX11y lead to a delayed plant growth protein..	56
B.5.3. Distribution and effect of PEX11 fusion proteins on peroxisomes in <i>A. thaliana</i> plants. ....	57
B.5.4. The effect of hormones and sucrose on the growth of <i>PEX11</i> transgenic seedlings ..	60
B.6. Promoter activity of <i>AtPEX11D</i> .....	64
B.6.1. <i>In silico</i> prediction of AtPEX11D promoter elements .....	64
B.6.2. A minimal promoter region of 258bp is essential for the appropriate expression of <i>AtPEX11D</i> .....	65
B.6.3. The <i>AtPEX11D</i> promoter drives expression in a light cycle depended manner .....	67
B.6.4. The minimal promoter is more active than the full-length promoter.....	69
C6.5. Heat shock did not alter expression from the <i>AtPEX11D</i> promoter .....	72

B.6.6. Auxin, methyljasmonate, abscisic acid and tween induces the <i>AtPEX11D</i> promoter...	73
B.7. Search for a potential transcription factor regulating <i>AtPEX11D</i> .....	77
B.7.1. A yeast one-hybrid screen identified the transcription factor SOL1 as a potential regulator of <i>AtPEX11D</i> expression .....	77
B.8. SOL1 expression increases the number of peroxisomes and the formation of small peroxisome clusters .....	81
B.9. SOL1 influences <i>AtPEX11D</i> promoter driven GUS expression .....	82
<b>C. Discussion</b> .....	83
C.1. PEX11 from the three kingdoms .....	83
C.2. Sorting of the PEX11-fusion proteins to the peroxisomal membrane is conserved throughout the three kingdoms.....	84
C.3. Overexpression of PEX11 proteins leads to peroxisome proliferation and cluster formation .....	85
C.3.1. Overexpression of <i>AtPEX11D</i> led to a disintegration of ER membrane structures .....	90
C.4. Overexpression of PEX11 might cause a dominant negative effect on peroxisomes.....	91
C.5. Overexpression of <i>AtPEX11A</i> causes growth defects .....	94
C.6. Some hormones affect PEX11 overexpression plants .....	96
C.7. A minimal promoter region sufficient for the expression of the <i>AtPEX11D</i> gene as well as the search for potential regulatory factors.....	97
C.8. Tissue specific regulatory elements are present upstream of the minimal promoter .....	99
C.9. The expression of <i>AtPEX11D</i> seems to be light but not heat induced.....	100
C.10. The transcription factor SOL1 affects <i>AtPEX11D</i> expression in plant cells.....	101
<b>D. Materials and Methods</b> .....	109
D.1. Bacteria .....	109
D.1.1. Bacterial strains .....	109
D.1.2. Bacterial stock.....	109
D.1.3. Bacterial media .....	109
D.1.4. Preparation of electro competent <i>E. coli</i> TOP10, DH5 $\alpha$ or DB3.1 cells .....	110
D.1.5. Transformation of electrocompetent <i>E. coli</i> and <i>A. tumefaciens</i> cells .....	110

D.1.6. Transformation of chemically competent <i>E. coli</i> .....	110
D.2. Yeast.....	111
D.2.1. Yeast strains .....	111
D.2.2 Yeast media.....	113
D.2.3. One step yeast transformation.....	113
D.2.3. High efficiency yeast transformation.....	114
D.2.4. Plasmid isolation from yeast.....	114
D.2.5. Filter Lift Assay .....	115
D.2.6. Liquid $\beta$ -galactosidase assay .....	115
D.3. Plant.....	116
D.3.1. Growth medium.....	116
D.3.2. Growth condition .....	117
D.3.3. Sterilization of <i>Arabidopsis thaliana</i> and <i>Nicotiana benthamiana</i> seeds.....	117
D.3.4. Transient expression in <i>N. benthamiana</i> leaves.....	117
D.3.5. Floral Dip of <i>A. thaliana</i> plants .....	118
B.3.5.1. Culture preparation .....	118
D.3.5.2. Plant preparation.....	118
D.3.6. Isolation of genomic DNA from plants.....	118
D.3.6. Protoplast isolation of <i>A. thaliana</i> .....	119
D.3.7. Protoplast transformation of <i>A. thaliana</i> .....	120
D.2.8. Fluorometric GUS measurements of <i>A. thaliana</i> protoplasts .....	120
D.3.8. GUS staining.....	121
D.3.9. Paraffin Embedding .....	122
D.3.10. Cyro-cuttings of agarose embedded samples .....	123
D.4. DNA.....	124
D.4.1. Buffers and solutions .....	124
D.4.2. Polymerase chain reaction (PCR).....	125
D.4.3. Agarose gel electrophoresis .....	125
D.4.4. Restriction digest .....	126

D.4.5. Ligation .....	127
D.4.6. Clean plasmid isolation from bacteria with a kit .....	127
D.4.7. Quick and Dirty plasmid isolation from bacteria .....	127
D.4.8. DNA purification from an agarose gel .....	128
D.4.9. Gateway® cloning .....	128
D.4.10. TOPO-TA cloning.....	130
D.4.11. Cloning of PEX11 fusion proteins from yeast, human and plant.....	130
D.4.11. Mutagenesis of the full length AtPEX11D promoter .....	132
D.5. RNA .....	133
D.5.1. RNA isolation with TRIzol from plant material .....	133
D.5.2. Reverse transcriptase (RT) reaction.....	134
D.6. Microscopy and photography.....	134
D.6.1. Stereo microscopy .....	134
D.6.2. Light microscopy .....	134
D.6.3. Confocal microscopy of plant peroxisomes.....	135
Sample preparation.....	135
Settings.....	135
D.6.4. Statistical analyses .....	135
D.6.5. Digital photography .....	136
Supplementary .....	141
Abbreviations .....	143
Bibliography .....	146
Curriculum Vitae .....	157
Acknowledgments .....	158





## Abstract

Peroxisomes are highly dynamic organelles present in nearly all eukaryotic cells. In higher plants, peroxisomes (PX) are involved in a variety of essential physiological and biochemical processes such as photorespiration, lipid catabolism and biosynthesis of plant hormones such as auxin and jasmonic acid. Over 30 proteins, the so-called peroxins (PEX proteins), are known to be involved in PX biogenesis. Among these the PEROXIN 11 (PEX11) protein family members were identified as PX proliferation factors. In a collaborative effort we studied the effects on PX appearance mediated by the three PEX11 family members of *Saccharomyces cerevisiae* (ScPEX11, ScPEX25 and ScPEX27), the three human (PEX11 $\alpha$ ,  $\beta$  and  $\gamma$ ), and the five *Arabidopsis* PEX11 protein family members (AtPEX11-A to E). My study focused on the effect and function of the PEX11 proteins in plants and aimed to tackle two aspects.

i) The capacity of PEX11-protein family members of the three kingdoms (yeast, animal and plant) to induce peroxisomal proliferation in *N. benthamiana* and *A. thaliana* plants. PEX11 proteins from the three different organisms were over-expressed transiently by agro-infiltration and by production of stable *A. thaliana* transgenic lines. By evaluating the PX appearance (size and number) the degree of functional conservation of the PX proliferation factors was evaluated as well as their effects on plant growth. Our experiment showed that all PEX11 proteins, despite their origin (yeast, human or plant), are efficiently targeted to the peroxisomal membrane. The overexpression of the various PEX11 proteins affected the peroxisome appearance and induced the formation of peroxisomal cluster to different degrees. This suggests that although the localisation to peroxisomes is conserved throughout the three kingdoms the individual PEX11 proteins may differ in some of their functions.

ii) The transcription factors regulating *PEX11* expression in plants are not known, thus we studied in detail the expression of *AtPEX11D* facilitating the identification of a putative transcription factor regulating *AtPEX11D* expression. *AtPEX11D* was chosen as it showed the strongest effect on PX shape and number. First I studied the expression pattern of *A. thaliana* *PEX11D* under various conditions. Next I performed a promoter deletion studies. Five different deletion constructs of the *AtPEX11D* promoter region were created and cloned into a GUS reporter system to study their expression activity in plants. By this means, a short promoter region sufficient to mediate expression was identified. This region was cloned into the yeast One-Hybrid system and a screen for transcription factor(s) binding specifically to this *AtPEX11D* promoter sequence was performed. This approach allowed me to identify a number of potential

transcription factors. One selected transcription factor could be confirmed to induce *AtPEX11D* promoter activity and PX formation in plant cells.

## Zusammenfassung

Peroxisomen sind Organellen, die in fast allen eukaryotischen Zellen vorkommen und von einer einfachen Membran umhüllt sind und spezielle metabolische Funktionen ausführen. In höheren Pflanzen sind Peroxisome (PX) in eine Vielzahl von physiologischen und biochemischen Stoffwechselfunktionen involviert, wie z.B. in der Photorespiration und der Biosynthese von Lipiden und Hormonen, wie Auxin oder Jasmonaten. Es sind 30 sogenannten Peroxine (PEX Proteine) bekannt, die eine wesentliche Rolle in der Biogenese von PX spielen. Innerhalb dieser Proteingruppe spielt vor allem die PEROXIN11 (PEX11) Protein Familie eine wesentliche Rolle in der Proliferation von PX.

In einer gemeinschaftlichen Studie mit zwei anderen Arbeitsgruppen wurde die Auswirkung von PEX11 Proteine aus drei unterschiedlichen Organismen, Hefe (*S. cerevisiae*: ScPEX11, ScPEX25 und ScPEX27), Mensch (in Humanen Nierenzellen: PEX11 $\alpha$ ,  $\beta$  und  $\gamma$ ) und Pflanzen (*A. thaliana*: AtPEX11A bis-E), auf die Erscheinungsform und Anzahl der Peroxisome untersucht.

Meine Arbeit bezieht sich hauptsächlich auf die Untersuchung aller PEX11 Proteinen aus den unterschiedlichen Organismen (Hefe, Mensch und Pflanze) und deren Auswirkung auf die Erscheinungsform und Anzahl von Peroxisomen in pflanzlichen Organismen wie *Arabidopsis thaliana* und *N. benthamiana*. Diese Untersuchungen wurden einerseits transient in Blätter von *N. benthamiana*, andererseits in stabilen transgenen *A. thaliana* Linien vorgenommen. Alle PEX11 Proteine aus den drei verschiedenen Organismen konnten an die peroxisomale Membran binden und die meisten PEX11 Proteine hatten einen starken Effekt auf die Anzahl und Erscheinungsform von Peroxisomen. Diese Ergebnisse zeigen, dass die PEX11 Proteinfamilie einen hohen Konservierungsgrad bezüglich der Lokalisierung der PEX11 Proteine zwischen den unterschiedlichen Organismen aufweist.

Ein weiterer Aspekt meiner Arbeit war die Analyse des *AtPEX11D* Promoters und die Suche nach möglichen Transkriptionsfaktoren. Es ist nur sehr wenig darüber bekannt, wie die PX Proliferation sowie die Expression von *PEX11* Genen in Pflanzen reguliert wird. Um die Expression und einen möglichen Transkriptionsfaktor zu identifizieren haben wir die Promoteraktivität von *AtPEX11D* analysiert. *AtPEX11D* wurde näher untersucht da dieses Protein bei Überexpression die stärksten Effekte auf PX zeigte. Die Promoteraktivität dieses Genes wurde mit Hilfe eines GUS Reporter Systems unter verschiedenen Bedingungen untersucht. Mit Hilfe von Deletionskonstrukten wurde ein essentieller Bereich in der Promotersequenz von *AtPEX11D* ermittelt, welcher die Expression reguliert. Mittels eines Hefe

One-Hybrid Screens wurden mögliche Transkriptionsfaktoren isoliert und für einen konnte ein Einfluss auf die *AtPEX11D* Promoter Expression und induktion von PX gezeigt werden.

## A. Introduction

### A.1. Peroxisomes

Peroxisomes are single-membrane-bounded organelles present in nearly all eukaryotic cells like yeast, plant and mammalian cells. They are highly dynamic and unlike mitochondria or chloroplasts they do not contain own DNA or ribosomes. Therefore, all proteins necessary for the assembly and biogenesis of peroxisomes, such as matrix or membrane-associated proteins are encoded in the nucleus, and thought to be synthesized on free cytosolic ribosomes (Lazarow and Fujiki 1985) and imported into the peroxisomes (Johnson and Olsen 2001; Mano and Nishimura 2005).

Peroxisomes have been first described by Rhodin in 1958 as distinctive organelles surrounded by a single membrane, containing a core granular like structure and biochemically characterised by deDuve in 1966. Originally the central function of peroxisomes was believed to be the metabolism of fatty acids and detoxification of hydrogen peroxide. In the meantime, it was shown that peroxisomes are also involved in other important metabolic processes and have species-specific functions (Mano and Nishimura 2005; Hayashi and Nishimura 2006; Brown and Baker 2008). In mammals key enzymes are found in peroxisomes, involved in cholesterol, bile acids, and plasmalogen synthesis (Brown and Baker 2008). In single cell organisms such as *H. polymorpha* peroxisomes are involved in the process of methanol oxidation as well as in the metabolism of alkylated amine or alkane (Veenhuis et al. 1987; Brown and Baker 2008). In plant cells peroxisomes take part in the biosynthesis of essential hormones (reviewed in Kaur et al. 2009) and in photorespiration (Hu et al. 2002). However, it seems that the detoxification of hydrogen peroxide is a common feature in almost all eukaryotic peroxisomes (Corpas et al. 2001; Hayashi and Nishimura 2006).

#### A.1.1. Plant peroxisomes

In higher plants, peroxisomes are divided into five groups based on their different functions (Hayashi and Nishimura 2006).

(1) Leaf peroxisomes are involved in the processes of photorespiration and photomorphogenesis, a light-mediated developmental process. (2) The so-called glyoxysomes

located in germinating seeds are involved in the lipid metabolism and the glyoxylate cycle. (3) The gerontosomes are located in senescent tissues, using glyoxysomal enzymes to catabolise lipids whereas (4) root nodule peroxisomes are involved in nitrogen fixation by biosynthesis of ureide, which is then transported from the nodules to the above ground parts of the plant in leguminosae. (5) The last group represent unspecialized peroxisomes, which are relatively undifferentiated peroxisomes located throughout the whole plant. A common feature of all peroxisomes is the detoxification of reactive oxygen species. (Hu et al. 2002; Lipka et al. 2005; Hayashi and Nishimura 2006; Mullen and Trelase 2006).

### *A.1.1.1. Metabolic function of peroxisomes in plant cells*

#### A.1.1.1.1. Detoxification of reactive oxygen species (ROS)

In peroxisomes reactive oxygen species (ROS) like hydrogen peroxide ( $\text{H}_2\text{O}_2$ ) or superoxide radicals ( $\text{O}_2^{\cdot-}$ ) occur as by-products of various metabolic reactions such as the photorespiration pathway,  $\beta$ -oxidation of lipids, or during polyamine oxidation (Corpas et al. 2001; Kaur et al. 2009). Therefore peroxisomes contain several enzymes, such as catalase (CAT), necessary for the removal and degradation of these toxic by-products. Catalase can use the produced  $\text{H}_2\text{O}_2$  in order to oxidize other substrates and thereby detoxify it or  $\text{H}_2\text{O}_2$  can be directly detoxified by converting it into water ( $\text{H}_2\text{O}$ ) (Corpas et al. 2001).

However in plants, it has been shown that not only catalase but also ascorbate peroxidase (APX) (Bukelman and Trelase 1996) or superoxide dismutase (del Rio et al. 1998) play an important role in the degradation of reactive oxygen species (Mano and Nishimura 2005). APX has a higher affinity of binding  $\text{H}_2\text{O}_2$  compared to catalase and is therefore involved in the degradation of low concentrations of hydrogen peroxide by reducing it to water via the ascorbate-glutathione cycle (Kaur et al. 2009). The superoxide dismutase is crucial for the detoxification of  $\text{O}_2^{\cdot-}$  into  $\text{O}_2$  and  $\text{H}_2\text{O}_2$  (del Rio et al. 1998) which is then converted to  $\text{H}_2\text{O}$  and  $\text{O}_2$  by catalase (Figure 1, modified after Kaur et al. 2009).

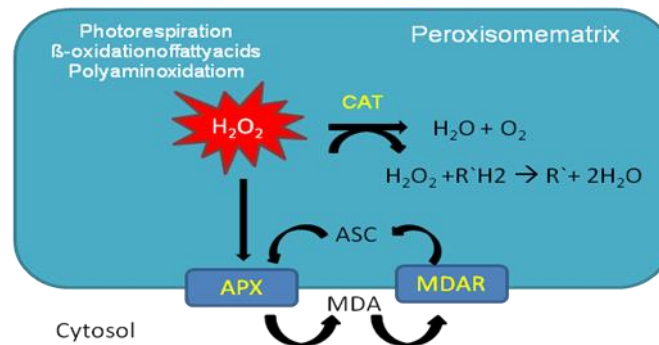


**Figure 1: Detoxification of ROS in peroxisomes via catalase (CAT) or ascorbat peroxidise (APX) via the ascorbate-gluthation cycle (modified Figure after Kaur et al. 2009).**

**CAT:** catalase; **APX:** ascorbat peroxidise; **MDA:** monohydroascorbat; **MDAR:** monodehydroascorbat reductase; **ASC:** ascorbat.

#### A.1.1.1.2. Lipid Metabolism

Oilseed plants such as the brassicaceae *Arabidopsis* are not able to gain energy from starch or sugars during germination (Mano and Nishimura 2005). Therefore lipids, mainly triacylglycerols (e.g. palmetic acid) are stored in so-called oil bodies located in cells of the endosperm and cotyledons and used as energy and carbon source for germination (Hayashi and Nishimura 2006). The conversion of fatty acids into succinate occurs in peroxisomes via  $\beta$ -oxidation and the glyoxylate cycle (Cooper and Beevers 1969). During germination this succinate is used to provide the carbon to build sucrose until photosynthesis (calvin-benson cycle) can take place (Hayashi and Nishimura 2006).

In higher plants these specific peroxisomes are called glyoxysomes and are the site of fatty acid  $\beta$ -oxidation and the glyoxylate cycle (Hayashi and Nishimura 2006). In contrast, in human cells the breakdown of fatty acids is split between two different cell organelles, the peroxisomes and mitochondria. In mammalian cells peroxisomes are not able to degrade short-chain fatty acids, the breakdown of these fatty acids occur in mitochondria (Hashimoto 1996; Wanders and Waterham 2006, Mano and Nishimura 2005).

### A.1.1.1.3. Peroxisomal fatty acid $\beta$ -oxidation

In plant peroxisomes the degradation of all fatty acids into acetyl-CoA takes place (Figure 2). During  $\beta$ -oxidation, two carbon units are released via an oxidation reaction and are available to bind to Coenzyme A (CoA) forming acyl-CoA by an acyl-CoA synthetase (ACX). Then the acyl-CoA is converted by cycling through the multifunctional protein (MFP), followed by 3-ketoacyl-CoA thiolase (KAT) activity into acetyl-CoA, representing the end product of the fatty acid  $\beta$ -oxidation pathway (Mano and Nishimura 2005).

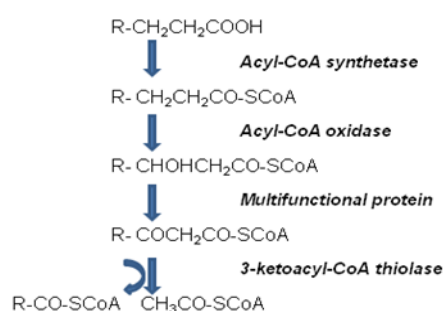


**Figure 2: Peroxisomal fatty acid  $\beta$ -oxidation.** Figure based on Hashimoto (1996) and Mano and Nishimura (2005). Conversion of fatty acid 2,4D (2,4-Dichlorophenoxy acetic acid) a synthetic auxin into acetyl-CoA.

### A.1.1.1.4. Glyoxylate Cycle

In plants, the end product of  $\beta$ -oxidation, Acetyl-CoA, serves as a substrate for the glyoxylate cycle which produces succinate during peroxisomal  $\beta$ -oxidation (Hashimoto 1996, Mano and Nishimura 2005). In mammalian cells the generated acetyl-CoA from the  $\beta$ -oxidation pathway enters the citric acid cycle (TCA cycle) where it is fully oxidized to carbon dioxide allowing cells to obtain energy from lipids. However in higher plants, the stored lipids are not only used for the generation of energy for growth but also for the biosynthesis of complex structures, needing a high amount of carbohydrates like cellulose or chitin (Mano and Nishimura 2005). Therefore the glyoxylate cycle is an additional metabolic pathway in higher plants by-passing the decarboxylation steps of the citric acid cycle to allow the synthesis of monosaccharides (Mano and Nishimura 2005). The main activity sites of these processes are the glyoxysomes in germinating seeds (Korneberg and Krebs 1957) and key enzymes involved in the glyoxylate cycle in glyoxysomes are: aconitase (ACO), malate dehydrogenase (MDH), citrate synthase (CSY), isocitrate lyase (ICL) and malate synthase (MLS) (Figure 3: modified from Hayashi and Nishimura 2006). During the glyoxylate cycle the acetyl-CoA gained from the fatty acid  $\beta$ -oxidation pathway



is converted into succinate required for an efficient gluconeogenesis or for respiration (Mano and Nishimura 2005).

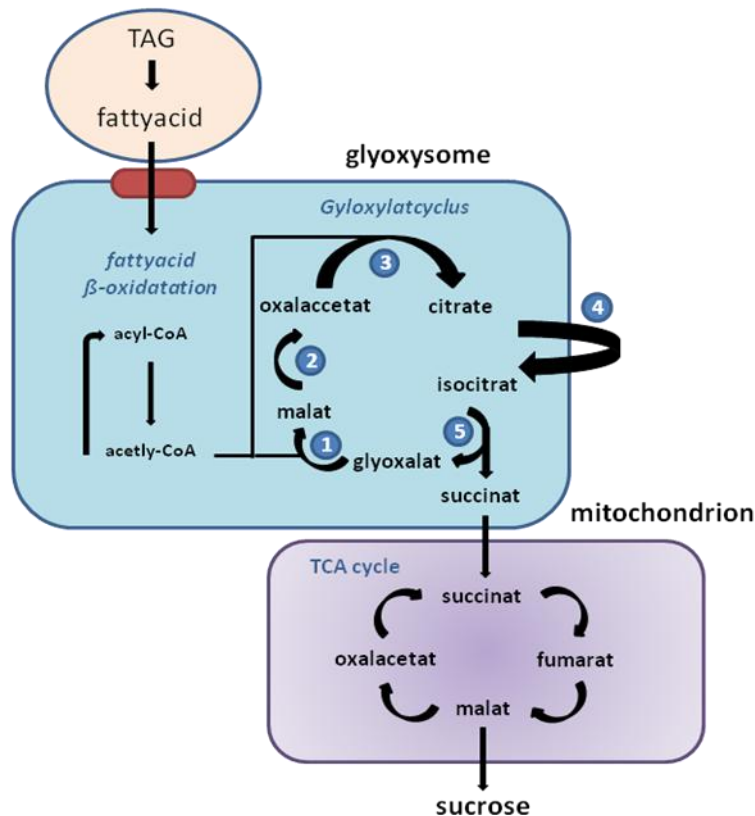


**Figure 3: The entire gluconeogenesis pathway from seeds containing stored TAG (triacylglycerol) during germination** (Figure modified after Hayashi and Nishimura 2006).

Conversion of fatty acids to succinate via the fatty acid  $\beta$ -oxidation pathway and the glyoxylate cycle in glyoxysomes. Enzymes involved in the glyoxylate cycle are: ① malat synthase, ② malat dehydrogenase, ③ citrate synthase, ④ actonitase (not located in the glyoxysome), and ⑤ isocitrat lyase.

However recent studies have shown that glyoxylate activity also occurs in senescent leafs, cotyledons and flowers (Pistelli et al. 1995) as well as in pollen (Zhang et al. 1994), indicating a developmental and metabolic control of the key enzymes involved in these processes.

### A.1.1.1.5. Photorespiration and the Glycolate pathway

The early atmosphere of the earth contained low amounts of oxygen. It is believed that peroxisomes have originally been responsible for the detoxification of cells by decreasing the  $O_2$

levels, which were toxic for most forms of life at that time (Nayidu et al. 2008). This suggests that photorespiration is an evolutionary relict.

Nowadays it is believed that the process of photorespiration operates alongside carbon assimilation in  $C_3$  plants in special peroxisomes, the so-called leaf peroxisomes, and seems to have a major effect on the cellular metabolism (Foyer et al. 2009). Photorespiration occurs during photosynthesis and is a process defined as a light depending  $O_2$  uptake and  $CO_2$  release (Tolbert 1971).

It occurs especially under high light or high temperature conditions as well as under low  $CO_2$  levels or water deficits. For example during drought stress the stomata of the cells close to prevent water loss, which leads to reduced  $CO_2$  levels. The low  $CO_2$  levels then trigger the activation of the photorespiratory pathway (Foyer et al. 2009).

The photorespiration pathway utilizes  $O_2$  and releases  $CO_2$  and is based on recycling phosphoglycolate. The process of photorespiration is divided between three different organelles: chloroplasts, leaf peroxisomes and mitochondria, forming a cycling glycolate pathway (Figure 4 based on Hayashi and Nishimura 2006 and Kaur et al. 2009).

The glycolate pathway is initiated in the chloroplast by the oxygenase activity of RubisCO, a key enzyme of  $CO_2$  fixation in photosynthesis, which can bind  $O_2$  instead of  $CO_2$ . This activity results in the formation of 2-phosphoglycolate, which are converted into glycolate by a phosphoglycolate phosphatase (PGLP1) (Hayashi and Nishimura 2006; Kaur et al. 2009). The glycolate is then passed on to leaf peroxisomes, where several enzymes such as the glycolate oxidase (GO), the hydroxypyruvate reductase and different aminotransferases convert the glycolate into the amino acid glycine (Hayashi and Nishimura 2006). The glycine is transported into mitochondria, where it is converted to serine by a glycine decarboxylase (GDC) and a serine hydroxymethyl transferase (SHMT) (Kaur et al. 2009). In the end the serine re-enters the leaf peroxisomes where it is converted into glycerate and then transported into chloroplast. The glycerate is then phosphorylated to 3-phosphoglycerate and enters the calvin-benson cycle, closing the glycolate pathway (Kaur et al. 2009).

### Glycolate cycle

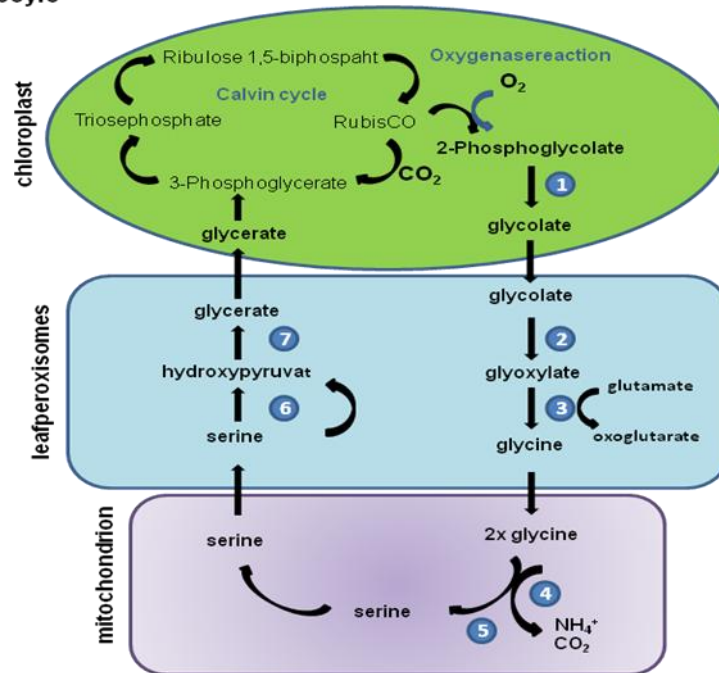


**Figure 4: Photorespiratory glycolate pathway in C3 plants** (Figure modified after Hayashi and Nishimura 2006 and Kaur et al. 2009).

① phosphoglycolate phosphatase (PGLP1) ② glycolate oxidase (GO) ③ glu:glyoxylate aminotransferase (GGT) ④ glycine decarboxylase (GDC) ⑤ serine hydroxymethyl transferase (SHMT) ⑥ ser:glyoxylate aminotransferase (SGT) ⑦ hydroxypyruvate reductase.

Even though the process of photorespiration lowers the photosynthetic activity and therefore often has a negative effect on plant growth, it is suggested to play a role in multiple signalling pathways, especially in plant hormone responses controlling growth or environmental and defence responses (Foyer et al. 2009).

#### A.1.1.1.6. Photomorphogenesis

A study by Hu et al. (2002) indicates a role of peroxisomes in light-mediated development, called photomorphogenesis. The authors could identify *TED3* as a homologous gene to the yeast and mammalian *PEX2*, which is involved in matrix protein import and peroxisome assembly. *TED3*-GFP fusion proteins showed a punctuated structure co-localising with the peroxisomal enzyme catalase, showing that the *TED3*-GFP is targeted to peroxisomes (Hu et al. 2002).

Interestingly, *ted3* mutants show some similarities to *TED3* overexpression plants, indicating that the *ted3* mutations lead to an increase in peroxisomal function (Hu et al. 2002).

The main result of this study (Hu et al. 2002) was that *ted3* mutants were able to rescue a *det1* mutant phenotype. *det1* mutants grown in the dark developed like wild-type plants grown under normal light conditions, whereas when grown under normal light conditions, they exhibit various growth defects, like smaller and paler leaves. Therefore, *DET1* is assumed to be a negative regulator of photomorphogenesis in plants.

Regarding the result, that *det1* mutants can be rescued by a *ted3* mutation, the authors suggested that *ted3* and therefore also peroxisomes could play a role in the photomorphogenic pathway which is negatively regulated by *DET1* (Hu et al. 2002).

### A.1.1.1.7. Biosynthesis of Hormones

Plant hormones are a group of naturally occurring substances which influence various physiological processes in plants. They occur in very low concentrations and mainly affect the growth and development of plants at specific time points. They are essential for the appropriate growth of plants and also influence cell death (Davies 2004).

So far, peroxisomes have been shown to play a role in the biosynthesis of three plant hormones: jasmonates (JA), auxins (e.g. IAA) and salicylic acid (SA) which are essential key players in a various number of metabolic and developmental processes (Woodward and Bartel 2005; Wasternack et al. 2007; Zolman et al. 2008; Reumann 2004; Kaur et al. 2009).

#### (A) Jasmonates

Jasmonates represent a group of plant hormones including jasmonic acid (JA) and methyl jasmonate (MeJA). They belong to the family of oxylipins produced by the oxidative metabolism of polyunsaturated fatty acids (Wasternack et al. 2007). Oxylipins are signalling molecules and capable of regulating genes involved in cell growth and biotic and abiotic stress responses (Kazan and Manner 2008).

The biosynthesis of JA is partitioned between two different organelles; the chloroplast and the peroxisome (Figure 5). It is initiated in the chloroplast, where  $\alpha$ -linolenic acid ( $\alpha$ -LeA), the substrate for numerous oxylipins, is subsequently converted into 12-oxo-phytodienoic acid

(OPDA). Afterwards the OPDA is transported via an ABC transporter (PAX1) through the peroxisomal membrane into their matrix. Upon import the OPDA is reduced to 3-oxo-2-cyclopentane-1-octanic acid (OPC:8), followed by 3 rounds of  $\beta$ -oxidation and conversion into jasmonic acid (Kaur et al. 2009).

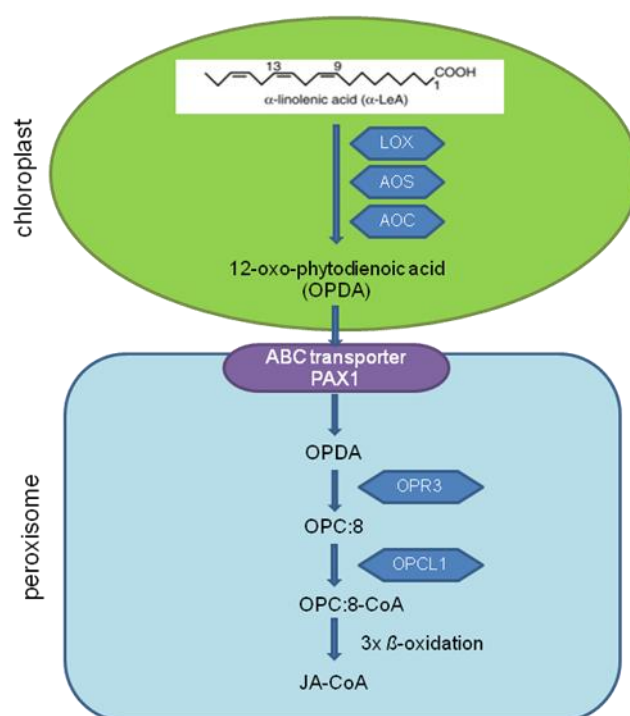


**Figure 5: Biosynthesis of jasmonic acid** (based on Wasternack et al. 2007 and Kaur et al. 2009).

**Chloroplast:** A conversion of alpha linolenic acid ( $\alpha$ -LeA) into 12-oxo-phytodienoic acid (OPDA) by lipxygenase (LOX), allene oxide synthase (AOS) and allene oxide cyclase (AOC) takes place.

**Peroxisome:** A conversion of OPDA to 3-oxo-2-cyclopentane-1-octanic acid (OPC:8) by oxophytodienoic acid reductase 3 (ORP3) occurs, followed by an activation to their responding CoA ester (OPC:8-CoA) with an OPC:8 CoA ligase1 (OPCL1). In the end JA-CoA is released after undergoing 3 rounds of  $\beta$ -oxidation.

Jasmonic acid can then be further modified in the cytosol into various jasmonic acid derivatives such as MeJA by a JA methyl transferase (Kazan and Manner 2008).

The produced JA as well as its derivatives can act as signalling molecules regulating a large number of JA-responsive genes (Kazan and Manner 2008) involved in various processes of plant development, as well as in plant defence (Wasternack et al. 2007).

Staswick et al. (1992) presented evidence that MeJA is involved in root elongation of *Arabidopsis* plants. Treatment with MeJA led to reduced root length in wild-type plants, allowing the

identification of JA signalling mutants. One of the first JA signalling mutants identified was the *coronatine insensitive1 (coi1)* mutant showing a reduced sensitivity to MeJA compared to wild type plants (Kazan and Manner 2008). This suggests that COI1 is somehow necessary for inhibiting root growth (Wasterneack et al. 2007). It is believed that COI1 is required as a repressor of the JA signalling pathway (Xie et al. 1998).

In addition it was also shown that JAs are involved in flower development in *Arabidopsis* plants by the analysis of *opr3* mutant plants, which have unviable pollen and are male sterile. This phenotype is due to a mutation in 12-oxophytodienoate reductase 3 (OPR3) and can be partially rescued by the addition of exogenous MeJA, but not by 12-oxo-phytodienoic acid OPDA (Stintzi and Browse 2000; Mano and Nishimura 2005). As shown in Figure 5, OPR3 protein is located in the peroxisomes and necessary for the conversion of OPDA into OPC:8. Therefore peroxisomes are believed to play an essential role in the biosynthesis of JA and in flower development (Wasterneack et al. 2007).

JAs also plays a major role in the defence mechanisms against various plant pathogens such as fungi (Vijayan et al. 1998) or insects (McConn et al. 1997). For example *Arabidopsis fad3-2, fad7-2* and *fad8* mutant plants are extremely vulnerable to the fungal root pathogen *Pythium mastophorum*, leading to root rot. It was shown that these mutants are not able to accumulate JA, due to low levels of linolic acid (Vijayan et al. 1998) used as a precursor for the biosynthesis of JA in peroxisomes (Figure 5). This phenotype can be rescued by treatment with exogenous MeJA, leading to plants that are unaffected by the fungus. The protective effect observed is thought to be mediated by a plant defence mechanism rather than the by a direct effect of the MeJA on the pathogen, due to no effect of exogenous MeJA on the growth of the fungus. It is therefore believed that MeJA represents a signalling molecule, which can initiate and coordinate plant defence mechanism after plant infection (Vijayan et al. 1998). Xu et al. (1994) have demonstrated that MeJA, together with ethylene, regulates the expression of osmotin, a pathogenesis-related (PR) protein involved in plant defence responses.

The JAs signalling pathways are involved in a various number of plant physiological processes and therefore need tight regulation. The biosynthesis of JA is regulated by a positive feedback loop, in which genes encoding for the biosynthesis of JA are activated by JA and MeJA. In general JAs play an important role in plant development as well as in the defence against various pathogens, by either regulating directly the biosynthesis of JAs or using JAs as signalling molecules regulating genes involved in the defence mechanisms (Kazan and Manner 2008).

### (B) Auxin

Auxins are essential plant hormones playing a key role in a various number of plant growth related process, such as vascular tissue development, root initiation, tropistic response, leaf senescence or flower and fruit development (Davies 1994; Estelle and Somerville 1987).

So far, four naturally occurring auxins in plants are known (Figure 6): the indole-3-acetic acid (IAA), the indole-3-butyric acid (IBA), the 4-chloroindole-3-acetic acid (4-Cl-IAA) and the 2-phenylacetic acid (PAA) (Simon and Petrašek 2011).

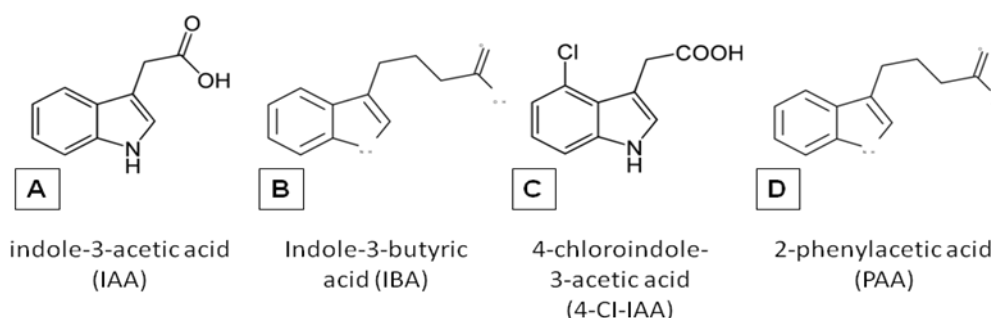


**Figure 6: The four endogenous auxins occurring in plants** (Figure modified after Simon and Petrašek 2011).

**A)** indole-3-acetic acid (IAA) **B)** indole-3-butyric acid (IBA) **C)** 4-chloroindole-3-acetic acid (4-Cl-IAA) and **D)** 2-phenylacetic acid (PAA) .

Plants have evolved several pathways for the synthesis of auxins like tryptophan (Trp) dependent or Trp-independent pathways, using tryptophan or indole as precursor, respectively (Woodward and Bartel 2005). However, none of these pathways is fully understood.

In addition a role of peroxisomes was suggested in the biosynthesis of the natural occurring auxin IAA. IAA is the most abundant native auxin involved in a various number of developmental processes in plant cells (Davies 1994).

IBA, like IAA, is a naturally occurring auxin involved in the regulation of lateral root formation. It was suggested that IBA is converted into IAA by a process similar to the  $\beta$ -oxidation in peroxisomes (Fawcett et al. 1960).

This hypothesis found support by a genetic screen for IBA-resistant *Arabidopsis* plants, providing additional evidence that the conversion of IBA into IAA is performed by a process similar to  $\beta$ -oxidation (Zolman et al. 2000). They identified *Arabidopsis* mutants show a resistance to the inhibitory effect of IBA on root elongation, but remain sensitive to IAA. Some of the identified IBA-resistant mutants also showed a sucrose dependent growth phenotype, growing only very

slowly on media without sucrose, as well as a 2,4-DB-resistance. This implicates that these mutants were unable to utilise fatty acids to gain energy for growth by  $\beta$ -oxidation, thereby indicating that the conversion of IBA to IAA is achieved by a  $\beta$ -oxidation activity (Hayashi et al. 1998, Zolman et al. 2000).

Some of the IBA-responsive mutants found during the screen did not show a sucrose dependent or 2,4-DB resistant phenotype. This suggests that the general fatty acid  $\beta$ -oxidation is not affected in these mutants, but they might be unable to catalyze specific IBA  $\beta$ -oxidation (reviewed in Kaur et al. 2009).

Zolman et al. (2007) revealed evidence that IBR3, a putative acyl-CoA dehydrogenase, seems to act in the first step of IBA  $\beta$ -oxidation, which yields the corresponding CoA ester, whereas IBR1 and IBR10 have been implicated to be involved in the following steps of the IBA  $\beta$ -oxidation. *IBR1* encodes for a short chain dehydrogenase/reductase (SDR), whereas *IBR10* resembles an enoyl-CoA hydratase/isomerase (Zolman et al. 2007, 2008; reviewed in Kaur et al. 2009).

### (C) Salicylic acid

Salicylic acid (SA) is a phenolic phytohormone and plays an important role in plant growth and development as well as in pathogen response (Davies 2004). Hoft van Huijsduijen (1986) already showed that SA treatment of tobacco plants induced the synthesis of pathogenesis-related (PR) proteins, as well as resistance to viruses like the alfalfa mosaic virus (AIMV). Nearly one decade later Xu et al. (1994) showed that SA, like JAs, are important signalling molecules involved in the regulation of plant defence mechanisms, by inducing in combination with MeJA the gene expression of PR-1b proteins.

In addition SA or a derivative seems to act as a long-distance signal initiated at the site of infection, leading to the induction of a resistance in other parts of the plant. This process is called systemic acquired resistance (SAR) (Vijayan et al. 1998).

However, despite the importance of SA in plant defence its biosynthesis is not well understood. It is believed to be synthesized via the shikimate pathway, mainly localized in chloroplasts, by the processing of chorismate by the isochorismate synthase (ICS) to isochorismate and then further to salicylic acid and pyruvate via pyruvate lyase (PL) (Wildermuth et al. 2001).



Even though the main site of SA biosynthesis is probably located in chloroplasts, there is evidence indicating that peroxisomes are maybe also involved in the biosynthesis of SA (Reuman et al. 2004; reviewed in Kaur et al. 2009).

An *Arabidopsis* genome-wide screen was performed to identify new proteins from peroxisomes, by searching for proteins carrying a putative major or minor peroxisomal targeting signal PTS1 or PTS2. Several proteins were found and proposed to be involved in the biosynthesis of plant hormones such as SA (Reuman et al. 2004).

Another possible pathway for the biosynthesis of SA was suggested by processing of phenylalanine, derived from the shikimate pathway, to a *trans*-cinnamic acid. The further processing of the cinnamic acid to SA involves the reduction of two carbons via a  $\beta$ -oxidation, suggesting that this step is localized in peroxisomes (Wildermuth et al. 2001, reviewed in Kaur et al. 2009).

### A.1.1.1.8. Pathogen response

Several studies have revealed an important role of peroxisomes in pathogen response. The strongest evidence has been provided by *pen* mutants, identified during a screen aimed to identify non-invasive pathogens in *Arabidopsis* (Lipka et al. 2005; reviewed in Kaur et al. 2009).

The *PEN2* gene encodes a glycosyl hydrolase, which has catalytic activities and is localised in peroxisomes. It was shown that *PEN2* induces callose deposition at the site of infection as well as the activation of glucosinolates, when exposed to microbe-associated molecules (MAMPs) such as bacterial flagellin (Clay et al. 2009). *pen2* mutant plants fail to induce callose deposition after treatment with Flg22, a synthetic molecule resembling flagellin, providing evidence that *PEN2* plays an important role in the innate immune response (Clay et al. 2009; reviewed in Kaur et al. 2009).

Localisation experiments showed that *PEN2*-GFP fusion proteins localize to peroxisomes and that they accumulate at the site of infection (Lipka et al. 2005). It is suggested that the H<sub>2</sub>O<sub>2</sub> produced beside the generation of glyoxylate, triggers the pathogen resistance in plants (reviewed in Kaur et al. 2009).

### A.1.2. Peroxisome Biogenesis

The formation and assembly of peroxisomes has long been a matter of debate. Since the early 1970s different model systems have been proposed and rebutted. The prevailing model during the early 1970 was the “ER-vesiculation model”, where the organelles were believed to be derived from the rough endoplasmatic reticulum (ER) (reviewed in Mullen et al. 2001).

This model was then replaced by the “growth and division model” in 1985 by Lazarow and Fujiki, in which the peroxisomal proteins were synthesized on free polyribosomes in the cytosol rather than on the ER (Lazarow and Fujiki 1985). It was suggested that a post-translational import of peroxisomal proteins occurs, which are responsible to induce growth and fission of mature pre-existing peroxisomes. Since the 1980 this “growth and division model” has been generally accepted (reviewed in Mullen et al. 2001).

However, recent studies have led to a modification of the “growth and division model” once again, suggesting a role of the ER, proposing an “ER semi-autonomous peroxisome and replication” model in plant peroxisome biogenesis (reviewed in Mullen and Trelease 2006). This model suggests that the peroxisomal membrane proteins group I (PMP1, such as PEX16 and PEX10), as well as ascorbate peroxidase (APX), after being translated in the cytosol, are sorted to the ER. Both, APX and ER-inserted PMPs, travel through the ER membrane towards a specialised region of the ER the so-called peroxisomal ER (pER). Here nascent ER-vesicle are formed and released into the cytoplasm, and mature into an intermediate sorting compartment (ERPIC)(reviewed in Mullen et al. 2001; Kaur et al. 2009). In plant cells these ERPICS can be transported and fused to pre-existing mature peroxisomes, delivering the PMPs as well as membrane lipids to the peroxisomes (reviewed in Kaur et al. 2009).

Currently, due to the lack of available pex mutants a *de novo* formation of peroxisomes has not been observed in plant cells. However, the PEX proteins in yeast and mammalian species inducing the ERPICs to assembly to intermediate vesicles, which eventually form new peroxisomes (reviewed in Titorenko and Mullen 2006 and Mullen and Trelease 2006), are present indicating that a similar mechanism exists in plants.

#### A.1.2.1. Peroxins

Extensive research in yeast as well as in human and rat have identified a group of genes essential for the function of peroxisomes (Distel et al. 1996; Fujiki 2000; Mano and Nishimura 2005). These genes are called the *PEX* genes and their protein products are referred to as peroxins

(Brown and Baker 2008). To date 31 PEX proteins (see Table 1) have been identified in yeast and are known to be involved in the general process of peroxisome biogenesis (Kiel et al. 1996). So far 20 orthologues in mammals (Brocard and Hartig 2007; Platta and Erdman 2007) and 16 orthologues in plants have been identified (Mullen et al. 2001; Hayashi and Nishimura 2006). These proteins can be divided into three groups depending on their different function (see Table 1):

- i) PEX proteins involved in membrane protein import.
- ii) PEX proteins involved in the matrix protein import.
- iii) PEX proteins involved in the proliferation machinery.

PEX11 Genes in yeast	Orthologues in mammals	Orthologues in plants	Characteristics	Function in biogenesis	Molecular function
PEX1		PEX1	AAA-type ATPase	Matrix protein import	ATP-dependent dislocation of Pex5p
PEX2		PEX2	RING-finger	Matrix protein import	Photomorphogenesis in plants
PEX3		PEX3.1/PEX3.2		PMP-targeting; de novo formation	Membrane anchor of Pex19p, PX assembly in plants
PEX4		PEX4	Ubc	Matrix protein import	Mono-ubiquitination of Pex5p
PEX5		PEX5	WoodF-motifs; TPR region, ubiquitinated	Matrix protein import	PTS1-receptor
PEX6		PEX6	AAA-type ATPase	Matrix protein import	ATP-dependent dislocation of Pex5p
PEX7		PEX7	WD40 motif	Matrix protein import	PTS2-receptor
PEX8			Coiled-coil domain; leu-zipper	Matrix protein import	Connection of docking- and RING complex; cargo release (?)
PEX9	Eliminated wrong ORF				
PEX10		PEX10	RING-finger	Matrix protein import PX assembly in plants	ER/PMP
PEX11	PEX25/PEX27	PEX11A/PEX11B/ PEX11C/PEX11D  PEX11E	PMP, C-terminal DsF motif for plant PEX11 (c-d)	Proliferation	<i>Function in plants:</i> PEX11A: elongation/duplication; PEX11B: PX structure; PEX11C and D: elongation; PEX11E: duplication
PEX12		PEX12	RING-finger	Matrix protein import	
PEX13		PEX13	SH3-domain	Matrix protein import	Member of the docking complex
PEX14		PEX14	PXXP-motif; phosphorylated	Matrix protein import	Member of the docking complex
PEX15	PEX26		Phosphorylated	Matrix protein import	Membrane anchor of Pex6p
PEX16		PEX16	PMP-targeting	Proliferation; de novo formation	PX assembly/structure (?) in plants
PEX17		PEX17		Matrix protein import	Member of the docking complex
PEX18	PEX20		WoodF-motifs; ubiquitinated	Matrix protein import	PTS2-co-receptor in Sc
PEX19		PEX19.1/PEX19.2	CAAX-box; farnesylated	PMP-targeting; de novo formation PMP	Class I receptor and chaperone; soluble escort of PMPs to ER/PX
PEX20	PEX18/PEX21		WoodF-motifs; ubiquitinated	Matrix protein import	PTS2-co-receptor in most fungi
PEX21	PEX20		WoodF-motifs; ubiquitinated	Matrix protein import	PTS2-co-receptor in Sc
PEX22		PEX22		Matrix protein import	Membrane anchor of Pex4p
PEX23	PEX30/PEX31/PEX32		DysF	Proliferation Growth	Regulation in Yf
PEX24	PEX28/PEX29			Proliferation	Separation of peroxisomes in Yf
PEX25	PEX11			Proliferation	Elongation of peroxisomes
PEX26	PEX15			Matrix protein import	Membrane anchor of Pex6p in Hs
PEX27	PEX11			Proliferation	Elongation of peroxisomes
PEX28	PEX24			Proliferation	Separation of peroxisomes in Sc
PEX29	PEX24			Proliferation	Separation of peroxisomes in Sc
PEX30	PEX23		DysF	Proliferation	Growth regulation in Sc
PEX31	PEX23		DysF	Proliferation	Growth regulation in Sc
PEX32	PEX23		DysF	Proliferation	Growth regulation in Sc

**Table 1: The 31 Peroxins and their orthologues in mammals and plants** (adapted from Mullen et al. 2001; Hayashi and Nishimura 2006; Brocard and Hartig 2007; Platta and Erdmann 2007).

AAA: ATPase associated with diverse cellular activities; CAAX-box: farnesylation motif; DysF: Dysferlin domain; Hs: Homo sapiens PMP: peroxisomal membrane protein; PX: peroxisome; PXXP: class II SH3 interacting motif; RING: really interesting new gene; Sc: *Sacharomyces cerevisie*; SH3: Src homology 3; TPR: tetratricopeptide repeat; Ubc: ubiquitin-conjugating enzyme; WD40: 40amino acid long domain containing conserved Trp-Asp; Yl: Yeresinia

### A.1.2.2. Peroxisome Assembly and Formation

The formation and assembly of peroxisomes is a multi-step process including three key stages: (1) The formation of peroxisomal membrane, (2) the import of peroxisome matrix proteins, (3) and the proliferation of pre-existing peroxisomes.

#### *A) The formation of peroxisomal membrane*

So far, two classes of peroxisomal membrane proteins (PMPs), the Class I and Class II PMPs, are known to be involved in the formation of peroxisomal membranes. The Class II PMPs (like AtPEX3 or AtPEX19) are synthesized on free cytosolic ribosomes and are then subsequently imported into the peroxisomal membrane leading to the growth of pre-existing mature peroxisomes. In contrast, the Class I PMPs (AtPEX16 and AtPEX10) are thought to route via the ER towards their final destination, which is either a pre-existing mature peroxisome or a nascent “mature” peroxisome via the *de novo* pathway (Mullen et al. 2001; Mullen and Trelease 2006; Fang et al. 2004; reviewed in Platta and Erdmann 2007).

The following three PMPs – PEX3, PEX16 and PEX19 have been shown to have orthologues in *Arabidopsis*, playing an essential role during the early steps of peroxisomal membrane assembly and maintenance in a various number of organisms. Their absence leads to no detectable peroxisomes (Mullen and Trelase 2006; reviewed in Kaur et al. 2009).

#### *B) The import of peroxisome matrix proteins*

The peroxisomal import of matrix proteins can be divided into four steps: i) a receptor-cargo interaction ii) a receptor-cargo docking to the peroxisome membrane iii) a receptor-cargo translocation and iv) the cargo release into the cytosol (Platta and Erdmann 2007; Brown and Baker 2009).

Proteins which are designated to be transported into peroxisomes contain specific peroxisome targeting signals (PTSs) necessary for the sufficient recognition and transport into the peroxisomal matrix. So far, two main peroxisome-targeting signals (PTSs) are known to be involved in this process, PTS1 or PTS2 (Johnson and Olsen 2001). PTS1 is localized at the C-

terminus of the protein containing a carboxyl terminal tripeptide consisting of the three amino acids Ser-Lys-Leu (SKL) or similar variants such as (Ser/Ala/Cys)-(Lys/Arg/His)-Leu (Gould et al. 1994). Although the sequence of this carboxyl terminal tripeptide is conserved throughout the different kingdoms (yeast, mammals and plants) slight divergences could be observed (Hayashi et al. 1995; Brocard and Hartig 2006; Kragler et al. 1998). PTS2 is localised at the N-terminal side of the proteins with a consensus sequence (Arg/Lys)-(Leu/Val/Ile)-X<sub>5</sub>-(His/QIn)-(Leu/Ala) and was first described by Swinkels et.al in 1991.

Besides the peroxisomal targeting signals cytosolic receptors are essential for a proper transport of these proteins to the peroxisomes (Brown and Baker 2008).

PEROXIN5 (PEX5) and PEROXIN7 (PEX7) have been identified as the two major cytosolic receptors binding to the PTSs of the proteins and targeting them to the peroxisomal membrane (Kragler et al. 1998; Brocard and Hartig 2006). Even though PEX5 and PEX7 are present in all three kingdoms the mechanism of protein transport is slightly different (Figure 7 based on Brown and Baker 2008). In plants like *Arabidopsis* the PTS1 pathway with PEX5 depends also on the PTS2 receptor PEX7 (Ramón and Bartel 2010). In mammals two splicing variants of PEX5 exist, leading to two different transport pathways both involving PEX5. In yeast two completely independent transport pathways exist, the PTS1 with PEX5 as the cytosolic receptor and PTS2 with PEX7 and two additional co-receptors, PEX18 and PEX21 (Figure 7 modified after Brown and Baker 2008).

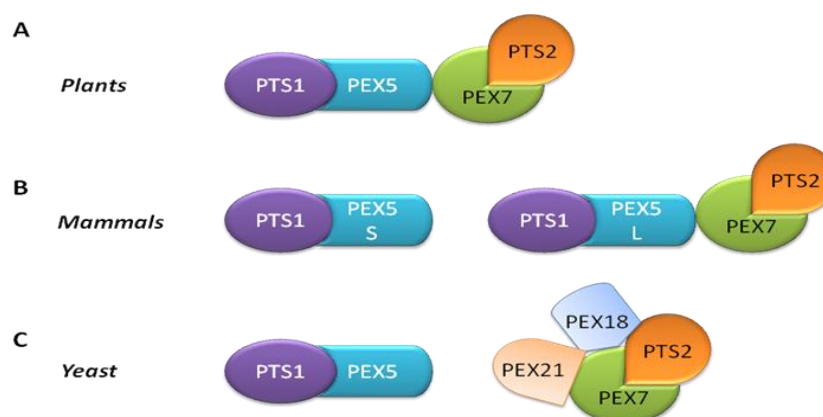


**Figure 7: PTS1 and PTS2 receptor-cargo recognition in various organisms** (based on Brown and Baker 2008).

**(A)** In *Arabidopsis* the PTS2 pathway is completely depended on the PTS1 binding to the PEX5 receptor. **(B)** In mammals two splicing variants exists: PEX5<sub>S</sub> (short isoform) and PEX5<sub>L</sub> (long isoform). PEX5<sub>L</sub> and PEX5<sub>S</sub> both function as PTS1 receptors, whereas PEX5<sub>L</sub> is also required together with PEX7 for PTS2 binding. **(C)** In yeast PEX5 requires PTS1, and in addition co-receptors PRX18 and PEX21 are required for the binding of PTS2 two.

The docking complex necessary for the appropriate transport of matrix proteins through the peroxisomal membrane consists of two PEROXINS (PEX13 and PEX14) in plants and in mammals and additionally PEX17 in yeast (Brown and Baker 2008). In *Arabidopsis* it has been shown that PEX13, an integral membrane protein, binds to the PEX7-PEX5 complex via the PTS2 pathway (Mano et al. 2006), whereas PEX14 binds directly to PEX5 (Nito et al. 2002).

The mechanism underlying the translocation of the proteins across the peroxisomal membrane and their release into the lumen of the peroxisomes is still unknown. The current knowledge suggests that RING-domain-containing PEROXINS (PEX2, PEX10 and PEX12) allow a translocation of the receptor-cargo complex through the peroxisomal membrane (Platta and Erdmann 2007; Brown and Baker 2008). Concerning the release of the proteins into the lumen of the peroxisomes it is suggested that Pex8p together with Pex20p interacts with Pex5p in yeast (Wang et al. 2003).

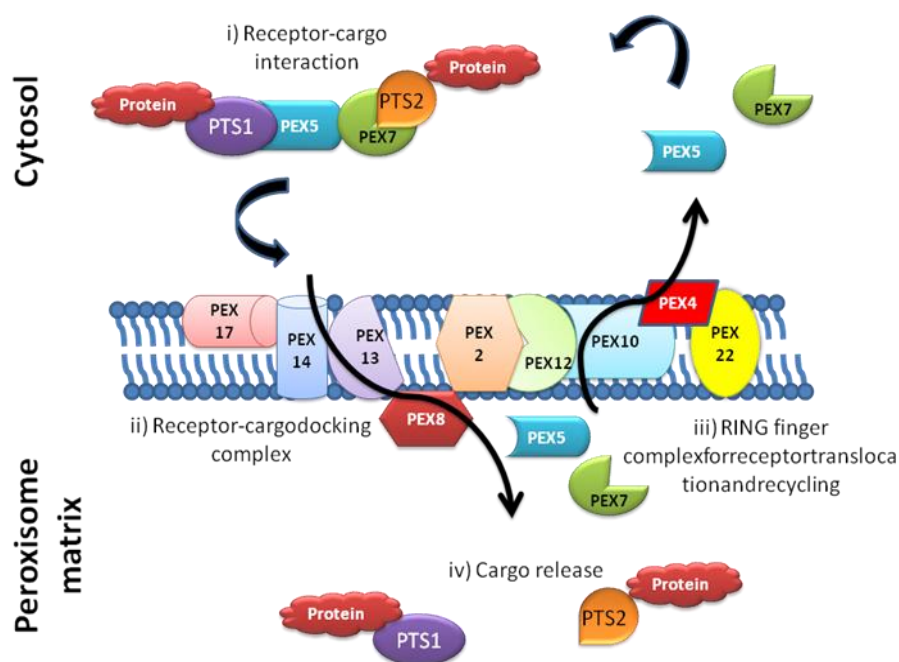


**Figure 8: Overview of peroxisomal matrix protein import** (based on Brown and Baker 2008).

The matrix proteins are binding to either a PTS1 or PTS2 targeting signal binding to a cytosolic receptor PEX5 and/or PEX7, the so called receptor-cargo interaction. This complex then targets the proteins of the docking complex (PEX13, PEX14 and PEX17) and are translocated through the peroxisomal membrane into the peroxisomal matrix. There the cargo (matrix protein) is released into the lumen and the receptors are recycled via the RING finger complex (PEX2, PEX10 and PEX12) back into the cytosol, with the support of PEX8 (in yeast) together with PEX4, which is anchored to the membrane by PEX22.

### C) Proliferation

Eukaryotic cells are able to regulate the number, area and size of their organelles responding to environmental changes. The inhibition or division of the nucleus as well as the Golgi apparatus is coupled to the cell cycle, whereas the division of organelles like the chloroplasts, mitochondria or the peroxisomes are regulated by division processes (Osteryoung and Nunnari 2003; Yan et al. 2005).

An important process regulating the size and number of peroxisomes in eukaryotic cells is the so-called proliferation. This process leads to a significant increase of peroxisomes per cell. It allows the cells to quickly react upon environmental changes like herbicides, ozone or during senescence (Pastori and Del Rio 1997; Lazarow and Fujiki 1985).

This process consisting of several partially overlapping steps: (i) enlargement of pre-existing peroxisomes (ii) elongation of peroxisomes (iii) membrane constriction (iv) fission of the peroxisomes and finally (v) distribution (Fagarasanu et al. 2007; Kaur et al. 2009).

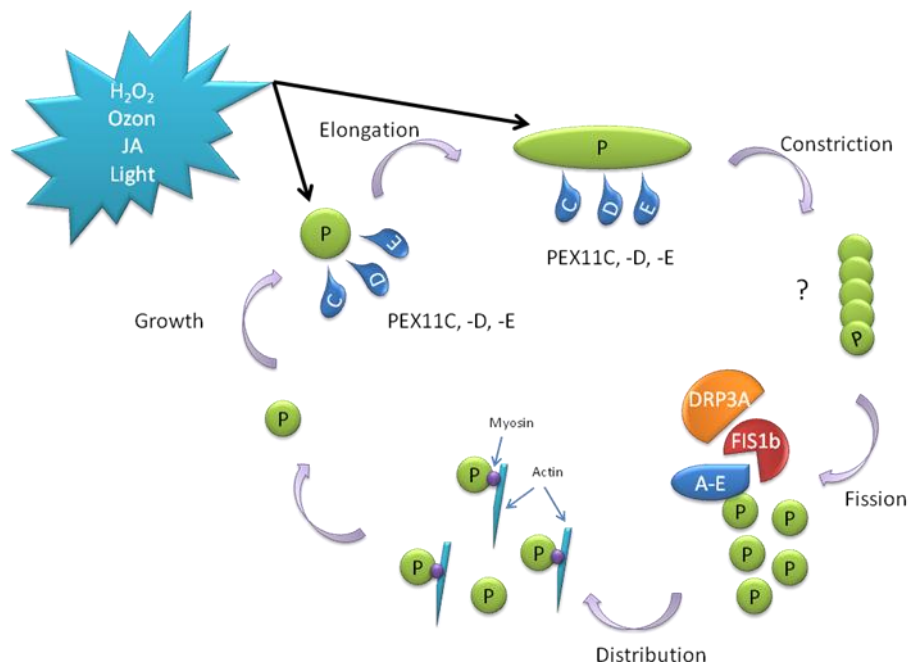


**Figure 9: Model of peroxisome proliferation in *Arabidopsis*** (modified after Lingrad and Trelase 2008 and Kaur et al. 2009).

Peroxisome proliferation can be induced by hydrogen peroxide, ozone, jasmonates (JA) or light. It's a process consistent of several overlapping steps: **i-ii) growth and elongation:** PEX11 (PEX11C, -D and -E) is involved in the early steps of PX proliferation. **iii) membrane constriction:** not much is known about the constriction of peroxisomal membranes. **iv) fission of peroxisomes:** fission is enabled by the scission activities of DRP3A which is recruited to the peroxisomal membrane by FIS1b, which is previously recruited by the PEX11 gene family. **v) distribution:** finally the peroxisomes are distributed throughout the cell by various myosin proteins via the actin filaments.

In yeast a number of peroxisome membrane proteins (PMPs), like PEX11/PEX25/PEX27, PEX28/PEX29 and PEX30/PEX31/PEX32 have been identified to play an important role in the early steps of PX proliferation (Rottensteiner et al. 2003, Vizeacoumar et al. 2004, reviewed in Brocard and Hartig 2007). Among these, PEX11 was the first one to be identified and closer analyzed, revealing an important role in the enlargement and elongation steps during proliferation (Erdman and Blobel 1995).

Not much is known about the control of the constriction step, whereas several proteins have been revealed to be involved in the division and fission steps during proliferation (Kaur et al. 2009)

Recent studies in yeast and mammals have shown that specific dynamins and dynamine-related proteins (DRPs) are required for the fission process during proliferation (reviewed in Kaur et al. 2009). They belong to the group of large GTPases, a family of hydrolase enzymes, involved in various processes like vesicle trafficking in and out of the Golgi and cell and organelle division (Bliek 1999; Hinshaw 2000; Kauer et al.2009).

In yeast the dynamin-like protein Vps1p is involved in the fission event and required for the regulation of peroxisome abundance. Yeast *vps1* null mutants lead to few giant peroxisomes per cell and were not able to promote a normal peroxisome division (Hoepfner et al. 2001).

In human cells the dynamin-like GTPase DLP1 has been identified as a homolog to the yeast VPS1 and is known to regulate the dynamics of mitochondria as well as the ER (Li and Gould 2003). Recent studies have suggested a role of DLP1 in the division process of peroxisomes. Silencing of DLP1 dynamin leads to a significant decrease of peroxisome number. It is believed that PEX11 recruits DLP1 to the peroxisomal membrane and by this means peroxisome division is initiated (Li and Gould 2003; Koch et al. 2003).

In *Arabidopsis* two dynamin-related proteins, DRP3A and DRP3B, have been reported to play a role in the division process of two organelles: mitochondria and peroxisomes (Mano et al. 2004; Zhang and Hu 2009; reviewed in Kauer et al. 2009). In an *Arabidopsis* mutant screen a protein named aberrant peroxisome morphology 1 (AMP1), functioning in the maintenance of peroxisome numbers, was identified. Mutant plants have significantly larger peroxisomes and a decreased number of organelles (Mano et al. 2004; Zhang and Hu 2009).

Beside the DRPs another protein family, the *FISSION1* (*FIS1*) gene product is involved in the peroxisomal and mitochondrial division machinery. FIS1 related proteins are integral membrane proteins targeting both membrane systems (Zhang and Hu 2008, 2009). In yeast and mammals,



FIS1 acts as an adaptor for DPL1 (mammals) or VSP1 (yeast), by recruiting them to peroxisomes or mitochondria, which leads to membrane fission (Zhang and Hu 2008, 2009). In human cells PEX11, FIS1 and DRP are involved in the process of peroxisome proliferation. Studies by Li and Gould (2003) as well as Koch et al. (2004, 2005) have shown that PEX11 and FIS1 are involved in peroxisome elongation and constriction and that the human FIS1 and DLP1 interact with each other directly. This is not the case for PEX11 and DLP1 (Koch et al. 2010).

In *Arabidopsis* two homologues of FIS1, FIS1A and FIS1B, have been identified and shown to support peroxisomal and mitochondrial division (Lingard and Trelase 2008; Zhang and Hu 2009). A study from Lingard and Trelase in 2008 revealed that all five AtPEX11 homologues (AtPEX11A to E) physically interact with FIS1b, whereas no interaction could be observed with FIS1a or DRP3A. They suggest that PEX11 promotes peroxisome elongation as well as the recruitment of FIS1b to the peroxisomal membrane. Afterwards FIS1b seems to recruit DRP3A to the membrane, initiating the fission step of peroxisome proliferation (Lingard and Trelase 2008). The divided peroxisomes are then transported inside the cell with the help of various myosin proteins via actin filaments (Lingard and Trelase 2008).

### A.1.3. Induction and regulation of Peroxisomes Proliferation

Peroxisomes are highly sensitive organelles which can adapt to environmental changes. In order to do that, they must quickly react upon external stimuli by changing their size, number and protein content, defined as proliferation.

In yeast such as *Sacharomyces cerevisiae*, peroxisome proliferation is induced by fatty acids, e.g. oleic acid. So called oleate responsive elements (ORE) were found in the promoter region of several genes encoding peroxisomal proteins like the *POX1* as well as the *ScPEX11* gene (Karpichev et al. 1997, 1998; Gurvitz et al. 2001). So far, two proteins, OAF1 and OAF2, also named PIP2, (Karpichev et al. 1998; Rottensteiner et al. 1997), have been identified to act as transcription factors binding to such ORE sequences by forming a heterodimer OAF1/PIP2 (Rottensteiner et al. 1997).

In mammals, a peroxisome proliferator activator receptor  $\alpha$  (PPAR $\alpha$ ) was identified playing an important role in the regulation of genes involved in the lipid homeostasis, including all peroxisomal  $\beta$ -oxidation genes in mammalian cells (Lemberger et al. 1996). This receptor binds to the peroxisome proliferator response element (PPRE) located in the promoter region of genes

involved in the lipid homeostasis, thereby activating their gene transcription (Berger and Moller 2002).

Beside PPAR $\alpha$ , two additional isoforms PPAR $\delta/\beta$  and PPAR $\gamma$  are known: PPAR $\delta/\beta$  is ubiquitously expressed, whereas PPAR $\gamma$  is mainly expressed in adipose tissue and PPAR $\alpha$  is highly expressed in liver, kidney, heart and muscles cells (Schoonjans et al. 1996; Berger and Moller 2002). A various number of proliferation agents (PA) such as clofibrate, a hypolipidemic drug, was shown to induce expression of HsPEX11 $\alpha$  and thereby promoting peroxisome division in mammalian cells (Li et al. 2002b).

In contrast to the yeast and mammalian systems, very little is known about plant factors regulating the expression of genes involved in the peroxisomal proliferation machinery, like the *AtPEX11* gene family. No genes were found coding for PPAR homologous proteins or OAF1/PIP2 homolog proteins in the plant genome (Leon 2008, Kaur and Hu 2009).

A recent study could show that far red light can induce peroxisome proliferation in plant cells, requiring phytochrom A (phyA) and the up-regulation of the *AtPEX11B* gene, mediated by the bZIP transcription factor HY5 HOMOLOG (HYH) (Desai and Hu 2008).

The authors could show that phyA, as well as cryptochrom1 (cry1) and phyB led to a decrease in *AtPEX11B* expression in null mutant plants of these genes, with the strongest decrease observed in phyA null mutant plants, indicating an effect of phyA on *AtPEX11B* (Desai and Hu 2008). Based on an in silico analyses of the 219-bp promoter region upstream of the transcription start site (TSS) of the *AtPEX11B* promoter, a large number of light-response elements (LREs) like GATA, GT1, and I boxes, were found. These elements have been show to bind transcription factors, thereby regulating light-dependent gene activation (reviewed in Desai and Hu 2008). HYH and its homolog HY5, which are very common transcription factors shown to play a role in the regulation of genes during photomorphogenesis, were analysed for their binding activity to the *AtPEX11B* promoter (Desai and Hu 2008). Desai and Hu (2008) could show that even though HYH and HY5 share about 88% amino acid identity in their bZIP DNA-binding domain, only HYH was observed to bind to the *AtPEX11B* promoter analysed by an electrophoretic mobility shift assay (EMSA), indicating a specific binding of HYH to the promoter region of *AtPEX11B*.

In addition, it is known that peroxisome proliferation in plant cells can be induced in post-germinative growth as a response to herbicides, ozone or during senescence (Pastori and del Rio 1997; Lopez-Huertas et al. 2000) but the mechanism underlying these processes are still unknown.

### A.1.4. The PEX11 gene family

PEROXIN11 (PEX11) protein family members are peroxisomal membrane proteins (PMP) which seem to play a key role in peroxisome proliferation in nearly all eukaryotic cells. All PEX11 proteins of higher organisms are similar in their amino acid composition and harbour a conserved PEX11 domain similar to the one found in yeast ScPEX11 (formerly PMP27) (Erdmann and Blobel 1995).

#### A.1.4.1. Yeast *PEX11*

The yeast ScPEX11 protein has been shown to play a key role in the proliferation machinery of peroxisomes. Yeast cells lacking *PEX11* are able to grow on glucose and ethanol media, whereas the utilization of oleate is limited. *PEX11* lacking cells harbour few giant peroxisomes per cell, suggesting a role in the division and fission process during proliferation (Erdmann and Blobel 1995; Marshall et al. 1995). As expected for a proliferation factor over-expression of *ScPEX11* leads to a significant increase of peroxisomes per cell (Sakai et al. 1995; Marshall et al. 1995; Li and Gould 2002; Tam et al. 2003).

Recently additional PMPs have been identified such as PEX25/PEX27 belonging to the PEX11 protein family as well as Pex28p/Pex29p or Pex30p/Pex31p/Pex32p, playing a role in peroxisome proliferation in yeast (Rottensteiner et al. 2003; Tam et al. 2003). ScPex11, ScPex25 and ScPex27 share common structural motifs (~10% identity and ~18% similarity) and ScPex11 is thought to be peripheral membrane protein (Marshall et al. 1995).

#### A.1.4.2. Human *PEX11*

In mammalian cells three *PEX11* genes, *HsPex11 $\alpha$* , *HsPex11 $\beta$*  and *HsPex11 $\gamma$* , have been identified. A phylogenetic analysis revealed that *HsPex11 $\alpha$*  is more closely related to *HsPex11 $\beta$*  than to *HsPex11 $\gamma$*  (Abe and Fujiki 1998; Tanaka et al. 2003).

All three human PEX11 proteins are peroxisomal membrane proteins and HsPEX11 $\alpha$  and HsPEX11 $\beta$  exposes both N- and C-terminal ends to the cytosol, like shown by immunofluorescence microscopy experiments. The human HsPEX11 $\beta$  seems to be essential for the survival of mammalian cells. It has been shown that *PEX11 $\beta$* -deficient mice have developmental delays, hypotonia and enhanced neuronal apoptosis, resembling the effects of the Zellweger Syndrom in humans (Li et al. 2002a).

In contrast, mice lacking PEX11 $\alpha$  are externally indistinguishable from wild-type mice, having a normal developmental pattern and showing no detectable defect of peroxisome proliferation (Li

et al. 2002b). Overproduction of PEX11 $\alpha$  led to an induced peroxisome proliferation in mouse and human cultured cells (Li and Gould 2002b).

The over-expression of the HsPEX11 $\gamma$  leads to an enlargement and clustering of peroxisomes (Li et al. 2002a).

In addition, we could observe that over time the expression of all human PEX11 proteins clearly led to the formation of PX clusters after an previous increase in PX number as well as an elongation of PX in human kidney cells (HEK293T) compared to a control (Koch et al. 2010).

### A.1.4.3. Plant PEX11

Recent studies have identified five orthologues of the yeast *ScPEX11* gene in the plant *Arabidopsis thaliana*, referred to as *AtPEX11A* to *E*. The amino acid sequence alignment in Figure 10 (Lingrad and Trelase 2006) shows that the PEX11 proteins can be divided into two distinct classes. *AtPEX11C*, *-D* and *-E* belong to Class I, showing a high similarity to each other (75% average identity and 92% average similarity), whereas *AtPEX11A* and *-B*, belonging to Class II, are more divergent (exhibit 31% identity and 51% similarity to each other) (Figure 10 taken from Lingard and Trelase 2006).

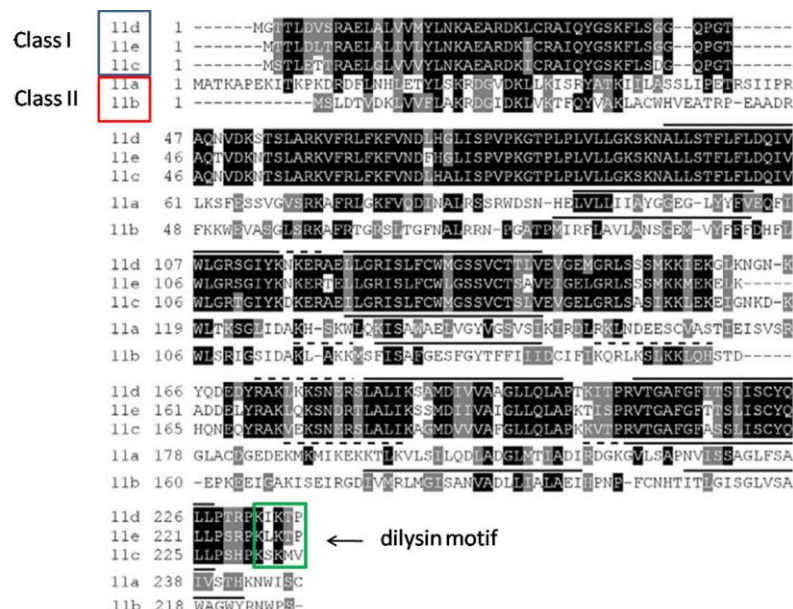


**Figure 10: Amino acid sequence alignment of AtPEX11A, -B, -C, -D and -E. AtPEX11 protein sequences were aligned using the ClustalW algorithm (Figure modified after Lingrad and Trelase 2006).**

(<http://www.ch.embnet.org/software/ClustalW.html>). Identical and similar residues were shaded black and gray, respectively, with BOXSHADE ([http://www.ch.embnet.org/software/BOX\\_form.html](http://www.ch.embnet.org/software/BOX_form.html)) Transmembrane domains were predicted using TMpred

([http://www.ch.embnet.org/software/TMPRED\\_form.html](http://www.ch.embnet.org/software/TMPRED_form.html)), and are over-lined in black. Basic clusters of amino acid residues are over-lined with dashes. Dilysine motifs are boxed in red.

Interestingly, the Class I *AtPEX11* gene family members possess a C-terminal dilysine motif with the sequence–KXXXX (Figure 10, indicated with a green box), also known as the ER retrieval motif. This motif is thought to facilitate binding of coatomers and was first observed in rats. It is believed that the dilysin motif of PEX11 binds to a coat protein 1 (COP1), thereby recruiting an ADP-ribosylation factor (ARF1) (Passreiter et al. 1998). Studies by Anton et al. (2000) provide some evidence that together PEX11 and coatomers are involved in the process of peroxisome division by promoting membrane vesiculation (reviewed in Kaur et al. 2009).

Recent studies revealed that all five *AtPEX11* proteins localize to peroxisomes in cell suspension cultures (Lingard and Trelease 2006) as well as in transgenic *A. thaliana* plants (Orth et al. 2007).

The orientation of the N- and C-termini of the *AtPEX11* family members relative to the peroxisomal membrane was determined by myc-tagged versions of the proteins in cell suspension cultures of *A. thaliana* as well as in tobacco BY2 cells. The results revealed that both termini of *AtPEX11B*, -C, -D and -E face the cytosol, whereas *AtPEX11A* exposes its C-terminus to the peroxisomal matrix (Lingard and Trelease 2006).

In addition, the *AtPEX11A* protein possesses three predicted trans-membrane domains (TMDs), whereas the other four *AtPEX11* proteins (*AtPEX11B*, -C, -D and -E) have four TMDs, highlighted in Figure 10 with solid lines (Lingard and Trelease 2006).

Orth et al. (2007) analysed the subcellular localisation of the different *AtPEX11* isoforms in transgenic plants expressing CFP-PEX11 fusion proteins under control of the strong 35S promoter, together with an YFP-PTS1 fusion protein. They observed a consistent pattern of distinct morphological changes to the organelles in 10 to 15 independent T2 lines overexpressing each of the five CFP-*AtPEX11* fusion proteins (Orth et al. 2007).

They could observe an elongation as well as an increased proliferation of peroxisomes. Over-expression of CFP-PEX11A or CFP-PEX11B fusion proteins mainly resulted in peroxisome elongation (Orth et al. 2007).

Over-expression of the CFP-PEX11C, CFP-PEX11E and CFP-PEX11D fusion proteins, belonging to Class I, mostly lead to peroxisomal clustering and an increased number of peroxisomes (Orth et al. 2007).

In addition, analysis of RNAi silencing plants with different degrees of silencing of *AtPEX11A*, *AtPEX11B* or *AtPEX11E* (as a representative for Class I *AtPEX11*) show that the *AtPEX11* proteins

are to some part redundant in their regulation of peroxisome proliferation. *AtPEX11A*, *AtPEX11C*, *AtPEX11D* and *AtPEX11E* appear to play a stronger role in peroxisome proliferation than *AtPEX11B* (Orth et al. 2007).

Different results were obtained by Lingard and Trelase (2006), who found that in cell suspension cultures of *Arabidopsis*, myc-tagged versions of PEX11C and PEX11D initiate peroxisome elongation without fission, whereas PEX11E leads to an increase in peroxisomal number without elongation. *PEX11B* leads to peroxisome aggregation without changes in peroxisome abundance or length. Cells transformed with myc-*AtPEX11A* show a significant difference regarding the amount of elongated peroxisomes over a time period of 72h. First only a small percentage (about 5%) of the cells show elongated peroxisomes, increasing to about 37% after 36h and then declining to the same level as the control (Lingard and Trelase 2006).

These differences may be due to the different experimental setups used: a transient expression in *Arabidopsis* and BY2 tobacco cell suspension cultures by Lingard and Trelase (2006) versus constitutive expression in transgenic *A. thaliana* plants by Orth et al. (2007).

## B.2. Results

### B1. Expression profiles of the five *AtPEX11* members in *A. thaliana* plants

The five *Arabidopsis PEX11* genes were previously shown to be expressed in siliques, leaves, roots and suspension cultures, except for *AtPEX11A* (Lingard and Trelase 2006).

An own database research (eGFPbar.utoronto.ca/ status 2011) suggests a high expression of *AtPEX11A* (At1G47750) in water imbibed seeds (after 24h) and pollen (especially in tricellular pollen). Tissue specific expression of *AtPEX11A* was predicted in stamen and guard cells.

*AtPEX11B* (At3G47430) shows an induction of expression after light exposure and a quite high expression in cotyledons, cauline and rosette leaves and flowers (especially in sepals) as well as in water imbibed seeds. A tissue specific expression is measured in mesophyll cells of leaves and the stigma.

*AtPEX11C* (At1G01820) shows a high expression in cauline and senescent leaves as well as in dry seeds. The gene is highly expressed in the vascular tissue and less in the mesophyll cells and guard cells of the leaf. In addition the expression seems to be light induced.

*AtPEX11D* (At2G45740) is highly expressed in cotyledons, cauline, adult or senescent leaves as well as in sepals or water imbibed seeds after 24h. A tissue specific expression of *AtPEX11D* is detected in mesophyll cells of leaves as well as in guard cells and in the lateral root cap.

The last *PEX11* member, *AtPEX11E* (At3G61070) shows a high expression in pollen and water imbibed seeds (24h). A lower expression is detected in flower tissues (especially petals) and the stamen. No or very weak expression is measured in cotyledons, cauline or rosette leaves.

To evaluate the microarray data, a Northern Blot analyses was performed with the help of Nikola Winter with *PEX11* specific probes (Figure 11). Here *AtPEX11A* and *AtPEX11E* could not be detected and *AtPEX11B* showed a very low expression in seedlings and flowers and was barely detectable in senescent leaves. Our own analysis on existing microarray data as well as the Northern Blot analyses revealed a very low or no expression of the *AtPEX11E* gen in the analysed tissues.

*AtPEX11C* and *AtPEX11D* expression pattern appeared similar high in all examined tissues with the exception that *AtPEX11C* which was not detected in rosette leaves.

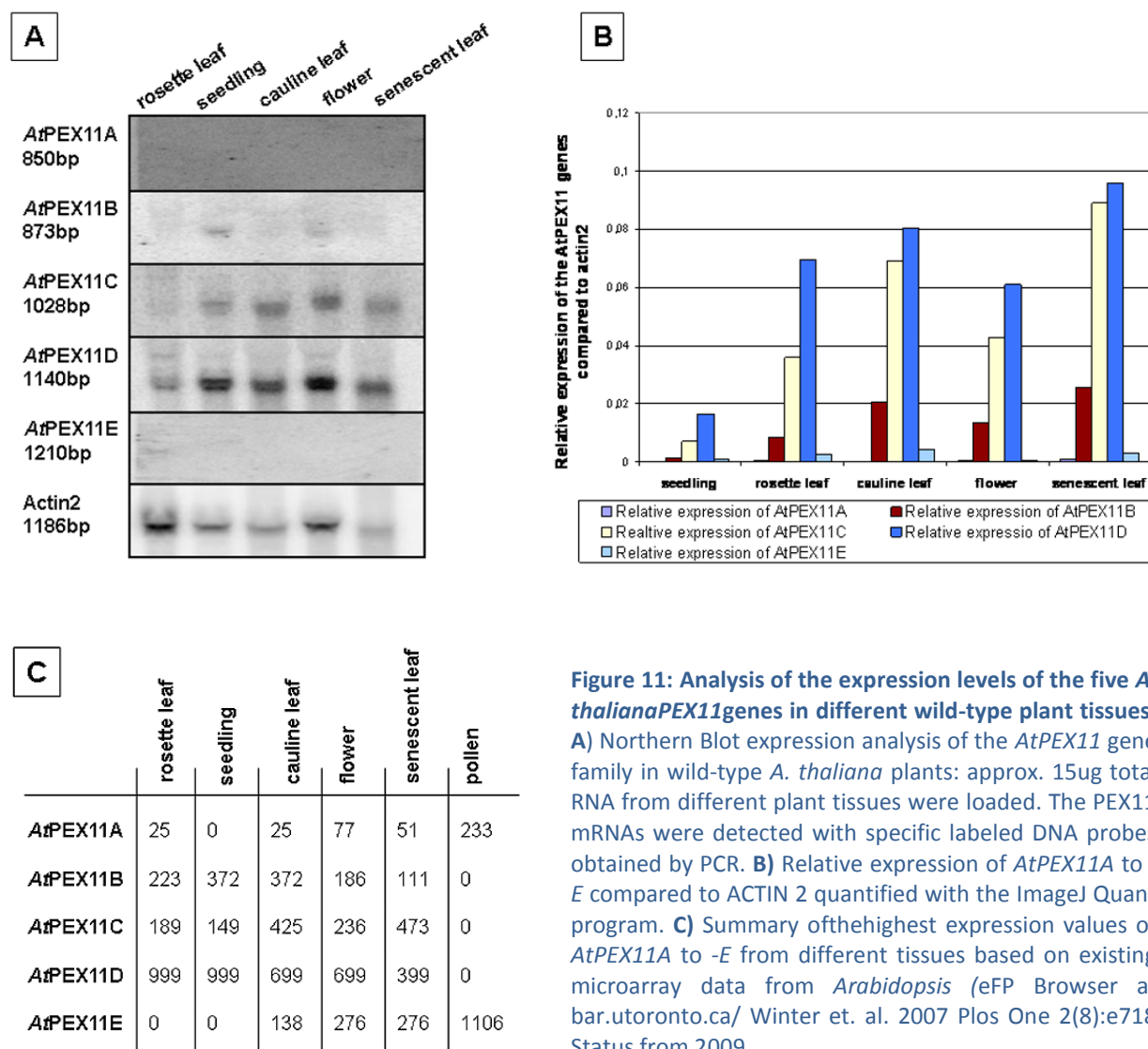


**Figure 11: Analysis of the expression levels of the five *A. thaliana* PEX11 genes in different wild-type plant tissues.** **A)** Northern Blot expression analysis of the *AtPEX11* gene family in wild-type *A. thaliana* plants: approx. 15ug total RNA from different plant tissues were loaded. The PEX11 mRNAs were detected with specific labeled DNA probes obtained by PCR. **B)** Relative expression of *AtPEX11A* to -*E* compared to ACTIN 2 quantified with the ImageJ Quant program. **C)** Summary of the highest expression values of *AtPEX11A* to -*E* from different tissues based on existing microarray data from *Arabidopsis* (eFP Browser at [bar.utoronto.ca/](http://bar.utoronto.ca/) Winter et. al. 2007 Plos One 2(8):e718 Status from 2009).

Taken together, the *AtPEX11D* transcripts showed the highest expression levels among all five family members, followed by *AtPEX11C*, whereas the two homologues belonging to the ClassII, *AtPEX11A* and *AtPEX11B*, exhibit low expression levels. Noteworthy, in the microarray analysis neither *AtPEX11B*, -*C* or -*D* were detected in pollen. Also *AtPEX11E* expression was not detected in the analyzed tissues in our study; a previous study by Orth et al. (2007) predicted a high expression of the *AtPEX11E* gene in a various number of tissues like leaf, senescent leaf, flower or seed based on their online microarray data.



## **B.2. Intracellular distribution of yeast, human and plant PEX11 fusion proteins in epidermal cells of *N. benthamiana***

To clarify whether the functions of the various PEX11 proteins are conserved throughout the three kingdoms we performed peroxisomal co-localisation experiments of transiently expressed fluorescent fusion proteins. This allowed us to compare the potential of plant, yeast and human PEX11 proteins to associate with peroxisomes (PX) and to analyse their capacity to induce peroxisomal proliferation in plant cells. The wild-type appearance of PX in epidermal cells of *N. benthamiana* leaves were evaluated with a red fluorescence protein (mCherry) carrying a C-terminal peroxisomal targeting signal (mCherry-SKL). Here the tagged PX appeared round shaped, well separated and most organelles were highly mobile (Figure. 12\_A). To analyse the effect of plant, yeast and human PEX11 proteins on the localisation and shape of PX we transiently co-expressed PEX11 yellow fluorescent protein fusions (YFP-PEX11) under the control of a 35S *CaMV* promoter, together with mCherry-SKL under the control of an estradiol induced promoter system (Curtis and Grossniklaus 2003; Koch et al. 2010).

Here all tested PEX11 fusion proteins localised to the peroxisomal membranous structures, which were at least partially tagged by mCherry-SKL (Figure 12\_B to 12\_D). In addition, a strong clustering of PX was observed for all tested plant PEX11-fusion proteins, ScPEX11, HsPEX11 $\alpha$  and HsPEX11 $\gamma$  (Figure 12\_B to 12\_D, close ups). Exceptions were found with the two yeast fusion proteins ScPEX25 and ScPEX27 as well as the human HsPEX11 $\beta$  fusion proteins. Here no large clusters of PX were detected. About half of the PXs were located in small clusters, whereas the remaining PX resembled the wild-type situation with normal shaped and mobile peroxisomes (Figure 14). As an additional control to ensure that the N-terminal YFP tag had no effect on the PEX11 function we performed co-expression studies with mCherry-SKL and estradiol induced AtPEX11D without an YFP-tag (Figure 12\_B6). Here we could observe clustering of peroxisomes induced by AtPEX11D without an YFP-tag.

Taken together, our experiment suggests that all PEX11 proteins despite their origin are efficiently targeted to the peroxisomal membrane. However, their potential to affect peroxisomal proliferation appeared quite distinct.

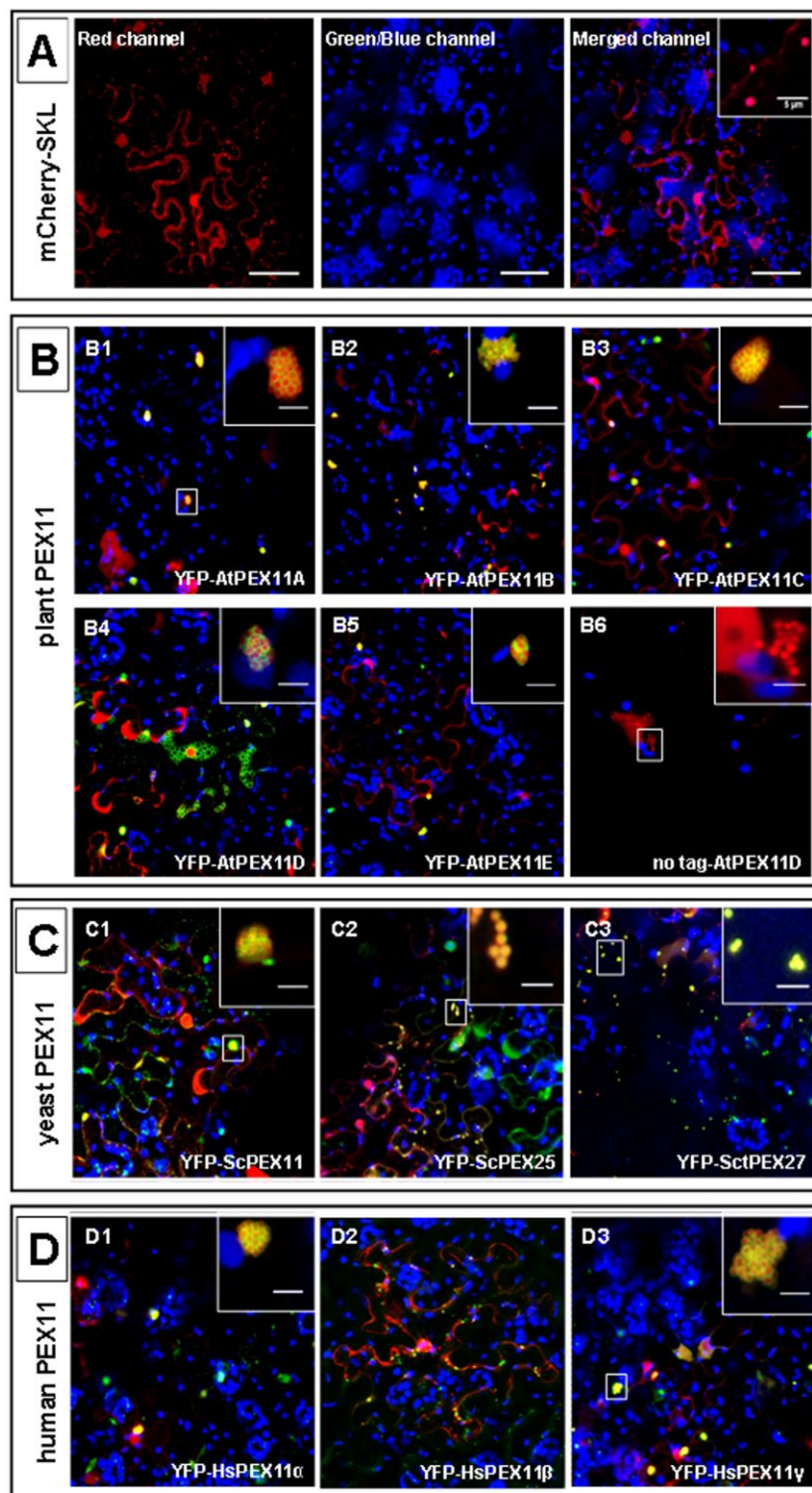


**Figure 12:** Co-expression of YFP-PEX11 fusion proteins from plant, human and yeast together with a red fluorescent PX marker (mCherry-SKL) 48h post infiltration in epidermal plant cells of *N. benthamiana*: **(A) Control:** estradiol-induced expression of the peroxisomal marker protein mCherry-SKL. Small, well-separated red-tagged PXs were visible. **(B) Arabidopsis** 35S promoter expressed **YFP-PEX11 fusion proteins AtPEX11A, AtPEX11B, AtPEX11C, AtPEX11D and AtPEX11E**, are detected at the membrane of PX in plant cells. Moreover, all these proteins and estradiol inducible **AtPEX11D** induce formation of PX clusters. **(C)** 35S promoter expressed **YFP-ScPEX11, -25 and -27 Yeast fusion proteins**. The tagged yeast PEX11 family members appear at the PX membrane and induce to various degrees PX clustering. **(D)**

Human derived PEX11 fusion proteins expressed by *35S::YFP-HsPEX11α*, *35S::YFP-HsPEX11β* and *35S::YFP-HsPEX11γ*. The human PEX11 proteins are detected at the PX membrane and except for HsPEX11β seem to induce PX clusters similar to the ones observed with the plant and yeast PEX11 fusion proteins. To allow high resolution imaging the cells were treated with F-actin depolymerizing cytochalasin D for 0.5h prior to imaging. This immobilized the movement of PX but did not induce clustering or alter the appearance of PX. Images are projected Z-stacks (20μm deep) of 6 optical slices, distance 4 μm; Scale bar: 40μm; small images: close-up of PX clusters, bar: 5μm; green channel: YFP, red channel: mCherry-SKL, blue channel: chloroplast auto-fluorescence.

### B.3. Plant, yeast and human PEX11 fusion proteins change the appearance of peroxisomes in plant cells.

To study the effects of the various yeast, human and plants PEX11 proteins on PX, we quantified the size, number and distribution of peroxisomes (PX) in the epidermal cells. The various PEX11-fusion proteins were co-expressed with mCherry-SKL and PX appearance was analysed 48h *post* infiltration. For each PEX11-fusion protein at least 3 independent co-expression assays were performed and in total 30 images (projected Z-stacks of 6 optical slices, distance 4 μm) were taken. The images were used to quantify the number, size and clustering of PX with the help of the ImageJ software (Collins 2007). We divided the PX into four categories with increasing size in μm of diameter (Table 2) and two additional categories for small and large peroxisomal clusters. Categories I and II represent very small and small PX, whereas category III encloses the normal-sized PX. Category IV represents enlarged PX, which are not clustered. The two categories A and B represent the small and large clusters formed after over-expression of PEX11 fusion proteins (Table 2). To calculate the total number of PX we included the PX appearing in small and large clusters. To achieve this we used 5 high-resolution images of small and large clusters from each PEX11-fusion protein from yeast, human and plant (see also materials and methods chapter D.6.4).

	Category I	Category II	Category III	Category IV	Category A Small cluster	Category B Large cluster
Diameter [μm]	0.0-0.5	0.51-0.87	0.88-1.9	1.91-2.75	2.76-6.16	6.17-27.55
Area [μm <sup>2</sup> ]	0-0.21	0.21-0.59	0.59-2.98	2.98-5.96	5.96-29.80	29.80-596.04

**Table 2: Six categories of peroxisomal sizes and clusters were assigned:** Category I and II for very small and small PX (0.0-0.87μm in diameter), Category III for normal sized PX (0.88-1.9μm) and categories IV for enlarged PX (1.91-2.75μm). The categories A and B represent small (2.96-7.16μm) and large (6.17-27.55μm) peroxisomal clusters formed after over-expression of the different PEX11 fusion proteins.

By quantifying the number and size of PX of the different PEX11 fusion proteins we could answer two questions:

- 1) Does the average size and/or number of peroxisomes (PX) change due to the expression of yeast, human and plant PEX11 fusion proteins?
- 2) Does the over-expression of the PEX11 fusion proteins alter the distribution of peroxisomes (PX) in plant cells?

### B.3.1. Heterologous PEX11 fusion proteins alter the size and number of peroxisomes in plant cells

First, as a control, epidermal leaf cells of *N. benthamiana* were transformed with the peroxisomal marker protein signal mCherry-PTS1 (SKL) alone to evaluate the shape, size and abundance of PX in the infiltrated plant tissues under normal conditions. A single epidermal cell shows an average of 25 PX (Figure 13: control), which are round shaped, well separated and highly mobile.

The over-expression of the five plant PEX11 fusion proteins led to a change in number and area of PX for four AtPEX11 fusion proteins (Figure 13), except for the AtPEX11A fusion protein showing a slight decrease in PX number and area compared to the control. AtPEX11C, AtPEX11B and AtPEX11D led to approx. twice as many PX per cell compared to the control, whereas AtPEX11E only induced a slight increase in PX numbers. AtPEX11A, AtPEX11C, AtPEX11D and AtPEX11E cover a smaller area indicating that these fusions induced the formation of smaller PX compared to the control.

Concerning the yeast homologues ScPEX25 and ScPEX27, the over-expression of these proteins led to an increase of PX number and area. Especially the over-expression of the ScPEX27 fusion protein led to three times more PX per cell compared to the control (approx. 75 PX per cell/ control approx. 25 PX per cell). In contrast, the yeast ScPEX11 fusion protein had no obvious effect on the number of PX per cell, but they cover a smaller area, suggesting that the PX are smaller in size compared to the control. Concerning the three human PEX11 orthologues, no obvious changes regarding the number or area of PX were observed induced by HsPEX11 $\alpha$  fusion protein, whereas in the presence of the HsPEX11 $\gamma$  fusion protein a larger area of PX as well as a higher amount of PX per cell were observed. Note that the human HsPEX11 $\beta$  seemed to increase the number of PX per cell, but due to a too small number of successful infiltrations and images

(n=3) available, no quantification was performed and is therefore marked as not determined (n/d).

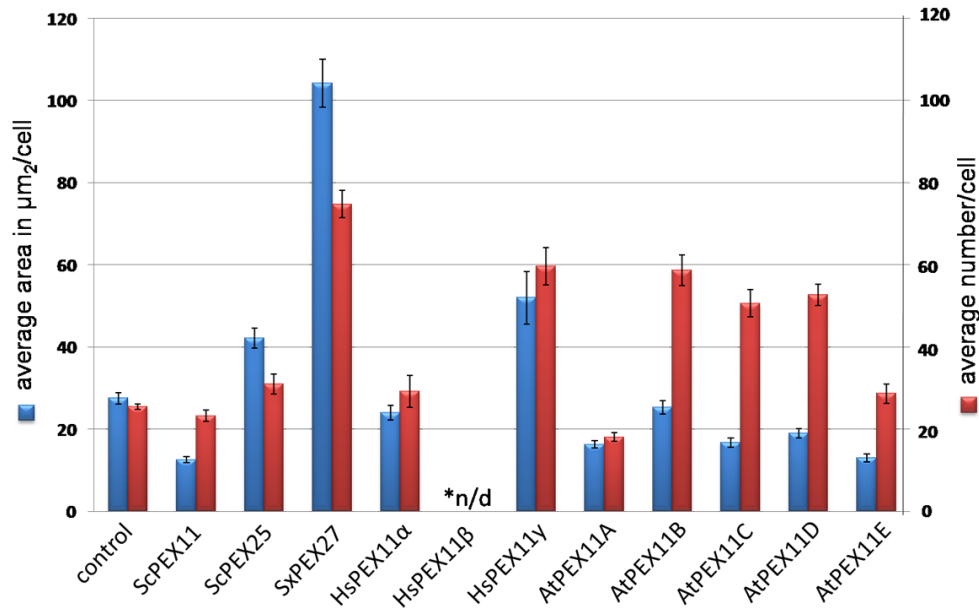


**Figure 13: Statistical analysis of peroxisome (PX) abundance and area 48h post infiltration.** Blue bars: Average area of all PX per cell in  $\mu\text{m}^2$ . Red bars: Average number of PX per cell. Error Bars: Standard error of means; 3 independent infiltration experiments were performed with a total n= 30 images representing approximately 190 cells. \*n/d = not determined.

Beside the analysis of the size, number and area of PX we also evaluated the effect on the morphology of PX.

### B3.2. Over-expressing yeast, human and plant PEX11 fusion proteins lead to cluster formation of peroxisomes

Considering the question, whether over-expression of the various PEX11 fusion proteins effects the distribution of peroxisomes (PX), we evaluated the appearance of clusters.

We were able to observe a significant shift induced by each PEX11-fusion protein towards the formation of small or large peroxisomal clusters and a decrease of the abundance of separated small and normal sized PX, summarized in category I to IV (see Figure 14). All five *Arabidopsis* PEX11 fusion proteins led to cluster formation containing nearly all PX inside small and large clusters (Figure 14: Category A and B). The two human PEX11 fusion proteins HsPEX11 $\alpha$  and HsPEX11 $\gamma$  as well as the yeast ScPEX11 showed about 80% cluster formation (both categories A and B taken together), whereas for the two remaining yeast PEX11 fusion proteins, ScPEX25 and

ScPEX27, only 50% of the PX were located in clusters, which were small. In contrast to the other PEX11 fusion proteins the over-expression of *ScPEX25* and *ScPEX27* did not lead to the formation of large PX clusters (Figure 14). Again no quantification of PX clusters was performed for the human HsPEX11 $\beta$  fusion protein, due to the small number of images. However, the few obtained images (see example in Figure 12) seem to indicate the formation of a lower number of clusters compared to the plant or the two other human PEX11 fusion proteins. Here the situation resembles more that of the two yeast PEX11 proteins, *ScPEX25* and *ScPEX27* (Figure 12\_C2/C3 and 14).

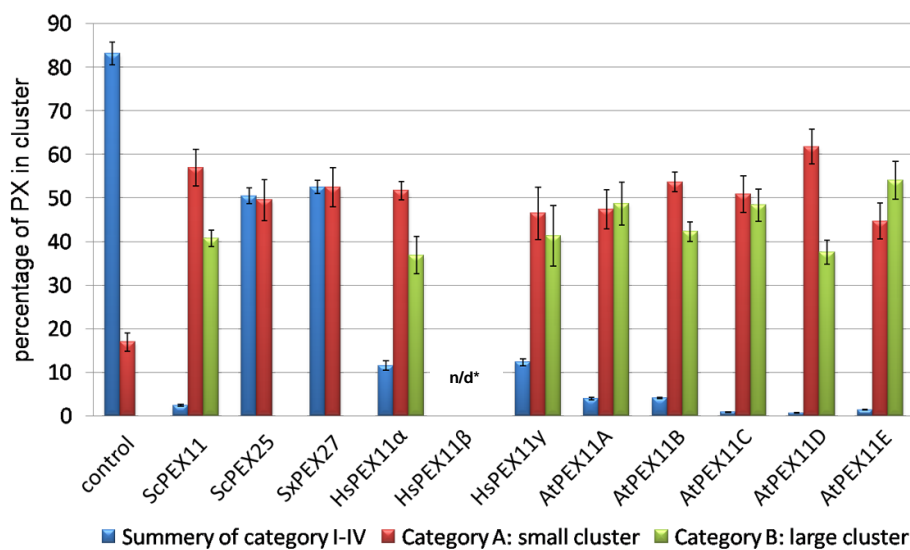


**Figure 14: Peroxisomal cluster formation after over-expressing yeast, human and plant YFP-PEX11 fusion proteins in epidermal leaf cells of *N. benthamiana*.** Blue bars: summarized percentage of PX of category I to IV. Red bars: Category A: percentage of PX located in small clusters. Green bars: Category B: percentage of PX located in large clusters; Error bars: Standard error of means; 3 independent infiltration experiments were performed analysing n= 30 images (represent approximately 190 cells), n/d\* = not determined.

### B.4. Over-expression of the plant AtPEX11D fusion protein leads to the formation of aberrant membrane structures

Of all five AtPEX11 proteins, AtPEX11D seemed to be the most interesting. The gene is highly expressed in all analysed tissues and over-expression did not only lead to the formation of (PX) clusters, but also induced aberrant membrane structures (AMS) tagged by the YFP fusion protein (Figure 15). Also in infiltrated epidermal cells the protein appeared readily in association with endoplasmic reticulum (ER)-like structures. To further analyse its subcellular distribution, we infiltrated *N. benthamiana* leaves expressing a GFP version tagging the endoplasmic reticulum (ER-GFP-KDL, line 16c; Ruiz et al. 1998) with agrobacteria harbouring the mCherry-PTS1



construct. This allowed us to evaluate the appearance of the ER mesh and the relative localization and appearance of PX under wild-type conditions.

The microscopic images indicate that the ER appears normal as a cortical net and that PX are well separated forming no clusters and they were often found in the proximity of the ER (Figure 15\_A). Most importantly the red and green fluorescent signals never overlapped and no aberrant ER-structure or clustering of PXs were observed. Note that PXs were often found adjacent to the chloroplast (CP) and that a weak red fluorescence mCherry-PTS1 signal also appeared in nuclei (N).

In contrast, after co-infiltration of mCherry-SKL (red) with YFP-PEX11D fusion constructs (green) in wild-type *N. benthamiana* leaves, peroxisomal clusters (PXC) (Figure 15\_B and 15\_C1) appeared together with aberrant membrane structures (AMS) (Figure 15\_C and 15\_C2). Noteworthy, the mCherry-PTS1 construct was not found to tag the AMS.

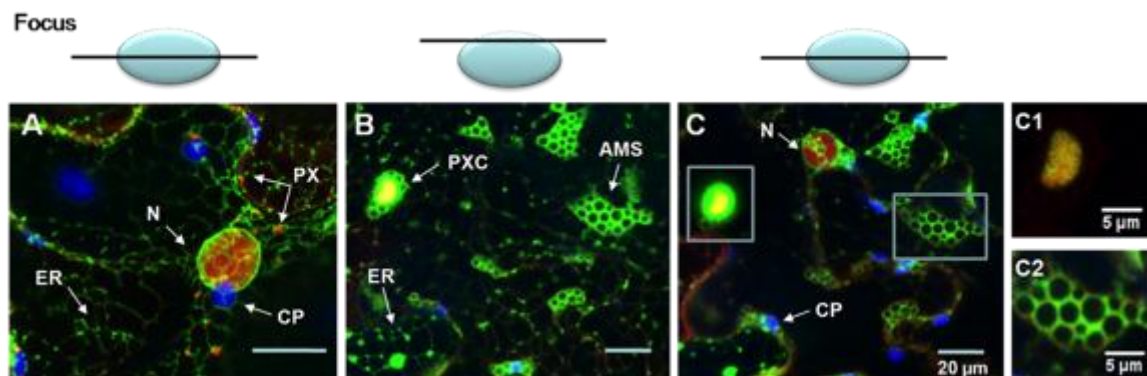


**Figure 15: ER-like and aberrant membrane structures appeared after over-expression of YFP-AtPEX11D.**

**A) Control:** transgenic *N. benthamiana* epidermal leaf cells expressing a green fluorescent endoplasmic reticulum (ER)-tag. 48h post infiltration the peroxisomal marker mCherry-SKL (red) and the ER-GFP marker are shown. Peroxisomes (PX) are small round shaped dots in the proximity to chloroplasts (CP) and the ER appeared normal as a cortical mesh and forms a netlike structure and encircles the nucleus (green). An mCherry-SKL signal was also found in the nucleus (N). **B) Co-expression of mCherry-SKL with 35S::YFP-AtPEX11D.** Aberrant membrane structures (AMS) could be detected and peroxisomal clusters are formed (PXC). Image taken at the surface of the epidermal leaf cell shows the presence of the YFP-AtPEX11D fusion protein at ER-like structures. **C) Image of same epidermal leaf cell taken at a focal plane through the interior of the cell.** Images: green channel: ER-GFP (A) or YFP-AtPEX11D (B and C). red channel: mCherry-SKL, blue channel: chloroplasts auto-fluorescence. Scale bar: 20 μm; 5 μm

However, beside its association to PX membranes the AtPEX11D fusion protein was also detected in association to these aberrant membrane structures (AMS). In addition we observed an YFP-AtPEX11D-tagged mesh structure resembling the cortical ER (Figure 15\_B and 16\_B).

To identify the origin of the AMS and whether AtPEX11D also associates to the ER, we co-infiltrated constructs expressing the YFP-AtPEX11D protein and an ER-RFP marker (ER-RFP) and evaluated their distribution pattern 48h *post* infiltration. As shown in Figure 16, the AMS appeared to be filled with ER-RFP marker protein.

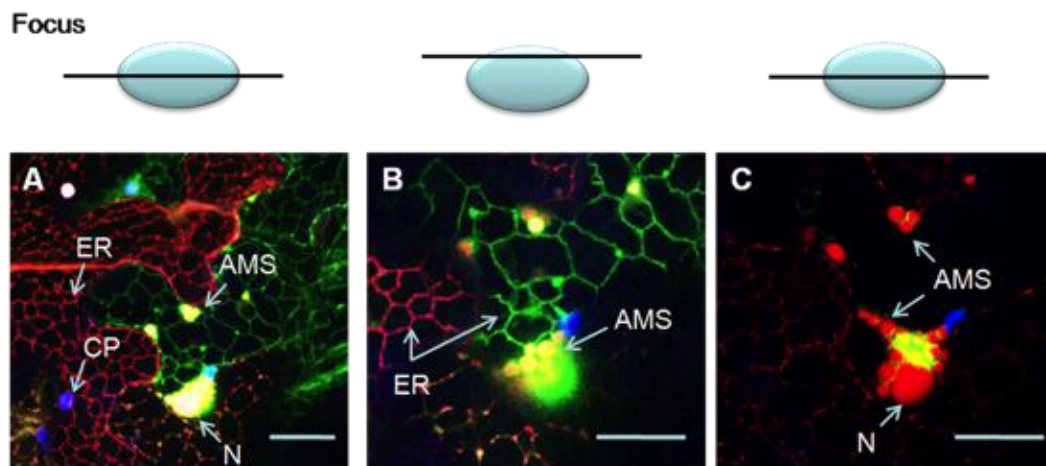


**Figure 16: ER-like structures and aberrant membrane structures appeared after over-expressing 35S::YFP-AtPEX11D in *N. benthamiana* epidermal leaf cells 48h *post* infiltration:** **A) Overviews of two epidermal leaf cells taken at the surface of the cells:** Co-infiltration of the ER-KDL-RFP marker (red) with the YFP-AtPEX11D fusion protein (green). Peroxisomes (PX) are not directly visible, only the peroxisomal membranes are tagged (green). The endoplasmatic reticulum (ER) is tagged in red and forms a netlike structure. Large aberrant membrane structures (AMS) are visible. **B) Crop Image of an aberrant membrane structure (AMS) taken at the surface of the cells:** In cells with a high AtPEX11D expression, no tagging of the ER with the AtPEX11D fusion protein is visible; instead the ER-RFP marker is trapped inside these aberrant membrane structures (AMS). **C) Crop Image of an aberrant membrane structure (AMS) taken at the interior of the cells:** Localisation of the ER-KDL marker in these structures visible, as well as a large cluster of peroxisomes embedded in the middle of the AMS structure. Images: green channel: YFP, red channel: ER-KDL-RFP, blue channel: *chloroplasts auto-fluorescence*. Scale bar: 20µm

A closer look at these AMS structures revealed a connection between the appearance of these AMS structures and a co-localization with an ER-RFP marker.

Like shown in Figure 17\_A, in cells, which did not show a high fluorescence of the YFP-AtPEX11D fusion protein, no AMS structure can be observed. In addition co-localization of the YFP-AtPRX11D fusion protein (Figure 17A\_green) with the ER-RFP marker (Figure 17A\_red) can be observed at mesh-like structures.

In Figure 17\_B, a cell is shown, containing a higher YFP-AtPEX11D expression as well as a few AMS structures. The ER-RFP marker is found to be entrapped inside of these AMS structures and therefore no netlike ER-structure is visible anymore with the ER-RFP marker (see arrows indicating no netlike ER-structures and the entrapped ER-RFP marker inside the AMS structures).



At the same time the YFP-PEX11D fusion proteins is still associated to a netlike ER structure (green, 17\_B arrow).

In Figure 17\_C, a cell was observed containing a large number of AMS structures filled with the ER-RFP marker. In contrast to Figure 17\_B the YFP-AtPEX11D fusion protein did not associate to ER-like structures anymore (Figure 17\_C, green) and a complete disintegration of the ER-netlike structures occurred. This indicates a correlation between the appearance of these AMS structures, and the tagging of ER-like structure by the YFP-AtPEX11D fusion protein.

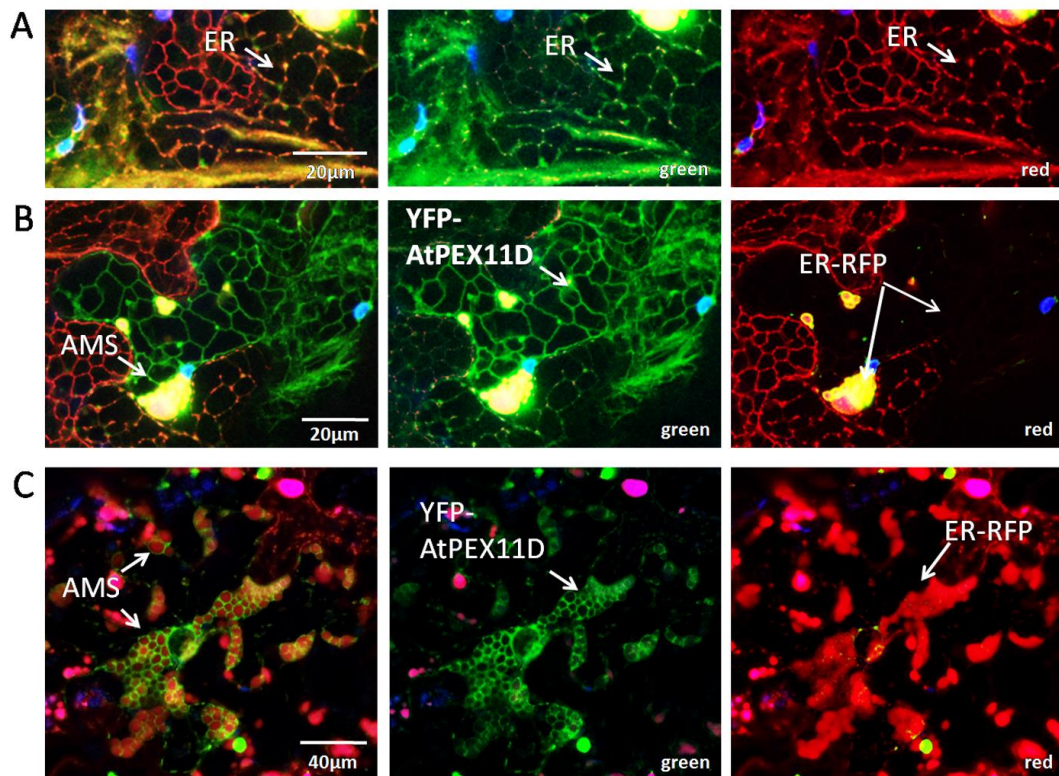


**Figure 17: ER-like structure and aberrant membrane structures appeared after over-expressing 35S::YFP-AtPEX11D in *N. benthamiana* epidermal leaf cells 48h post infiltration:** (A) Cells showing a co-localisation of the ER-like structure tagged with the YFP-AtPEX11D fusion protein and with the ER-RFP marker. No AMS structures visible. (B) The ER-like meshwork tagged with the YFP-AtPEX11D fusion protein starts to disintegrate and the ER-RFP marker is trapped inside the AMS structures. (C) Complete disintegration of the ER structure. The ER-RFP marker is trapped inside the AMS structures, filling a large cell area. No ER-like structures are associated with the YFP-AtPEX11D fusion protein anymore; instead the entrapped ER-RFP marker is surrounded by the YFP-AtPEX11D fusion protein. Images: green channel: YFP-AtPEX11D, red channel: ER-KDL-RFP, blue channel: chloroplasts auto-fluorescence. Scale bar: 20µm or 40µm.

In addition we evaluated, if the other PEX11 fusion proteins from yeast, plant and human also associate to the ER. Therefore, we had a closer look at the cell periphery of *N. benthamiana* epidermal leave cells, infiltrated with the different YFP-PEX11 fusion proteins together with the mCherry-SKL, 48h post infiltration. These experiments revealed, that nearly all the transiently over-expressed PEX11 fusion proteins, except for the two yeast fusion proteins ScPEX25 and

ScPEX27 as well as the HsPEX11 $\beta$  fusion protein, showed an association to an ER-like structure in green with the YFP-PEX11 fusion proteins (see Table 3).

Expressed protein	Average size of single PX ( $\mu\text{m}^2$ )	PX cluster formation	Average numbers of PX per cell	Aberrant membranous structures after 48h	Association to ER-like structures after 48h
AtPEX11A	0.90 $\pm 0.19$	+++	18 $\pm 1.09$	none	+
AtPEX11B	0.30 $\pm 0.07$	+++	58 $\pm 3.73$	none	+
AtPEX11C	0.33 $\pm 0.12$	+++	50 $\pm 3.29$	none	+
AtPEX11D	0.34 $\pm 0.09$	+++	52 $\pm 2.6$	+++	++
ScPEX11	0.48 $\pm 0.12$	++	23 $\pm 1.35$	none	+
ScPEX25	0.95 $\pm 0.01$	+	31 $\pm 1.35$	none	-
ScPEX27	0.95 $\pm$	+	74 $\pm 3.35$	none	-
HsPEX11 $\alpha$	0.67 $\pm 0.24$	++	29 $\pm 3.39$	none	+
HsPEX11 $\beta$ *	n/d	+	n/d	none	-
HsPEX11 $\gamma$	0.71 $\pm 0.27$	+++	59 $\pm 4.58$	+	+
mCherry-SKL	1.10 $\pm 0.01$	+/-	25 $\pm 0.66$	none	-

**Table 3: Summary of the transient overexpression studies and observed peroxisome effects of yeast, plant and human PEX11 fusion proteins in plant cells.** Cluster formation from no or low formation (+/-) to high amount of cluster formation (+++). \* data not determined n/d .

To confirm these data, co-infiltration studies with one of the yeast PEX11 fusion protein (ScPEX25) as well as with one human PEX11 fusion protein (HsPEX11 $\gamma$ ) were performed and analyzed 24h to 72h *post* infiltration. As a control (Figure 18\_A), transgenic *N. benthamiana* 16c leave tissues expressing the green ER marker protein (ER-GFP) were infiltrated with a red peroxisomal matrix protein PTS1 (mCherry-SKL).

This control experiment revealed the localization of the mCherry-SKL protein to small round shaped peroxisomes, whereas no association to the netlike ER structure or aberrant membrane structures (AMS) could be detected (Figure 18\_A). In addition, a newly constructed ER-RFP marker was infiltrated in these transgenic *N. benthamiana* 16c plants (Figure 18\_A) to confirm the appropriate localization of the ER-RFP marker, used for further analyses. As shown in Figure 18\_B the co-expression of the yeast ScPEX25 fusion protein with the ER-RFP marker did not lead to an detectable association of the ScPEX25 fusion protein (green) to the ER-structure (red),

whereas a co-localization of the human HsPEX11y fusion protein (green) with the ER-meshwork (red) was observed (Figure 18\_C).

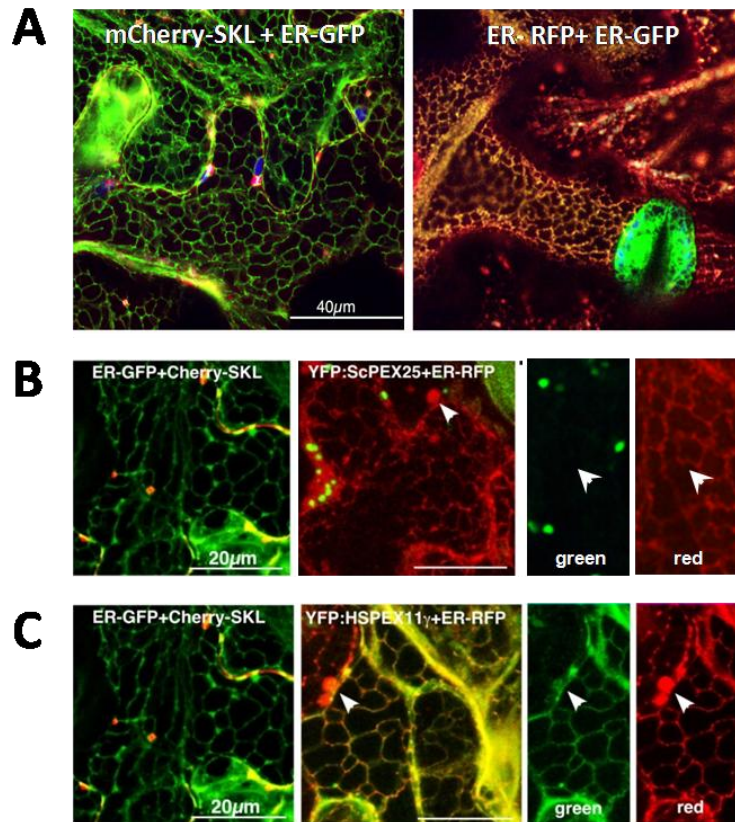


**Figure 18: Association of yeast and human PEX11 fusion proteins with the ER. (A) left: Control:** Co-expression of a peroxisomal matrix protein Cherry-SKL has been observed 72h *post* infiltration in transgenic *N. benthamiana* leaves (16C) carrying an ER-GFP marker. The ER appears as a typical meshwork at the cell periphery in green, whereas the mCherry-SkL marker localizes to small round shaped PX. No association of the mCherry-SKL marker to the ER can be observed. **(A) right:** In addition, co-localisation of a red ER-RFP marker with the green ER-GFP marker in transgenic 16C plants was shown. **(B)** No tagging of the ER netlike structure can be observed after over-expression of the yeast PEX11 fusion protein ScPEX25 in green, see arrow. **(C)** In contrast, the human HsPEX11y fusion protein (in green) associates to the ER meshwork (in red). Scale bar: 40µm and 20µm.

#### **B.4.1. Analysis of the dynamics of aberrant membrane and ER-like structures after over-expressing AtPEX11D**

To get a better insight into the formation of these aberrant membrane structures (AMS) as well as the observed ER-like structures we performed a timeline experiment and studied the dynamics and structure of the ER at three different time points (24h, 48h and 72 hours *post* infiltration). Co-infiltration experiments with the AtPEX11D fusion construct and an ER-RFP marker (*ER-RFP-KDL*) were performed as well as co-infiltration experiments with members of the yeast (*ScPEX25*) and human (*HsPEX11y*) *PEX11* gene family.

As a control *ER-RFP-KDL* was infiltrated alone and the ER-structures were analyzed over a time period of three days. No AMS were visible and no significant differences concerning the ER-structure could be observed (Figure 19\_a1-a3).

Twenty-four hours *post* infiltration of the AtPEX11D fusion protein together with an ER-RFP marker, a cortical netlike ER-structure was visible (red channel, Figure 19\_b1), whereas no sorting to the ER-like structures was observed of the YFP-AtPEX11D fusion protein (green channel). Peroxisomes already started to form small cluster and no aberrant membrane structures were visible.

The situation changed 48h *post* infiltration. In cells where the YFP-AtPEX11D was not expressed (Fig 19\_b2 left side) no AMS or ER-structures were observed with the ER-RFP marker, whereas cells expressing AtPEX11D (right side) showed a wide mashed pattern of an ER-like meshwork tagged by the YFP-AtPEX11D fusion protein. In these cells, no co-localization of the ER-RFP marker with the cortical netlike structure of the YFP-AtPEX11D could be observed. The ER-RFP marker got trapped inside the AMS (Figure 17\_B and Figure 19\_b2) and disintegration of the ER-structures occurred. Seventy-two hours *post* infiltration an even more sever disintegration of the ER structures (Figure 19-b3) could be observed.

The co-expression of the ER-RFP marker together with the human HsPEX11y led to a co-localization of the human YFP-HsPEX11y fusion proteins (green) with ER-RFP marker protein (red) 24 hours *post* infiltration, see Figure 19\_c1. PXs were small and round shaped and no aberrant membrane structures were observed. At 48 hours *post* infiltration PX were mainly located in small and large clusters, but still no aberrant membrane structures were visible. After 72h no association of the YFP-HsPEX11y fusion protein with the ER-RFP marker was observed and a sever disintegration of the ER could be detected (Figure 19\_c3).



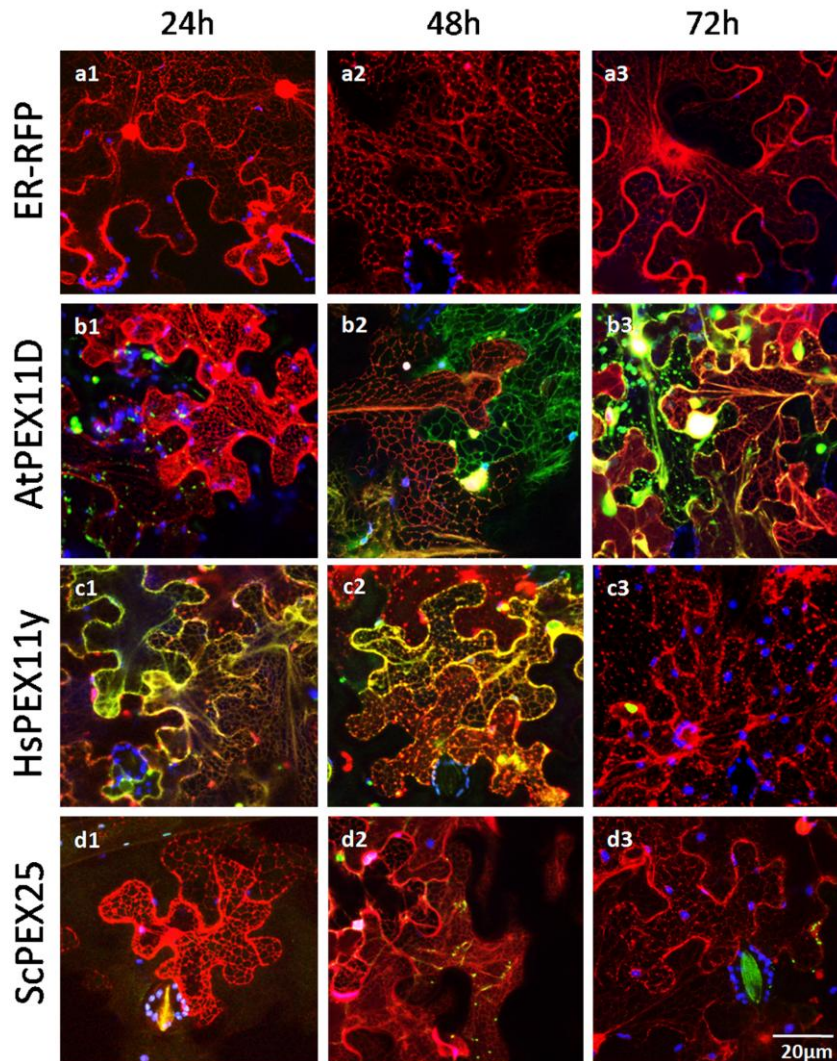


**Figure 19: Dynamics of ER-structure after over-expression of YFP-PEX11 family members in *N. benthamiana* 24h, 48h and 72h post infiltration. (a1-3) Control: ER-RFP-KDL: no aberrant membrane structures visible, ER-structure constant over 3 days. (b) Co-expression of YFP-AtPEX11D and ER-RFP marker. (b1) 24h post infiltration: netlike ER-structure visible with the ER-RFP marker, no tagging of ER-like structures with the YFP-AtPEX11D fusion protein, no aberrant membrane structures observed, normal peroxisomes as well as small clusters of peroxisomes. (b2) 48h post infiltration: ER-RFP marker associates to the ER in cells where the YFP-AtPEX11D is not highly expressed. In cells where the YFP-AtPEX11D gene is highly expressed ER-like structures are tagged by the YFP-AtPEX11D fusion protein, leading to a more wide meshed pattern of the ER. In addition the ER-RFP-KDL marker is trapped inside the aberrant membrane structures (AMS). (b3) 72h post infiltration: Disintegration of the ER-like structures tagged by the YFP-AtPEX11D fusion protein. ER-RFP marker trapped inside the AMS structures. (c1-3) Co-infiltration of human HsPEX11y with an ER-RFP-KDL marker: ER-RFP marker co-localized with the YFP HsPEX11y fusion protein already 24h post infiltration. The ER starts to disintegrate 48h to 72h post infiltration but no AMS appeared. (d1-3) Co-infiltration of yeast ScPEX25 with an ER-RFP-KDL marker: No AMS structures were detected throughout the whole experiments. In addition no association of the YFP-ScPEX25 fusion to the ER could be observed at any time point analysed. Images: green channel: YFP, red channel: ER-KDL-RFP, blue channel: chloroplasts auto-fluorescence. Scale bar: 20µm**

The over-expression of the yeast YFP-ScPEX25 fusion protein did not lead to the formation of large peroxisomal cluster or AMS (Figure 19\_d1-d3). No association of the YFP fusion protein to the ER structures was observed at any time point analyzed. (Figure19\_d).

### B.5. Analysis of transgenic *A. thaliana* lines expressing PEX11 fusion proteins

Transgenic *A. thaliana* lines expressing the various PEX11 proteins from yeast, human and plant under the control of the constitutive Cauliflower mosaic virus (CaMV) 35S promoter were established in the Col0 ecotype and analysed. All PEX11 proteins from yeast, human and plant were tagged with an N-terminal green fluorescence (YFP) marker.

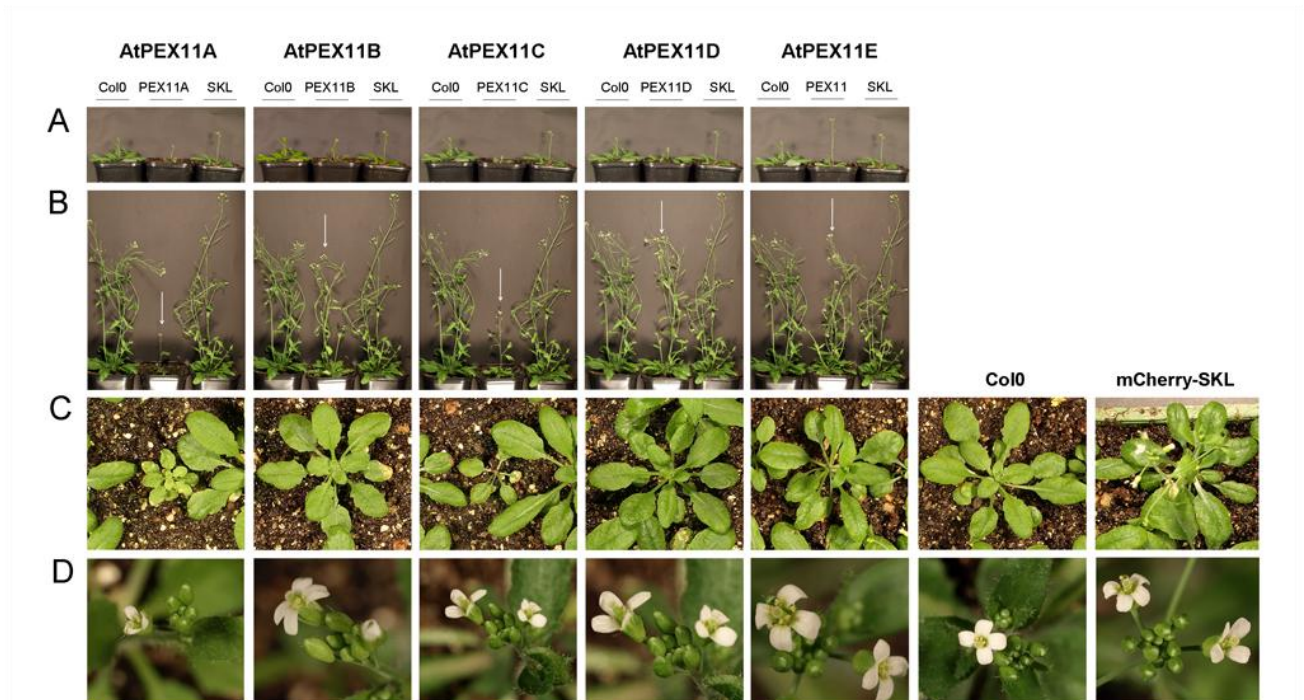
As a control, transgenic plants harbouring a peroxisomal red fluorescence mCherry marker (mCherry-SKL) expressed under the control of an estradiol inducible promoter (see methods) were analysed.

At least three transgenic lines were established and analyzed for each *AtPEX11* construct. Note that after several trials for the *AtPEX11A* construct only two independent stable transgenic lines could be established.

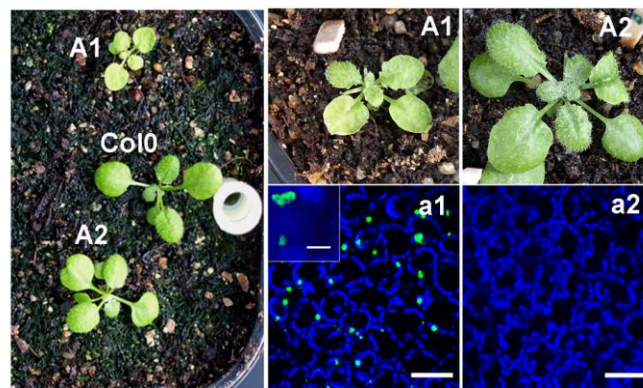
#### B.5.1. Over-expression of *AtPEX11A* lead to significant smaller plants with upward curved leafs

Figure 20 shows transgenic plants harbouring the five different *AtPEX11A-E* fusion proteins as well as control transgenic mCherry-SKL, at different developmental stages. Plants overexpressing *AtPEX11A* were significantly smaller compared to wild-type Col0 plants and the development of the inflorescence and flowers was delayed (Figure20\_C and 20\_D). Besides the significant reduction of size, a change in the morphology of rosette leafs could be observed. The leaves were curved upwards and in addition often bleaching of these leaves was observed (Figure20\_C and Figure21\_A1). Plants without an *AtPEX11A* expression resembled wild-type Col0 plants and did not show this phenotype (Figure21\_A2 and 21\_a2). No significant change concerning flower morphology was observed after overexpressing *AtPEX11A*. Plants overexpressing *AtPEX11C* showed a similar but less severe delay in leaf development as *AtPEX11A*. No changes in leaf shape or flower development of these plants could be observed. The over-expression of the

remaining three plant PEX11 proteins AtPEX11B, AtPEX11D and AtPEX11C did not lead to any significant phenotypical changes. They resemble Col0 plants as well as transgenic mCherry-SKL plants.



**Figure20: Phenotypal studies on transgenic *A. thaliana* plants overexpressing the plant AtPEX11 proteins at different developmental stages.**(A) Two weeks old plants.(B) 22days old plants.(C) Rosette(D) Flowers. Control plants: wild-type Col0 plants and transgenic mCherry-SKL expressing plants.



**Figure21: Phenotypal analysis of transgenic *AtPEX11A* plants.** (A1) Transgenic *YFP-AtPEX11A* plants are smaller with upwards curved leaves. (a1) CLSM image showing peroxisomal cluster formation in leaf tissue of the same plant. (A2) Transgenic *AtPEX11A* plants without expression are similar to Col0 wild type plants; (a2) no expression of the *YFP-AtPEX11A* protein is detected in this plant.



### B.5.2. Over expression of *ScPEX27* and *HsPEX11y* lead to a delayed plant growth

The over-expression of the yeast *ScPEX11* fusion protein as well as the human *HsPEX11y* fusion led to a delay in plant growth. The plants appeared to be smaller compared to the wild-type *Col0* plants or the transgenic mCherry-SKL plants at the same developmental stage like shown in Figure 22\_A to 22\_B. In addition the development of the inflorescence as well as flowering was delayed, but no morphological changes concerning leaf or flower structure were observed (Figure 22\_B and 22\_D). This could be observed in two independent transgenic lines overexpressing *ScPEX27* and *HsPEX11y*. The over-expression of the two remaining yeast *PEX11* homologues, *ScPEX11* and *ScPEX25* as well as the human *PEX11* orthologue *HsPEX11α*, did not have any significant effect on plant growth or plant morphology. Note that no transgenic plants overexpressing the human *HsPEX11β* were established and analyzed.

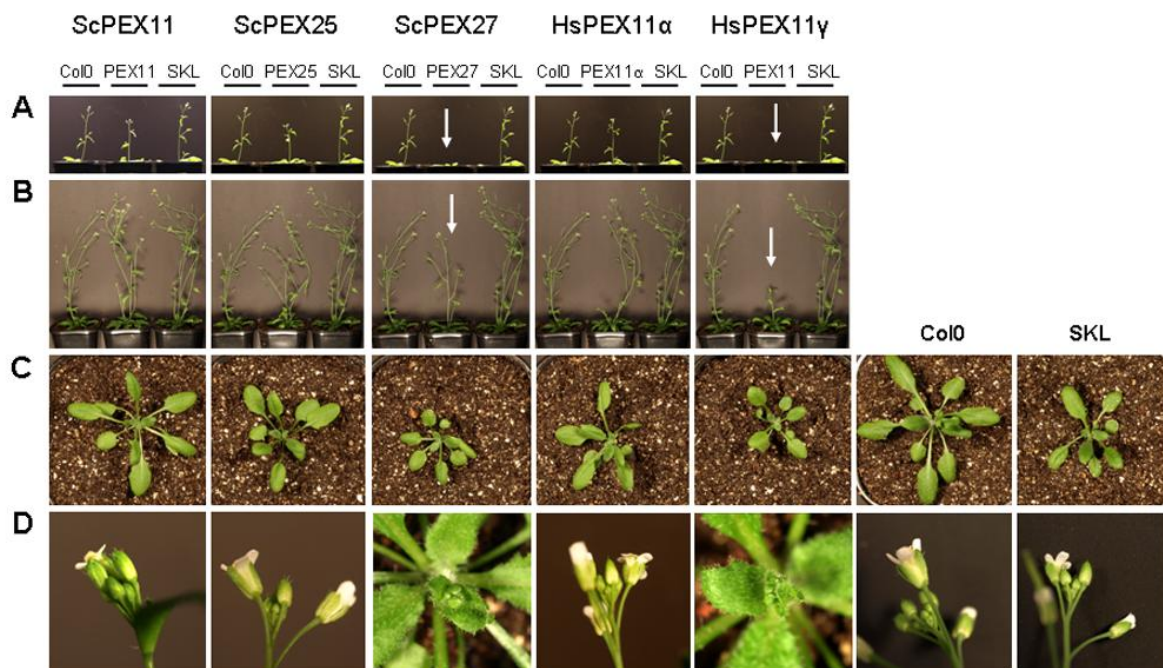


**Figure 22: Phenotypic analysis of transgenic *A. thaliana* plants expressing the yeast and human PEX11 proteins. (A)**Two weeks old plants. **(B)** 22days old plant **(C)** Rosette leaves **(D)** Flowers. *Control plants:* wild-type *Col0* plants and mCherry-SKL expressing plants.



### B.5.3. Distribution and effect of PEX11 fusion proteins on peroxisomes in *A. thaliana* plants

The control line harbouring the mCherry-SKL showed small, round shaped peroxisomes (PX) of approx. 1µm in diameter (Figure 23\_A), which were highly mobile and often found in proximity of chloroplasts. In contrast, the five *Arabidopsis* PEX11 fusion proteins sorted to the peroxisomal membrane and except YFP-AtPEX11B induced a shift towards formation of peroxisomal clusters (Figure 23\_B to F).

As shown in Figure 23, expression of the AtPEX11A, -C, -D and -E proteins led to the formation of more or less round shaped clusters in which the core area appeared devoid of the fusion proteins. The clusters were found to be closely associated to chloroplasts and often showed a slow movement. The only exception was AtPEX11B (Figure 23\_C). In this case the expressed YFP fusion was barely detectable and the PX appeared normal and well separated. Here no or few small clusters were detected which resembled the mCherry-SKL control shown in Figure 23\_A.

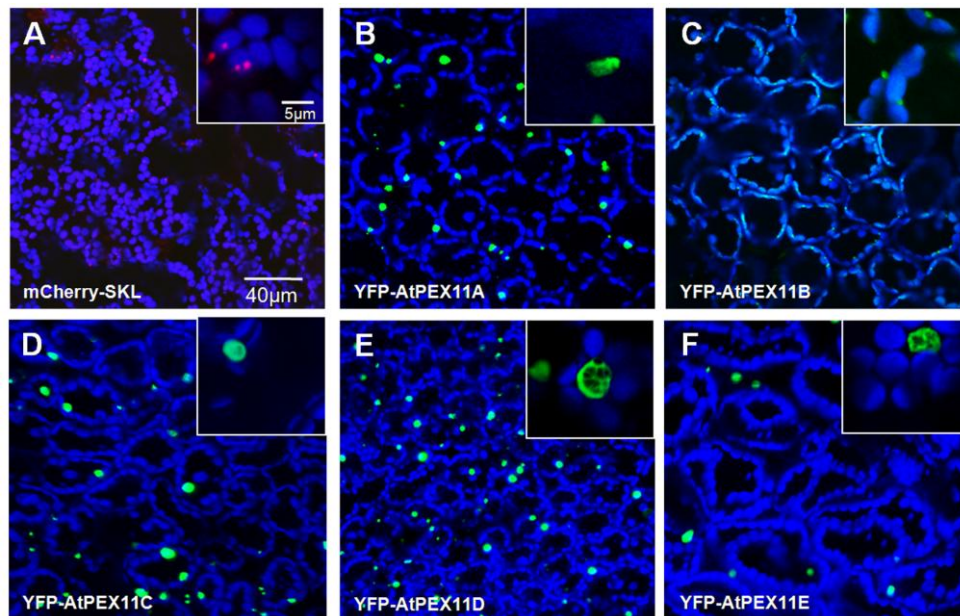


**Figure 23: CLSM images of epidermal leaf cells of transgenic *A. thaliana* plants expressing one of the five AtPEX11 YFP fusion proteins** (A) **Control:** Transgenic line expressing the mCherry-SKL construct tagging the PX. Here PX appeared normal as small, round shaped and highly mobile organelles. (B) **YFP-AtPEX11A transgenic:** Small and large PX clusters were detected and YFP- AtPEX11A was found at the PX membrane (see crop) and PX clusters. (C) **YFP-AtPEX11B transgenic:** PX appeared small and only a few small clusters were visible. (D-F) **YFP-AtPEX11D to -E transgenic:** Small and large peroxisomal clusters were visible. CLSM Images: green channel: YFP, red channel: mCherry-SKL, blue channel: chloroplasts auto-fluorescence. Scale bar: 40µm; 5µm.

To confirm that the observed cluster structures tagged with the various YFP-AtPEX11 fusion proteins are really PX, transgenic plants harbouring a YFP-PEX11 fusion protein together with a peroxisomal matrix protein (mCherry-SKL) were established and analysed for two of the five constructs: *AtPEX11A* and *AtPEX11D* (Figure 24 below). Therefore transgenic plants overexpressing YFP-AtPEX11A or YFP-AtPEX11D were transformed (see materials and methods) with the mCherry-SKL construct, and selected on growth medium via Basta (YFP-PEX11) and Hygromycin (mCherry-SKL) selection (see materials and methods).

In both cases the previously observed PX clusters (green) were now filled with the mCherry-SKL fusion protein (red) like shown in Figure 24 below.

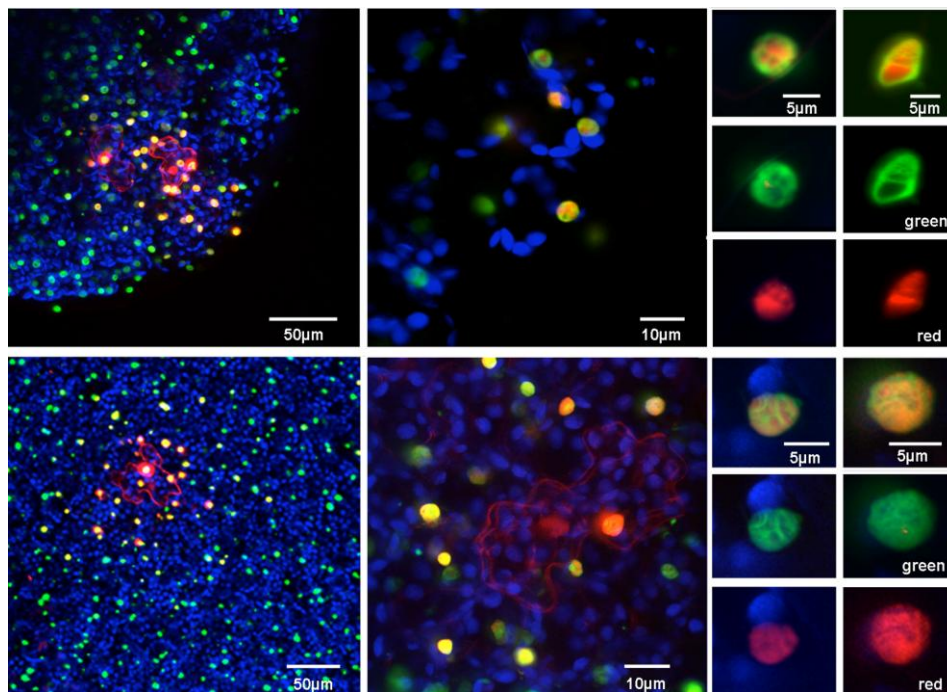


**Figure 24: CLSM images of epidermal leaf cells of transgenic *A. thaliana* plants expressing an YFP-AtPEX11 fusion protein together with the peroxisomal matrix targeting signal (mCherry-SKL)(A)** Transgenic plants overexpressing the YFP-AtPEX11A fusion protein together with the mCherry-SKL fusion protein. PX clusters can be observed in which the peroxisomal membrane is tagged by the YFP-AtPEX11A fusion protein (Crop: green), whereas the mCherry-SKL localises to the peroxisomal (Crop: red). **(B)** Transgenic plant overexpressing the YFP-ATPEX11D fusion protein together with mCherry-SKL. Again a localisation of the YFP-AtPEX11D fusion protein (Crop: green) to the peroxisomal membrane and the localisation of mCherry-SKL to the peroxisomal matrix (Crop: red). CLSM Images: green channel: YFP, red channel: mCherry-SKL, blue channel: chloroplasts auto-fluorescence. Scale bar: 50µm; 10µm and 5µm.

Besides the five *Arabidopsis* PEX11 fusion proteins, transgenic lines expressing the three yeast PEX11 homologues *ScPEX11*, *ScPEX25* and *ScPEX27* as well as two of the three human PEX11 orthologues, *HsPEX11α* and *HsPEX11γ*, were established and analysed. In these lines the tested

yeast and human YFP-PEX11 fusion proteins localised to the peroxisomal membrane. The ScPEX11 fusion proteins (Figure 25\_B) as well as the two human fusion proteins HsPEX11 $\alpha$  (Figure 25\_E) and HsPEX11 $\gamma$  (Figure 25\_F) led to the formation of PX clusters. The expression of the two yeast YFP-ScPEX25 and YFP-ScPEX27 constructs (Figure 25\_C and 25\_D) had no effect on the peroxisomal appearance and their distribution and size resembled that of the control (Figure 25\_A).

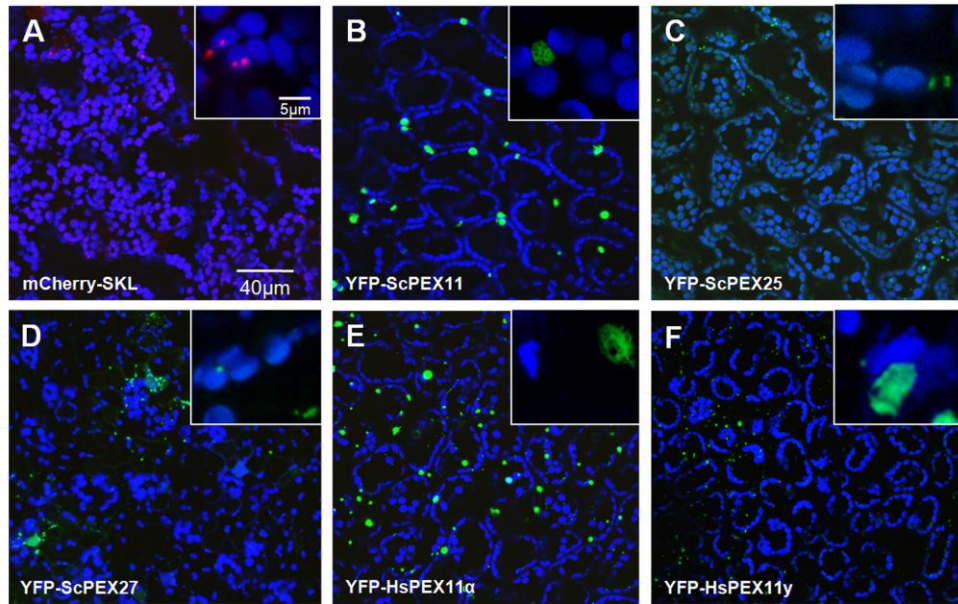


**Figure 25: CLSM images of epidermal leaf cells of transgenic *A. thaliana* plants expressing the various PEX11 proteins from yeast and human. (A) Control:** Transgenic line expressing the peroxisomal marker protein mCherry-SKL. Here PX appeared small, round shaped and highly mobile. **(B) YFP-ScPEX11:** PX cluster formation. **(C) YFP-ScPEX25:** small, well separated PX, only few and small clusters. **(D) YFP-ScPEX27:** same as ScPEX25. **(E) YFP-HsPEX11 $\alpha$ :** large PX cluster. **(F) YFP-HsPEX11 $\gamma$ :** PX cluster were visible. CLSM Images: green channel: YFP, red channel: mCherry-SKL, blue channel: chloroplasts auto-fluorescence. Scale bar: 40µm; 5µm.

In addition cryo-cuttings of different plant organs were performed, to determine whether cluster formation of PX was restricted to a specific plant organ. Here representative transgenic plants expressing YFP fusions of ScPEX11 (yeast), HsPEX11 $\gamma$  (human) or AtPEX11D (plant) were used to perform cryo-cuttings of a rosette leaf, a whole flower bud, an ovule and the anthers. As shown in Figure 26, in all three transgenic lines and all analysed plant organs PX clusters could be detected in all tested plant tissues. No expression from the 35S promoter was observed in the ovules of ScPEX11 and HsPEX11 $\gamma$ , whereas overexpression of AtPEX11D showed a few PX inside of the ovule. No expression from the 35S promoter was observed in the pollen for any of the



analysed plants. Summarized the confocal inspection of the tissues revealed that the PX clusters appear throughout the various plant organs and no organ specific differences could be observed.

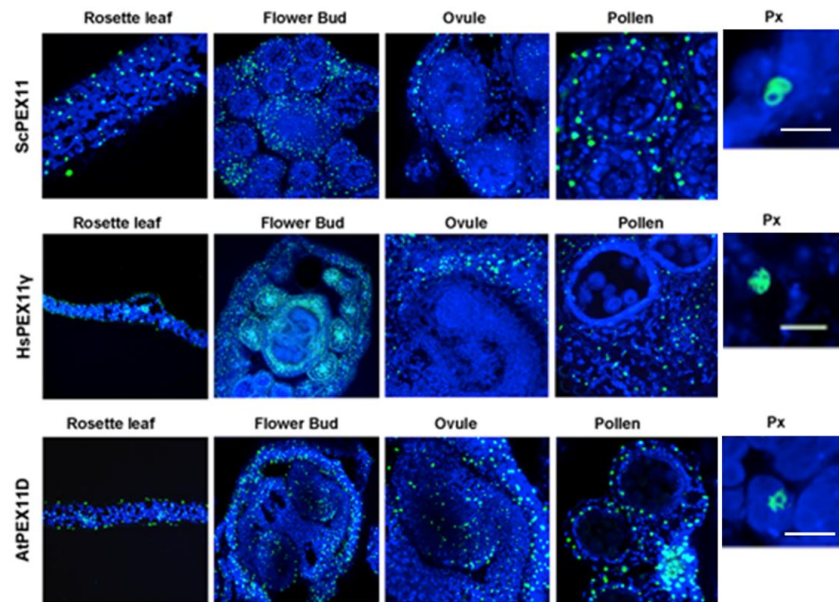


**Figure 26: CLSM images of cyro-cuttings through different plant organs of transgenic *A. thaliana* plants.** Analysed PEX11 proteins: YFP-ScPEX11, YFP-HsPEX11y and YFP-AtPEX11D. Analysed plant organs: rosette leaf, flower bud, ovule, pollen. Crop: Px. CLSM Images: green channel: YFP, blue channel: chloroplasts auto-fluorescence. Scale bar: 5µm.

### B.5.4. The effect of hormones and sucrose on the growth of *PEX11* transgenic seedlings

To analyse the effect of different hormone treatments as well as sucrose on the primary root growth, two independent transgenic *A. thaliana* lines expressing one of the five AtPEX11 fusion proteins (*AtPEX11A-E*) were grown on ½ MS medium. To test the effect of sucrose and/or hormones the medium was supplemented with 3% sucrose, in addition with methyl-jasmonate (10µM MJ), abscisic acid (1µM ABA), 1-Naphthaleneacetic acid (1µM NAA), or gibberellic acid (5µM GA). Their influence on growth was studied 7 days after germination under standard long day conditions (16h light/ 8h dark, 22°C). In addition, the growth effect of salt stress (100mM NaCl) was tested.

As shown in Figure 27\_A a significant defect in root elongation and a dwarf phenotype was observed for transgenic seedlings overexpressing *AtPEX11A*, *AtPEX11B* or *AtPEX11C*, whereas seedlings overexpressing *AtPEX11D* showed only a slight reduction of the root length compared

to wild-type Col0 plants. No significant difference in the root length of seedlings overexpressing *AtPEX11E* was observed compared to wild-type Col0 plants.

The addition of 3% sucrose into the growth medium led to an increase in the root length of transgenic seedlings overexpressing *AtPEX11A*, *AtPEX11B* or *AtPEX11C* (Figure 27\_B) compared to seedlings grown on medium without sucrose (Figure 27\_A). This suggests a partially rescue of the root elongation defect in transgenic lines expressing *AtPEX11A*, *AtPEX11B* or *AtPEX11C* fusion proteins observed on medium without sucrose. Seedlings overexpressing *AtPEX11D* did show a similar root growth as the control Col0 plants, whereas seedlings overexpressing YFP-*AtPEX11E* showed a slight increase in the primary root length compared to the control plants (Figure 27\_B).

The addition of 10 $\mu$ M methyljasmonate (MJ) into the growth medium ( $\frac{1}{2}$  MS medium with 3% sucrose) led to a rescue of the dwarf root phenotype observed for seedlings overexpressing *AtPEX11A* and *AtPEX11B* (compare Figure 27\_A, B and C), even though the root elongation of all plants, including the wild type plants are generally shorter. Seedlings overexpressing *AtPEX11C*, *AtPEX11D* or *AtPEX11E* did not show any significant differences in the root growth compared to plants grown on growth medium with 3% sucrose. For these plants the addition of MJ did not have any effect on root elongation, compared to plants grown on  $\frac{1}{2}$  MS medium with sucrose.

The supplementation of 1 $\mu$ M abscisic acid (ABA) into the growth medium led to an increase in the root length of seedlings overexpressing *AtPEX11A*, *AtPEX11D* or *AtPEX11E* compared to Col0 plants. Here ABA rescued the deficiency of the transgenic YFP-*AtPEX11A* line root growth observed on sucrose. In contrast, seedlings overexpressing *AtPEX11B* or *AtPEX11C* had a significant defect in root elongation and a dwarf phenotype similar to the situation observed for seedlings grown on  $\frac{1}{2}$  MS medium alone (Figure 27\_D and 27\_A).

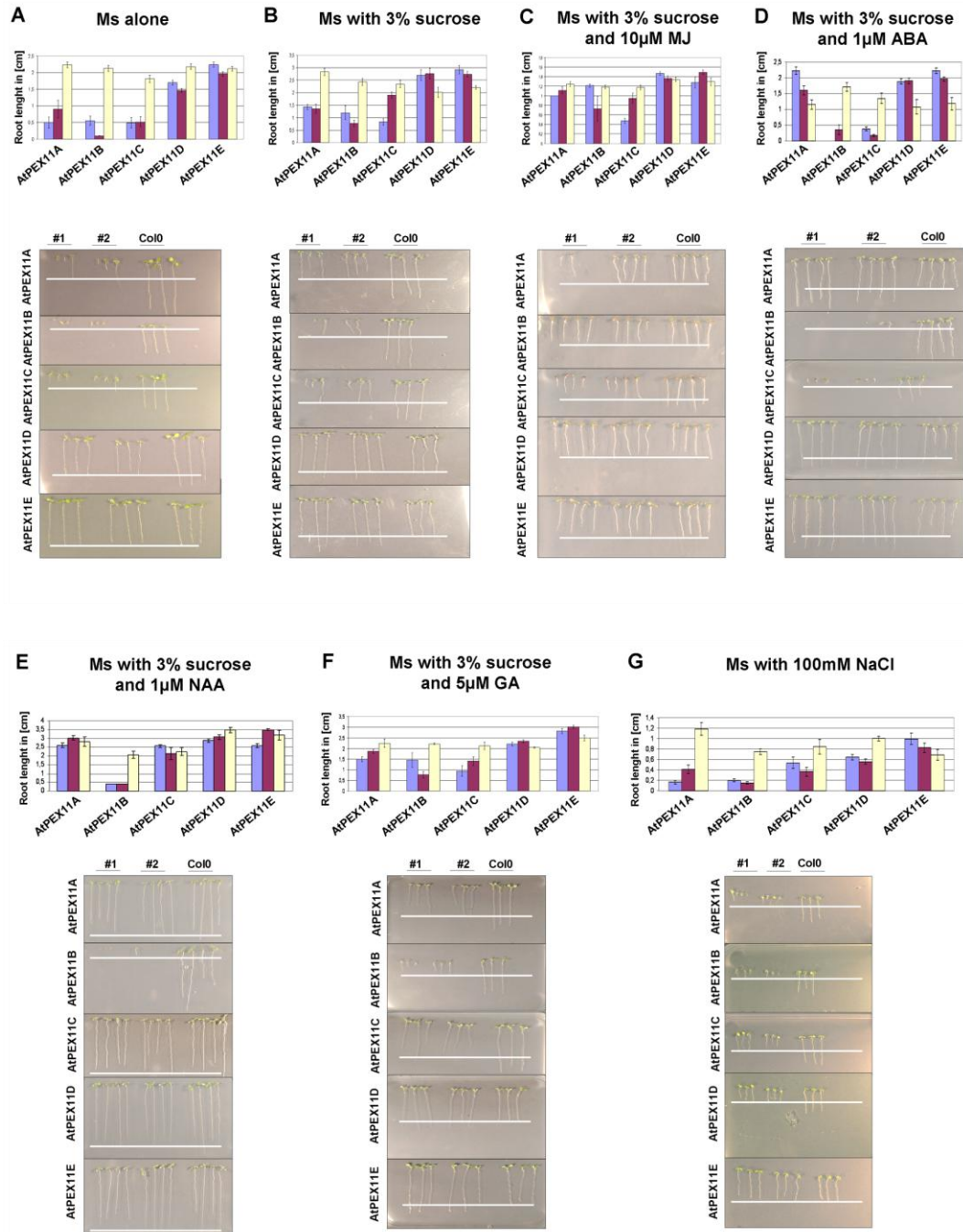


**Figure 27: Effects of sucrose and various hormone treatments on the root growth of transgenic *A. thaliana* plants overexpressing the different plant PEX11 fusion proteins.** T<sub>2</sub> progenies of these plants and wild type Col0 plants were grown for 7 days on ½ MS medium containing 0,5g MES, 4g Mourashige and Skoog medium with vitamins and 6g plant agar under normal light conditions (16h light/ 8h dark, 22°C). All plants were previously checked for their expression with a fluorescence microscope. **(A)** ½ MS medium without sucrose. **(B)** ½ MS medium with 3% sucrose. **(C)** ½ MS medium with 3% sucrose and 10μM MJ. **(D)** ½ MS medium with 3% sucrose and 1μM ABA. **(E)** ½ MS medium with 3% sucrose and 1μM NAA. **(F)** ½ MS medium with 3% sucrose and 5μM GA. **(G)** ½ MS medium with 100mM NaCl. n: two technical replica with 20 plants in total analysed.

The addition of 1-Naphthaleneacetic acid (NAA), a synthetic hormone of the auxin family, into the growth medium led to a rescue of the dwarf root phenotype observed for *AtPEX11A* and *AtPEX11C* on MS medium (Figure 27\_E). In contrast seedlings overexpressing YFP-*AtPEX11B* were either not able to germinate properly on medium supplemented with 1µM NAA (Figure 27\_E) or showed a strong reduction of growth suggesting hypersensitivity to auxin.

Again, the root growth of plants overexpressing *AtPEX11D* and *AtPEX11E* did not show any differences compared to Col0 plants.

Gibberelic acid (GA) was the last hormone analysed and showed a slight increase on root elongation for plants overexpressing *AtPEX11D* and *AtPEX11E* (Figure 27\_F). For seedlings overexpressing *AtPEX11A*, *AtPEX11B* and *AtPEX11C* the addition of 5µM GA did not lead to any positive or negative effect concerning root growth. These plants resembled the control situation on growth medium with 3% sucrose (compare Figure 27\_B and 27\_F), showing shorter roots compared to Col0 plants.

Finally I also analyzed the effect of salt stress (100mM NaCl) on root growth. In general, the addition of 100mM NaCl to the ½ MS medium (without sucrose) led to smaller plants. However, a slight negative effect on the root growth was observed for YFP-*AtPEX11D* transgenic plants (Figure 27\_G). YFP-*AtPEX11E* transgenic did not show any negative effect on root elongation compared to ½ MS medium.

Taken together, the most severe effects after the hormone treatment were shown for seedlings overexpressing *AtPEX11A*, *AtPEX11B* and *AtPEX11C* N-terminal YFP fusions. Seedlings overexpressing YFP-*AtPEX11A* showed a rescue of the dwarf phenotype after addition of 10µM MJ and 1µM NAA, and even a significant increase in root length was detected after supplementation of 1µM ABA. At the same time a rescue of the root phenotype of plants overexpressing YFP-*AtPEX11B* was only observed after the addition of 10µM MJ into the growth medium. The addition of MJ led to a partially rescue of the dwarf phenotype, whereas auxin led to a complete rescue of the phenotype. Plants overexpressing *AtPEX11C*, could be partially rescued with 10µM MeJA and completely after the addition of auxin, whereas ABA did not have any positive effects on root elongation.

GA and NaCl did not show a significant positive or negative effect on the root growth, for all overexpression lines analysed.

## B.6. Promoter activity of *AtPEX11D*

In contrast to the yeast and mammalian systems, nothing is known about factors regulating the expression of *AtPEX11* genes in plants. To get a better understanding of the dynamics of peroxisomes in living plants I studied the expression activity of one of the five endogenous *AtPEX11* genes. Therefore, an *in silico* analyses as well as a promoter activity study of the *A. thaliana* *PEX11D* under various conditions was performed.

*AtPEX11D* was chosen, due to its high endogenous expression impact on PX shape and number in transient assays and strong association to the ER (see chapter B3). According to the most recent available microarray data at [bar.utoronto.ca/](http://bar.utoronto.ca/) (status 2011), *AtPEX11D* is highly expressed in cotyledons, cauline, adult or senescent leaves as well as in sepals or water imbibed seeds (after 24h). Tissue specific expression of *AtPEX11D* was suggested to be in guard and mesophyll cells of leaves as well as in the lateral root cap and the procambium of roots. No expression was detected in the epidermis of the leaves and pollen. It was also predicted to be induced by heat stress, absisic acid (ABA) as well as light.

### B.6.1. *In silico* prediction of *AtPEX11D* promoter elements

According to our *in silico* analysis of the *AtPEX11D* promoter sequence (Figure 28) several regulatory motifs such as Y patches or regulatory elements (REG) might be present. Y patches are direction-sensitive plant corepromoter elements, appearing around the major transcription start sites (TSS). REGs are direction-insensitive elements that are preferentially found 100bp upstream of the TSS, containing many established cis-regulatory sequences (source: <http://www.ppdb.gene.nagoya-u.ac.jp>; Yamamoto and Obokata 2008). For the regulatory elements (REGs) an absisic acid responsive element and heat shock (stress) element were predicted.

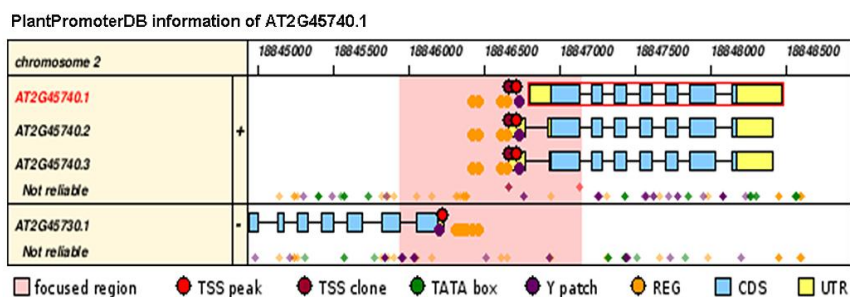


Figure 28: Predicted upstream promoter domains of *AtPEX11D* (AT2G45740) according to <http://ppdb.gene.nagoya-u.ac.jp> (Yamamoto and Obokata 2008).



### B.6.2. A minimal promoter region of 258bp is essential for the appropriate expression of *AtPEX11D*

To identify the essential promoter region driving the expression of the *AtPEX11D* five different deletion constructs (Figure30\_A) were generated and fused to a GUS/GFP reporter system (*AtPEX11Dprom::EGFP-GUS*; vector pKGWFS7), which allowed to follow the *in situ* expression by GUS staining. Based on the predicted regulatory motifs (Figure 28 and 29) the full-length upstream promoter of *AtPEX11D* (-732bp relative to the start codon) was divided into three different regions determined as region III (violet), region II (yellow) and region I (green) starting -151bp upstream of the UTR (-181 relative to the start codon; see sequence Figure 29). Five deletion constructs lacking one or two of these regions or part of them were established (Figure30\_A): **ΔII**: The complete region II of the *AtPEX11D* promoter, from -525bp to -409bp (relative to the UTR) was deleted. **ΔIa**: Part region I (first 129bp) was removed (-409bp to -280bp); **ΔIb**: The second part of region I was eliminated, (-280bp to -151bp); **ΔIa/ΔIb**: The complete region I has been deleted (-409bp to -151bp). **ΔIII/ΔII**: Both regions (III and II) were removed (-715bp to -409bp), here only region I remained intact.

Next transgenic plants harbouring the various promoter fragments were established and the tissue specific GUS expression, driven by the various deletion constructs was evaluated by GUS staining assays on seedlings (Figure 30\_B).

The full-length promoter drives expression of the GUS reporter (shown as blue staining) in cotyledons, young leaves, the hypocotyl and primary root in seedlings seven days after germination (Figure 30\_B1). A closer look at the deletion constructs revealed significant differences in their expression pattern compared to the full-length *AtPEX11D* promoter. A deletion of the complete region II led to a similar, but stronger expression pattern compared to the complete promoter region of *AtPEX11D* (Figure 30\_B2). The removal of the first 129bp of region I, defined as ΔIa, led to a significantly higher expression of the GUS reporter system in young leaves and primary roots.

```
Gaggatgatccaatgtggtgtacacagtacacataaaaagagtcaacatgatcaacggctagaatgaaagattg
aagagatgagtgcggtgacccaacgacgtgtttgtctgtttatcgggaaacgaagatgaccaaacgaagccctatctc
cgattacacacacaatcaaaagaagatcaagccaaaaacagaggcattgcgaatttaattgatcactctctctct
atctctgtcac acatctctcccaag (oligo) Gtatttcgaatcgaat

UTR
tcttttgattcttctatgattgtttacatttttcgtggtgtcttgatttttttgatcaaaactagtagaaattttccaatttctg
cctgcctgtgattagtagtagatatttgaatttgattagtaggtagaagaag(-1) ATG (+3)
```

**Figure 29: Sequence of the *ATPEX11D* promoter.** Yellow: upstream sequence used for the generation of the five deletion constructs; Grey: UTR; Bold: start codon.

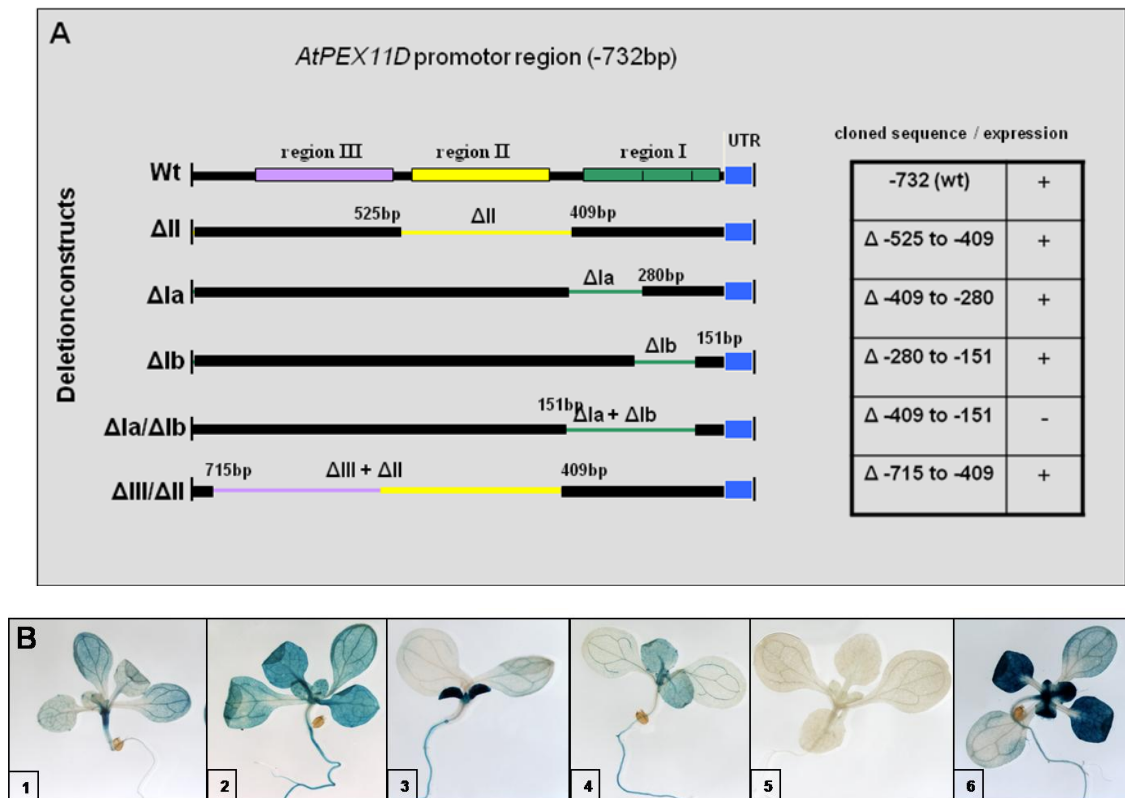


**Figure 30: Promoter study of *AtPEX11D*:** (A) Five different deletion constructs of the *AtPEX11D* promoter region (-732bp relative to the UTR as indicated in figure). Result of the GUS reporter analysis is shown on the right side. **Thin lines:** deleted promoter region, **thick black lines:** remaining promoter parts. (B) **Beta-glucuronidase (GUS) assay:** (1-6) 7 days old seedlings grown on MS medium with 3% sucrose under normal light conditions. (1) Full-length promoter drives expression of *AtPEX11D* in cotyledons, young leaves and primary root. (2)  $\Delta$ II: GUS expression pattern similar to that line with the full-length promoter. Note the stronger GUS signal. (3)  $\Delta$ Ia: very weak expression in cotyledons, very strong expression in young leaves, similar expression in primary root. (4)  $\Delta$ Ib: similar to full-length promoter. (5)  $\Delta$ Ia/ $\Delta$ Ib: no GUS expression at all. (6)  $\Delta$ III/ $\Delta$ II: expression in cotyledons, very strong expression in young leaves and primary root.

The deletion of the second part of region I, defined as  $\Delta$ Ib, showed a similar expression as the full-length promoter, except for a somewhat weaker expression in cotyledons (Figure 30\_B4).

No gene expression was observed after the deletion of the complete region I (30\_B5), indicating that this part of the promoter region is essential for an appropriate expression of the gene.

The complementary construct including only the region I( $\Delta$ III/ $\Delta$ II), referred to as minimal promoter, led to a significant increase in the expression of the GUS reporter system in young leaves compared to the full-length promoter region (Figure 30\_B6), which suggests that some negative regulatory sequences are existing upstream of region I.

By this means we identified a short DNA region of approximately 250bp (region I) necessary and sufficient for the expression activity, which was used in the following studies aiming to identify transcription factor(s) driving *AtPEX11D* expression (see chapter B.7.). The construct ( $\Delta$ III/ $\Delta$ II) will further be referred to as minimal promoter.

### B.6.3. The *AtPEX11D* promoter drives expression in a light cycle depended manner

Based on online microarray data from the eFP Browser at bar.utoronto.ca (Winter et. al. 2007 / Status 2011) a light cycle depended expression of the *AtPEX11D* (At2G45740) gene was proposed with the strongest expression between 8 and 12 hours after light exposure.

To confirm this data and to scrutinize the light exposure time necessary for the strongest gene expression, a time line experiment with the full-length promoter region of *AtPEX11D* was performed.

7 days old seedlings of transgenic *A. thaliana* plants were harvested after different times of light exposure (3h, 6h, 10h and 12h) and afterwards a GUS staining assay was performed. As shown in Figure 31 an increase in GUS expression was observed after 10h of light exposure. Especially in the cotyledons and the primary root and root tip a stronger expression of the GUS reporter system was detected compared to 3h of light exposure. No obvious differences were detected regarding the expression pattern and strength in young leaves. After 12h of light exposure a slight decrease in the strength of the GUS signal could be detected compared to 10h of light exposure.

Based on these results all following GUS expression experiments have been performed after 10h of light exposure to visualize possible differences between the constructs.

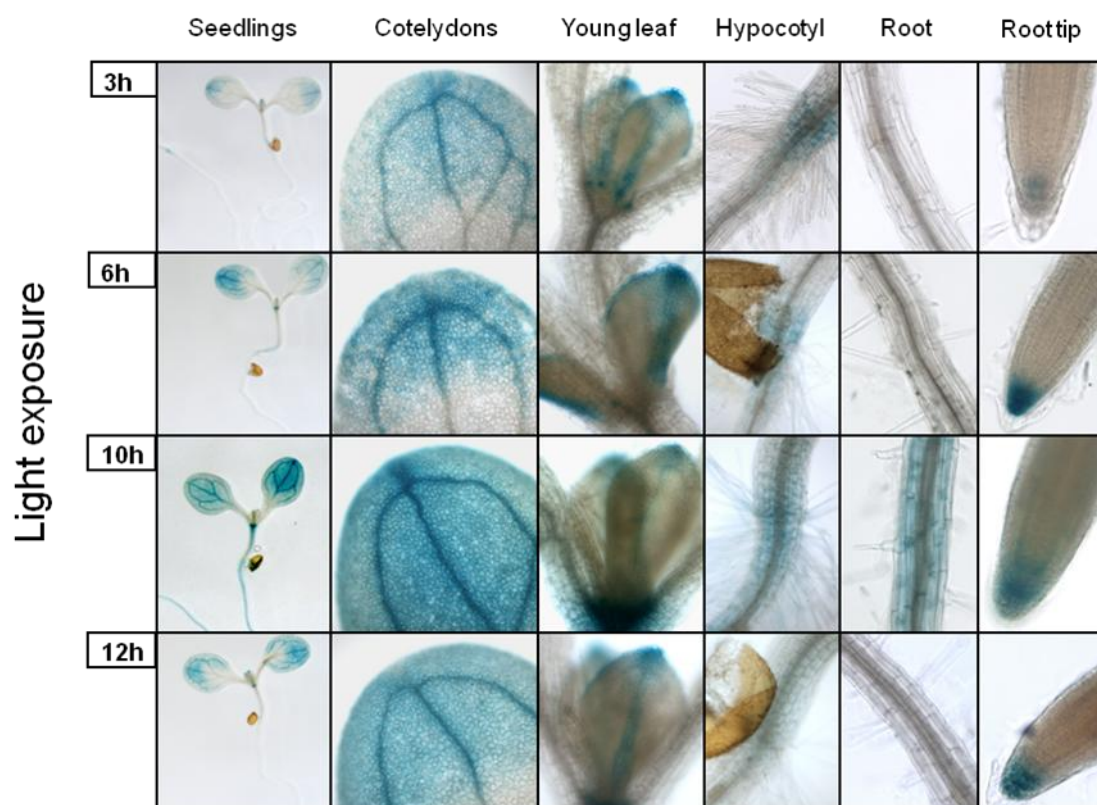


**Figure 31: Light exposure experiment on transgenic *A. thaliana* plants harbouring the full-length promoter of *AtPEX11D* driving a GUS reporter system.** 7days old seedlings were grown on ½ MS medium with 3% sucrose at 22°C and standard light conditions (16h light/ 8h dark). The GUS expression of these seedlings was analysed at 4 different light exposure time points (3h, 6h, 10h and 12h). Plant organs analysed: whole seedlings, cotyledons, young leaf, hypocotyls, root and root tip. Two independent *GUS::promoter* lines regulated by the full length region were analysed showing the same GUS expression: lines #4 and #6.

A shading experiment was performed to analyse the effect of light absence on the expression level driven by the *AtPEX11D* promoter. Unfortunately, the  $\beta$ -glucuronidase (GUS) assay of adult rosette leaves was not very informative due to a very patchy and irregular staining. For this fluorometric GUS measurement were performed using rosette leaves of adult transgenic plants with GUS under the control of the full-length and the minimal promoter. In addition the relative GUS activity regulated by the not active promoter of *AtPEX11D* ( $\Delta$ la/ $\Delta$ lb construct) as well as the general background activity of Col0 wild-type plants were evaluated.

As shown in Figure 32, a decrease in the GUS expression level of shaded plants compared to not-shaded plants was observed for minimal and full-length promoter constructs. Here the relative GUS activity of the not active promoter is barely above the background levels measured for the wild type Col0 plants. Also this experiment might suggest that shading has an effect on the

AtPEX11 full length and minimal promoter, this result has to be further confirmed due to only one technical replica with two independent measurements.

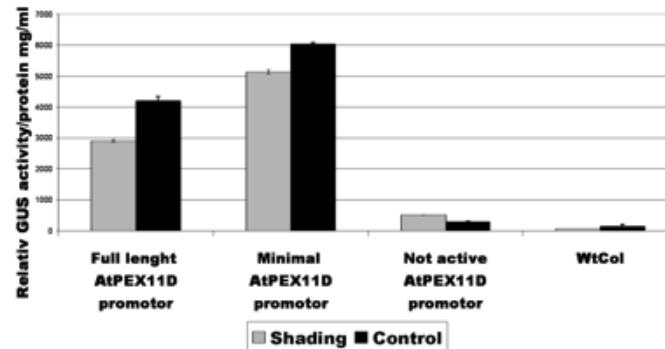


**Figure32: Fluorometric GUS measurements of plants after two days of shading.** Relative GUS activity decreases in plants after shading compared to plants exposed to long day light conditions (16h/8h). Decreased GUS activity can be observed with both full-length and minimal *AtPEX11D* promoter fragments. The measured GUS activity of the not active promoter fragment ( $\Delta 1a/\Delta 1b$ ) is similar the wild type. Gray bars: Shading, Black bars: Control, long day light exposure. Error bars: standard error of means; n=2 independent measurements of one biological replica.

### B.6.4. The minimal promoter is more active than the full-length promoter.

A more detailed analysis of the minimal promoter fragment (see chapter B.6.2 and Figure 30) revealed a significantly higher GUS expression in young leaves as well as a slightly higher expression in the primary root compared to the whole *AtPEX11D* promoter (Figure 33 below). However, no GUS expression was observed in the root tip of transgenic *A. thaliana* plants harbouring only the minimal promoter. In addition the GUS expression seems to be higher in the primary root in plants harbouring the minimal promoter region compared to plants regulated by the full length promoter. The cotyledons and the hypocotyl did not show significant difference between the whole and minimal promoter.

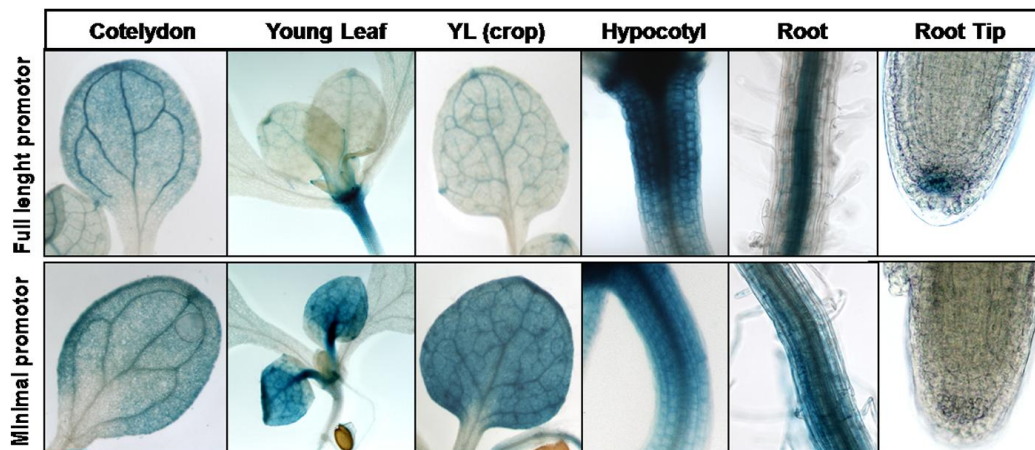


**Figure 33: Beta-glucuronidase (GUS) assay on transgenic plants. GUS under the control of the whole promoter of *AtPEX11D* versus the minimal promoter fragment.** All pictures were taken from 9 days old seedling grown on ½ MS medium with 3 % sucrose under normal light conditions. Following plant tissue were analysed in two independent plant lines for each GUS promoter construct: cotyledons, young leaf, young leaf crop, hypocotyls, primary root and root tip and inflorescence. Two independent *GUS::promoter* lines regulated by either the full length or the minimal promoter region were analysed showing the same GUS expression: Full length promoter (#4 and #6); minimal promoter (#5 and #6).

Regarding rosette leaves a slightly higher activity of rosette leaves in plants regulated by the minimal promoter region compared to the full length promoter can be observed (Figure 34 below). In addition, the GUS activity of the non-active promoter region ( $\Delta$ la/ $\Delta$ lb compare chapter B6.2) showed only a very slight activity compared to measured background activity of the GUS staining in wild type Col0 plants (Figure 34).

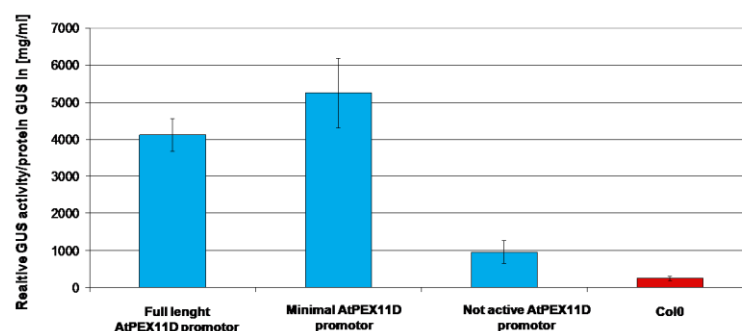


**Figure 34: Fluorometric GUS measurement of GUS activity in rosette leaves of transgenic plants regulated by the full length *AtPEX11D* promoter versus the minimal promoter fragment.** n: 2 independent replicas with 5 independent measurements in total.



Cross sections revealed also differences of GUS expression from the full-length or minimal *AtPEX11D* promoter, in addition to the results obtained for 9 days old seedlings grown on ½ Ms medium with sucrose (Figure 35).

The cross section through the stem showed a strong GUS staining of parenchyma cells as well as in the phloem (Figure 35) in plants regulated by the full length promoter of *AtPEX11D*. In contrast, no expression was detected in phloem cells of plants with GUS expression driven by the minimal promoter fragment and lower GUS staining in the parenchyma cells (Figure 35).

A cross section through a flower bud, showed a high expression in sepals, whereas only a very weak signal can be detected in the petals of the flower for both promoter constructs (Figure 35: Flower bud). A closer look at the carpel and ovules, revealed that the full length promoter drives a higher expression in ovules compared to the minimal promoter region (Figure 35: Carpel with ovule). In addition, a cross section through the primary root confirmed a stronger expression driven by the minimal promoter region compared to the expression observed in 9 days old seedlings regulated by the full-length promoter (Figure 35: root).

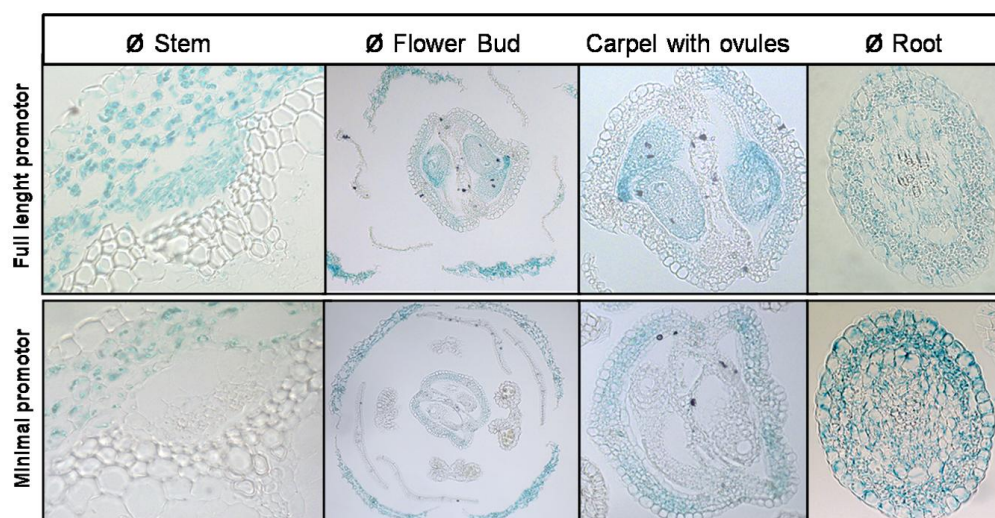


**Figure 35: Cuttings of paraffin embedded tissues from transgenic *A. thaliana* plants expressing GUS under the control of an intact or minimal promoter.** Tissues analysed: cross section through a stem, flower bud and through a primary root. Only one independent *GUS::promoter* line regulated by either the full length or the minimal promoter region was analysed: Full length promoter (#6); minimal promoter (#6).

### C.6.5. Heat shock did not alter expression from the *AtPEX11D* promoter

Based on online microarray data from AtGenExpress (Abiotic Stress by Kilian et. al., 2007, [bar.utoronto.ca/](http://bar.utoronto.ca/) Status 2011) a slight induction of *AtPEX11D* expression was predicted after a heat shock treatment: 18day old Col0 plants were stressed for 3h at 38°C, followed by a recovery at 25°C for 4 to 6 hours. Then a slight increase in the gene expression was detected in rosette leaves, indicated by arrows in Figure 36. In addition the *in silico* analysis of the *AtPEX11D* promoter predicted the localization of a heat shock (stress) element.

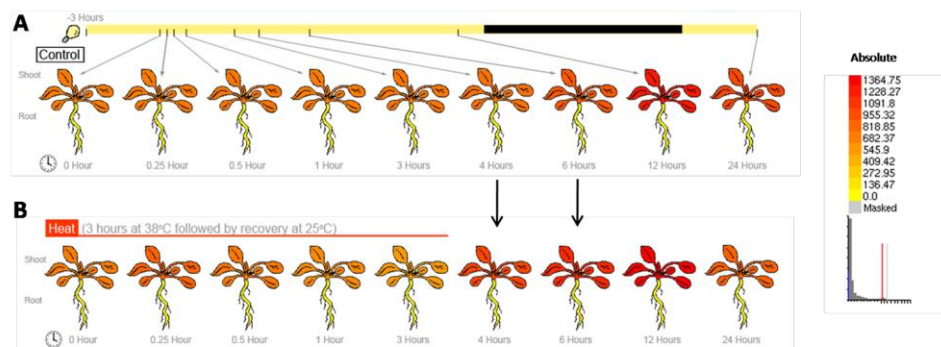


**Figure 36: Heat shock experiment of 18 day old *A. thaliana* Col0 plants analyzed for *AtPEX11D*mRNA levels (picture taken from eGFP Browser; [http://bar.utoronto.ca/efp\\_Arabidopsis/cgi-bin/efpWeb.cgi](http://bar.utoronto.ca/efp_Arabidopsis/cgi-bin/efpWeb.cgi)). As according to the online information the plants were grown under long day conditions (16h light/ 8h light) at 24°C and afterwards the RNA was isolated and hybridized to the ATH1 Gen Chip. (A) *Control*: plants grown under normal long day conditions at 24°C. (B) *Heat shock*: plants were stressed for 3hours at 38°C and afterwards recovered at 25°C (taken from eGFP Browser Stress series by Kilian et. al., 2007: [bar.utoronto.ca/](http://bar.utoronto.ca/) Status 2011).**

Therefore, a heat shock experiment with transgenic plants with GUS under the control of the complete *AtPEX11D* promoter or the minimal promoter fragment was performed. No significant differences between 9 days old seedlings exposed to 37°C for 4 hours compared to plants under control conditions (22°C) could be detected (Figure 37\_A). This was also the case for plants with GUS regulated by the minimal promoter region (Figure 37\_B).



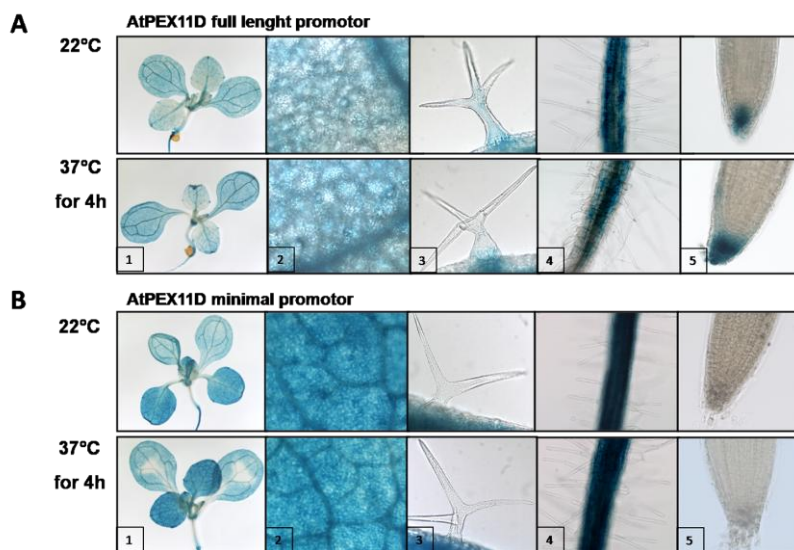


**Figure 37: Heat shock experiment on 9 days old transgenic *A. thaliana* plants with GUS under the control of the full-length or the minimal promoter of *AtPEX11D*.** Plants were grown under long day conditions (16h light/ 8h light) at 22°C on ½ MS medium with 3% sucrose. Plants were heat stressed at 37°C for 4h while control plants remained at 22°C. After a recovery of 4 hours a GUS staining assay was performed. **(A)** Seedlings with GUS regulated by the full-length promoter **(B)** Seedlings with GUS regulated by the minimal promoter. Plant material analyzed: **(1)** seedling, **(2)** young leaf, **(3)** trichome, **(4)** primary root and **(5)** root tip. Two independent *GUS::promoter* lines regulated by either the full length or the minimal promoter region were analysed showing the same GUS expression: Full length promoter (#4 and #6); minimal promoter (#5 and #6).

In addition, we noticed again a significantly higher expression of the GUS reporter in young leaves and the primary root, when it was regulated by the minimal promoter region (compare Figure 37\_A2, A4 to 37\_B2, B4). As before no GUS expression was detected in the root tip of plants regulated by the minimal promoter (Figure 37\_B5).

#### B.6.6. Auxin, methyljasmonate, absisic acid and tween induces the *AtPEX11D* promoter.

Based on our results concerning root development of transgenic *A. thaliana* plants overexpressing YFP-*AtPEX11D* as well as the predicted induction of expression after addition of absisic acid (ABA), a hormone assay was performed on the *AtPEX11D promoter::GUS* lines, to analyse the effect of various hormones on the promoter activity.

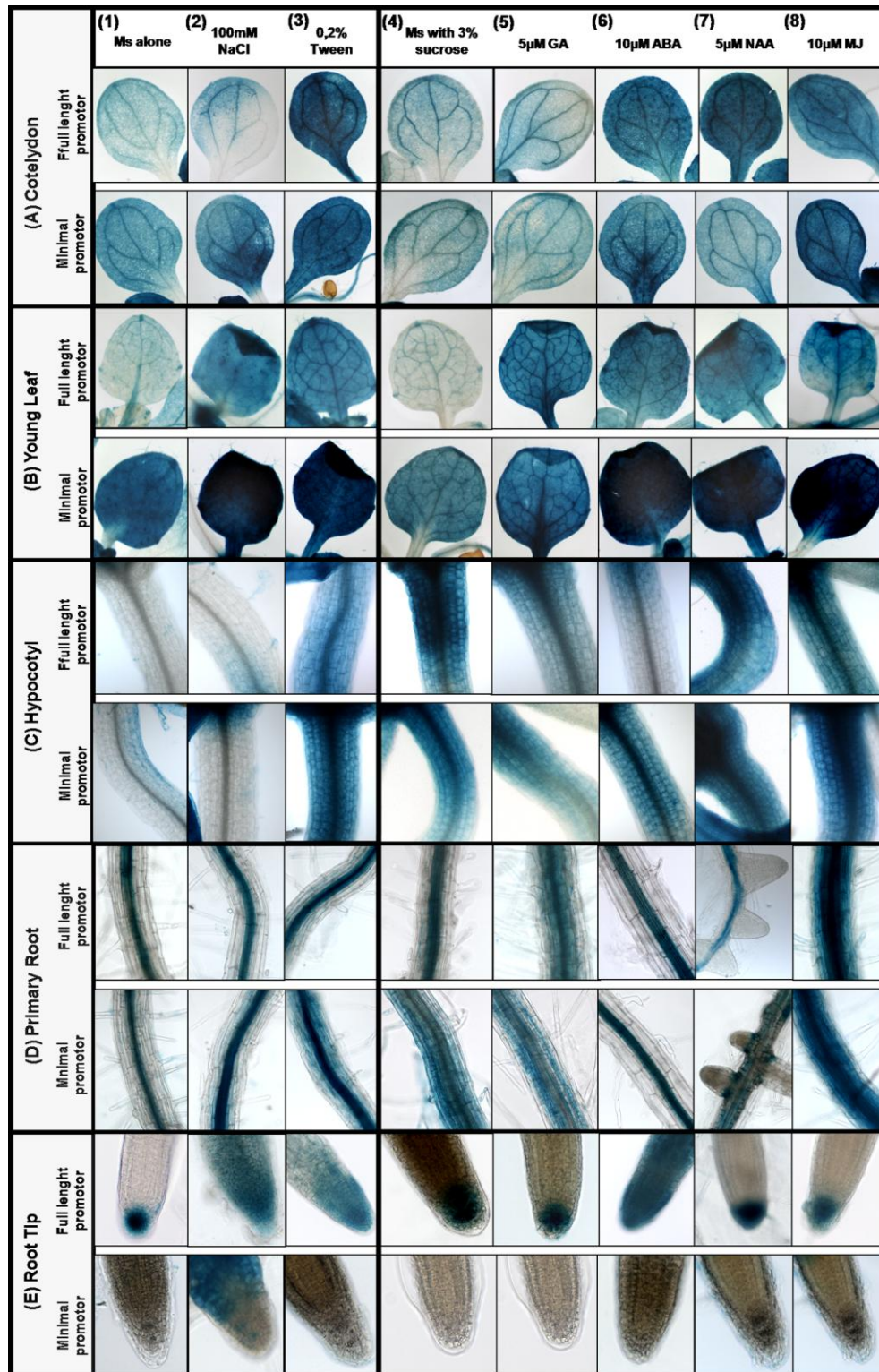


**Figure 38: Effect of various hormone treatments on the GUS expression regulated by the full length or minimal promoter region of *AtPEX11D* in transgenic *A. thaliana* plants.** Beta-glucuronidase (GUS) assay of 9 day old seedlings grown on different growth media under long day conditions at 22°C. **Plant material analysed:** (A) Cotyledons, (B) Young leaf, (C) Hypocotyl, (D) Primary root and (E) Root tip. **Growth medium:** (1) ½ MS alone (- sucrose), (2) 100mM NaCl, (3) 0,2% Tween, (4) ½ MS with 3% sucrose, (5-8) ½ MS with 3% sucrose supplemented with (6) 5μM gibberellic acid (GA), (7) 10μM abscisic acid (ABA) or (8) 10μM methyljasmonate (MJ). Two independent *GUS::promoter* lines regulated by either the full length or

the minimal promoter region were analysed showing the same GUS expression: Full length promoter (#4 and #6); minimal promoter (#5 and #6).

As shown in Figure 38 (A to C), an induction of the GUS reporter system after the addition of 0,2% Tween was observed in cotyledons, young leaves, the hypocotyl and the root tip in plants regulated by the whole *AtPEX11D* promoter. A similar result was observed for the minimal promoter.

In contrast, 100mM NaCl only led to a significantly higher GUS expression level in young leaves compared to plants grown on ½ MS alone, whereas no changes in the expression level were detected in the other plant organs like cotyledon or the hypocotyls (Figure 38\_A, C to E, lane 2).

The supplementation of GA, ABA, NAA and MJ into a ½ MS growth medium with 3% sucrose led to a higher GUS expression in young leaves compared to control plants (compare Figure 38\_B4 with 38\_B5 to B8). Both promoter fragments analysed showed the same effect. No changes in GUS expression were observed in cotyledons on growth medium containing 5µM GA (Figure 38\_A5), whereas all the other hormones (ABA, NAA and MJ) also induced GUS expression in cotyledons (Figure 38\_A6 to A8).

Only MJ led to significantly higher GUS expression levels in the primary root (compare Figure 38\_D4 with 38\_D8), whereas the other hormones (GA, ABA and NAA) mediated a similar expression like the control (see 38\_D4 to D7). A slight repression of the GUS signal was observed in the hypocotyl of plants grown on medium containing GA and NAA (Figure 38\_C5 and C6).

Again, no expression was detected in the root tips of plants with GUS regulated by the minimal promoter region, independent of hormone addition (Figure 36\_E4 to E8), whereas plants controlled by the whole promoter region showed a broader GUS expression in the root tip after the addition of GA (Figure 38\_E6).

A summary of visually quantified GUS expression levels under various hormone treatments and in diverse plant tissues is listed in Table 4 below.

**A: Gus expression regulated by the full length promotor**

Growth medium	Cotelydon	Leaf	Root	Root tip	Trichom	Hypocotyl
$\frac{1}{2}$ Ms – sucrose	++	+	+++	+++	+/-	+
100mM NaCl	++	++++	+++	++++	+++	+/-
0,2% Tween	+++++	++++	+++	+++	++	+++
$\frac{1}{2}$ MS + 3% sucrose	++	+	++	+++	+	+++
5 $\mu$ M GA	++	++++	+++	+++	+	+++
10 $\mu$ M ABA	++++	++++	+++	++++	n/d	+
5 $\mu$ M NAA	++++	++++	++++	+++	+++	+++
10 $\mu$ M MJ	++++	++++	+++++	+++	++	+++

**B: Gus expression regulated by the minimal promotor**

Growth medium	Cotelydon	Leaf	Root	Root tip	Trichom	Hypocotyl
$\frac{1}{2}$ Ms – sucrose	++	+++	+++	-	+	+
100mM NaCl	+++	+++++	+++	-	+	+/-
0,2% Tween	++++	++++	++++	-	+++	++++
$\frac{1}{2}$ MS + 3% sucrose	++	+++	++++	-	++	+++
5 $\mu$ M GA	++	+++	++++	-	++	+++
10 $\mu$ M ABA	++++	++++	++	-	+	+++
5 $\mu$ M NAA	++	++++	+++	-	+	+++
10 $\mu$ M MJ	+++++	+++++	+++++	-	+++	++++

**Table 4: Visual evaluation of GUS expression levels after a  $\beta$ -glucuronidase assay in 9 days old seedlings grown on different  $\frac{1}{2}$  MS media with additional hormones. (A) GUS expression regulated by the full-length promoter region (B) GUS expression regulated by the minimal promoter region. Expression was quantified visually from no expression (-) to high (++) or very high expression (++++).**

## **B.7. Search for a potential transcription factor regulating *AtPEX11D***

In contrast to the yeast and mammalian systems nothing is known about transcription factors regulating *AtPEX11* gene expression in plants. Therefore a yeast one-hybrid screen was performed to screen for potential transcription factors binding to the *AtPEX11D* promoter and potentially regulating *AtPEX11D* expression.

### **B.7.1. A yeast one-hybrid screen identified the transcription factor SOL1 as a potential regulator of *AtPEX11D* expression**

In order to search for potential transcription factors regulating the expression of the *AtPEX11D* gene an appropriate yeast screen strain had to be established. For this the minimal promoter region ( $\Delta III/\Delta II$ ) identified in course of the GUS promoter studies of *AtPEX11D* (see chapter B.6.2.) was introduced into modified integrative yeast YIPlac204 vector (see materials and methods: D.2.1), which allows for screening of putative binding factors fused to the activation domain and inducing a yeast reporter allowing growth on minimal media lacking the essential amino acid histidine (SC-HIS medium). In addition the promoter region lacking transcriptional activity ( $\Delta Ia/\Delta Ib$ , see chapter B.6.2.) was introduced into the integrative original yeast YIPlac211 vector with a LacZ interaction marker, which allowed the screening for beta GAL activity (blue stain). The strains carrying these two markers (minimal promoter allowing growth on SC-HIS and deficient promoter driving beta GAL activity) were combined by mating, resulting in a strain carrying both reporter systems, and was named screen strain 8.1. Interaction partners of the minimal promoter could then be identified by -His selection, whereas false positives could be identified and excluded by the additional LacZ (blue stain) reporter.

A high efficiency yeast transformation of the screen strain 8.1 was performed with two different cDNA libraries (see materials and methods D.2.1) and then selected on a SC-Ura, -Leu, -Trp, -His with 3mM ATZ medium used to counteract the basic minimal promoter activity. Of the originally 786 obtained clones for the library A, only 91 clones show consistent growth on the drop out medium (SC-Ura, -Leu, -Trp, -His + 3mM ATZ) after re-plating. In contrast, 356 clones were originally obtained after transformation with library B, from which only 11 clones could be confirmed to be stable on the drop out medium. Based on PCR analysis clones resembling the empty cDNA library vector were excluded from further analysis. For the remaining 89 clones a filter lift beta-GAL (blue stain) assay was performed to exclude potential false positive activator



clones, which also activate the deficient promoter region. As shown in Figure 39, no false positive clones could be detected.

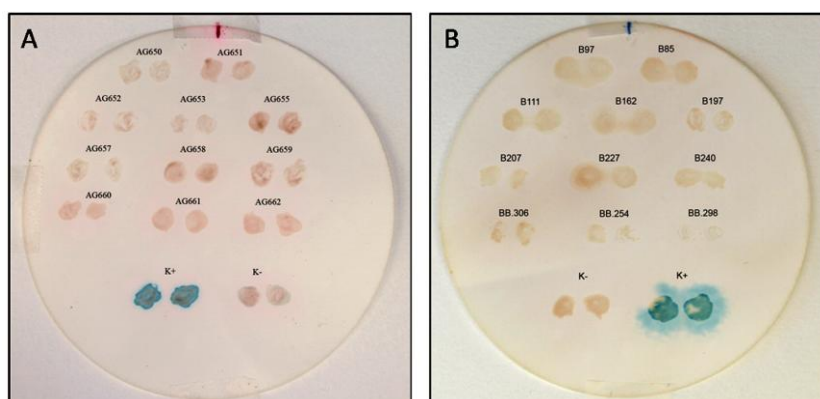


**Figure 39: Filter lift assay of yeast one hybrid clones were performed to exclude potential false positive activator clones. (A)** 11 exemplary clones of the library A together with a positive control (KNB1-KNAT) and negative control (empty pGAD10 vector) are shown. No blue staining (LacZ activity) can be detected for the potential interaction partners as well as the negative control. An intense blue signal (beta GAL activity) was detected for the positive control but not with the picked yeast colonies. **(B)** 11 clones of the library B were tested and also showed no staining.

Therefore all remaining 89 clones were sequenced and analysed further *in silico* (see supplementary table 4) for their potential to express a transcription factor. Based on this 23 potential candidates remained and were chosen for a re-transformation and re-evaluation in the screening strain 8.1. This revealed that only 7 of the 23 candidates again facilitate to grow on the selective HIS lacking medium supplemented with 3mM ATZ (Figure 40 and table 5).

ID	Results	ATG-number	His test	Liquid B-gal	Orientation	AD-fusion	ORF
B197	<i>Arabidopsis thaliana</i> leucine-rich repeat family protein mRNA, complete cds	AT2G17440	Grows	not sure	Forward	no AD fusion	1253-1578bp, only STOP missing at the end
A411	Tubulin9	AT4G20890	Grows	no	Forward	AD fusion	ORF, 910bp until STOP
A547	TCTP (translationally controlled tumor protein)	AT3G16640	Grows	no	Reverse	no AD fusion	ORF1: full lenght CDS of TCTP no ORF, Frame3
A600	F-box protein	At4G08098	Grows	no	Reverse	no AD fusion	704-870bp alignt with full lenght CDS no ORF, Frame 3
A685	transcription factor SOL1 (-TSO1-like)	At3G22760	Grows	yes, weak	Forward	no AD fusion	alignt with full lenght CDS from 293-1301bp
A691	4F5 protein-related, unknown protein	AT4G13615	Grows	yes, weak	Forward	AD fusion	ORF until Stop 291bp, full lenght protein from database 366bp

**Table 5: Summary of the 6 most interesting candidates based on data from the His assay and sequencing data. His assay:** Re-trafo of the candidates into the screen strain 8.1 and growth on selection medium (SC-

Ura-Leu-Trp-His + 3mM ATZ). **Liquid  $\beta$ -gal**: Transformation of candidates into delta 6/1 strain and further analysis of the activation of the LacZ reporter system driven by the minimal promoter. **Orientation**: orientation of the inserted fragment (candidate) in the pGAD10 vector. **AD-fusion**: are the candidates in an ORF with the promoter. **ORF**: open reading frame.

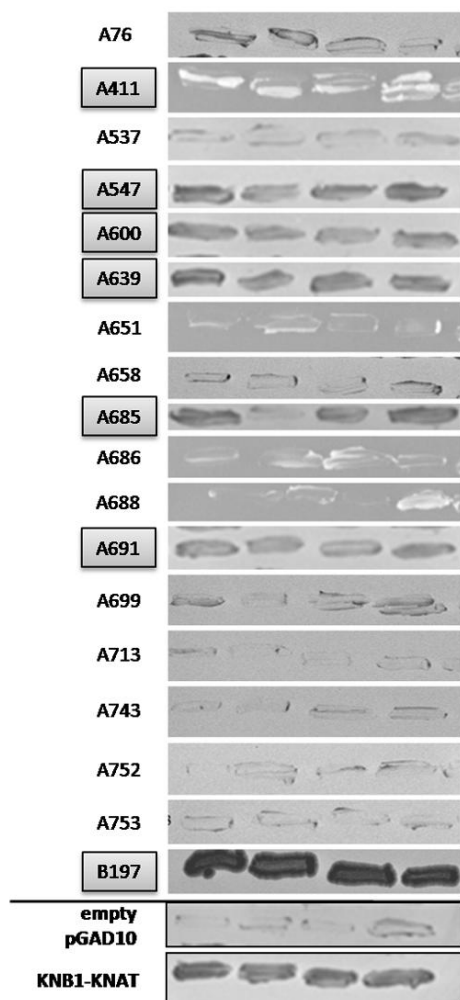


**Figure 40: -HIS growth assay of 18 potential candidates.** Four re-transformed screen strain colonies expressing each candidate construct were picked and tested on the SC-Ura, -Leu, -Trp, -His + 3mM ATZ for growth. Candidates with framed labels were able to grow on selective medium suggesting interaction of the expressed construct with the minimal promoter.

To confirm the 6 potential candidates, an integrative yeast Ylplac211 vector carrying the minimal promoter region driving LacZ expression was integrated into the YM4271 yeast strain referred to as delta 6/1 strain. A transformation of the candidates into this LacZ reporter delta6/1 strain allowed us to analyse the activation of the reporter in a different genomic context by the  $\beta$ -gal activity assay. As shown in Figure 41B, only two of the remaining six candidates, clones A685 and A691 (red box), showed a weak activation of the used *AtPEX11D* minimal promoter region. As a negative control, the same candidates were analysed with a liquid  $\beta$ -gal assay in the yeast screen strain 8.1, showing no induction of the LacZ reporter for negative selection and, thus, no unspecific activation of the promoter system.

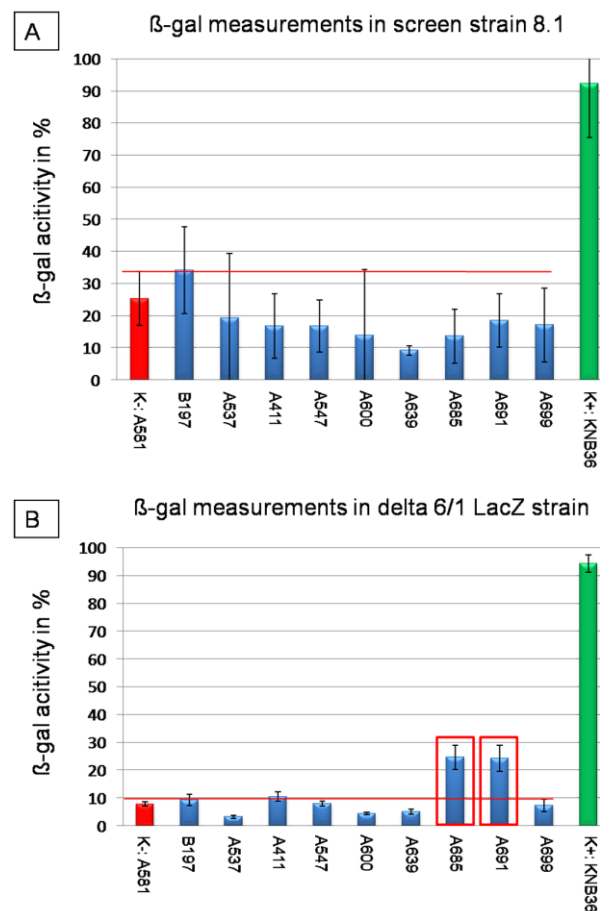


**Figure 41: Liquid β-gal assay of 6 potential candidates. The relative β-gal activity is stated in percentage (%).** **(A)** Control: Candidates transformed into the screen strain 8.1, in which interaction partners can be identified by His selection, whereas false positives can be identified and excluded by a not active promoter via the LacZ interaction marker. No activation of the deficient *AtPEX11D* promoter ( $\Delta I a/\Delta I b$ ) was observed, revealing no unspecific binding of the candidates to the minimal promoter region. **(B)** Candidates transformed into the delta 6/1 LacZ reporter strain, in which potential candidates can be identified via the LacZ marker by binding to the minimal promoter region. An activation of the minimal promoter region ( $\Delta I I I/\Delta I I$ ) was observed with two candidate factors, A685 and A691 (highlighted with a red box). This indicates that the two candidates are specifically binding to the minimal promoter region of *AtPEX11D*. n: two to three independent technical replicas with 5 to 8 independent biological measurements.

Based on the sequences and the results of the two reporter assays clone A685 was chosen as the most promising transcription factor candidate binding to the minimal promoter. The isolated clone harboured the full length cDNA sequence encoding the transcription factor SOL1 (TSO1-like; At3G22760).



## B.8. SOL1 expression increases the number of peroxisomes and the formation of small peroxisome clusters

To confirm that the identified putative transcription factor SOL1 is affecting *AtPEX11* expression and, thus, the number of peroxisomes (PX), SOL1 was cloned into a vector carrying an N-terminal YFP under the control of a strong 35S promoter (YFP-SOL1). Co-infiltration of constructs expressing YFP-SOL1 fusion proteins together with the peroxisomal matrix marker mCherry-SKL were analysed. In addition controls were performed by co-infiltration of constructs expressing a false positive 1 hybrid clone (YFP-TCTP) and a homeodomain transcription factor (YFP-KNAT1) to test whether the specific presence of SOL1 induced the formation of PX 96 h *post* infiltration due to its PEX11D promoter binding activity (Figure 42\_C and quantification results).

An obvious higher amount of PX/cell was observed in infiltrated *N. benthamiana* leaves, compared to plants infiltrated with the peroxisomal matrix protein alone (mCherry-SKL, Figure 42\_A) or YFP-TCTP or an YFP-KNAT1 fusion protein (provided by Daniela Fichtenbauer, Figure 42\_B). In addition, a SOL1 over-expression construct (in vector pEG100) without a tag (SOL1-no tag) was designed and compared to a KNB36-TAP tag control construct (provided by Daniela Fichtenbauer). This approach provided evidence that the observed cluster formation after SOL1 infiltration was not an effect of infiltration and expression of a protein or the YFP tag. As shown in Figure 42 the induction of small PX cluster formation as well as a significant increase in PX numbers per cell was observed only in the presence of a SOL1 construct compared to the control constructs (Figure 42: quantification).

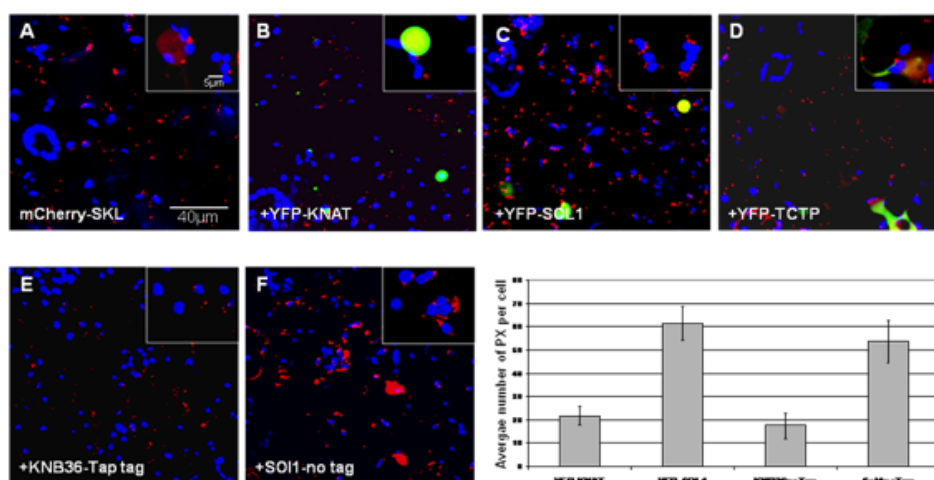


**Figure 42: Co-expression of a peroxisomal matrix protein, mCherry-SKL with a potential transcription factor SOL1 and different controls.** (A) mCherry-SKL control. (B) YFP-KNAT1 control. (C) YFP-SOL1. (D) YFP-TCTP constructs. (E) KNB36-TAP tag control. (F) SOL1-no tag. CLSM Images: green channel: YFP, red channel: mCherry-SKL, blue channel: chloroplasts auto-fluorescence. Scale bar: 40µm; 5µm;

Quantification: n = 6 independent images of two independent infiltration experiments (represent about 39 cells), Error bars: Standard Error of means.

### **B.9. SOL1 influences *AtPEX11D* promoter driven GUS expression**

Protoplasts from transgenic *A. thaliana* plants harbouring a GUS/GFP reporter system under the control of the full-length promoter region of *AtPEX11D* were isolated and transformed with the *YFP-SOL1* or the *YFP-KNAT1* control construct. Fluorometric GUS measurements showed that *YFP-SOL1* significantly increased the relative GUS activity regulated by the full-length promoter compared to the controls (Figure 43).

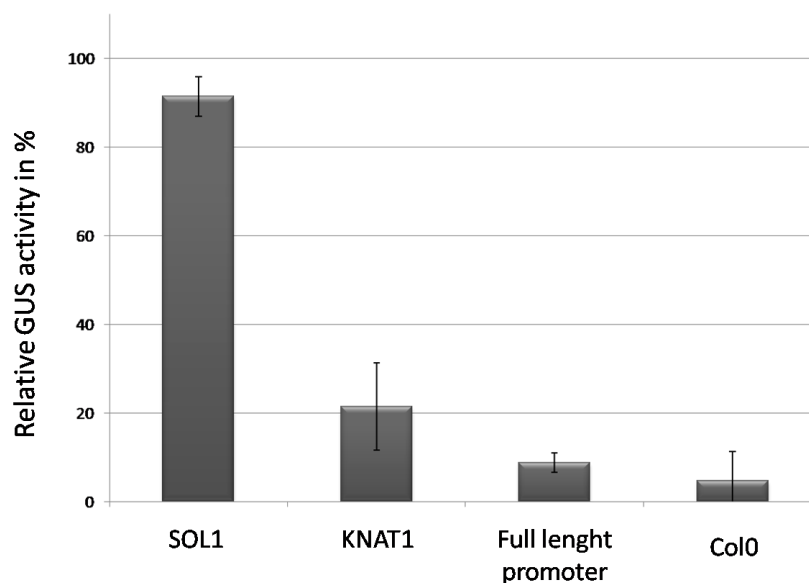


**Figure 43: Fluorometric GUS measurements of protoplasts transformation with an *YFP-SOL1* or control constructs. GUS expression is driven by the full-length promoter of *AtPEX11D*.**

After the transfection of isolated protoplasts with a *YFP-SOL1* construct a significant increase in the relative GUS activity in % compared to the controls was observed. Controls: transfection with *KNAT1*, background activity of full-length promoter alone and background activity of *ArabidopsisCol0*. n: two technical replica with 3 biological measurements for each one.

## C. Discussion

### C.1. PEX11 from the three kingdoms

Even though the metabolic pathways mediated by peroxisomes vary significantly between different eukaryotic organisms (Titorenko and Rachubinsky 2004) some general features concerning peroxisome biogenesis seem to be conserved throughout the kingdoms.

The *PEROXIN11* (*PEX11*) gene family, which encodes for peroxisomal membrane proteins involved in the proliferation of peroxisomes in yeast (Erdmann and Blobel 1995; Marshall et al. 1995) human (Schrader et al. 1998) and plant cells (Lingard and Trelase 2006; Orth et al. 2007), seems to be a conserved part of the cellular pathway building peroxisomes. A phylogenetic analysis of protein sequences of the *PEX11* family revealed a conserved amino acid region, which puts PEX11 proteins in a monophyletic group, in which the various PEX11 proteins can be divided into fungal (yeast), animal and plant subgroups (Orth et al. 2007). This suggests a single ancient *PEX11* gene, which evolved into the *PEX11* gene family and later on developed independently after the separation of these kingdoms (Orth et al. 2007, Nayidu et al. 2008).

Part of my work was based on the idea, that while some functions of the *PEX11* gen family members regulating peroxisome proliferation may have been conserved throughout evolution, others may be kingdom or species specific. Therefore, one main focus of my work was to evaluate the capacity of the different PEX11 proteins from human (HsPEX11 $\alpha$ , - $\beta$ , and - $\gamma$ ), plant *Arabidopsis thaliana* (AtPEX11A-E), and yeast *Saccharomyces cerevisiae* (ScPEX11, ScPEX25 and ScPEX27) to induce peroxisomal proliferation in plant cells.

PEX11 proteins from these different organisms were over-expressed either transiently by agro-infiltration in *N. benthamiana* or stable in *A. thaliana* transgenic lines. This approach allowed us to better understand the degree of evolutionary conservation of the PEX11 proteins and to deepen our knowledge concerning their function.

## C.2. Sorting of the PEX11-fusion proteins to the peroxisomal membrane is conserved throughout the three kingdoms

First the subcellular distribution of the five plant AtPEX11 fusion proteins has been analyzed in transient overexpression assays in epidermal leaf cells of *N. benthamiana*. For this the five different 35S::YFP-AtPEX11 fusion constructs have been co-expressed with the peroxisomal marker protein mCherry-SKL. The result of these studies suggested that each of the five plant AtPEX11 fusion proteins localizes to the peroxisomal membrane. This observation is in agreement with the AtPEX11 peroxisomal membrane association reported by Lingard and Trelease in 2006. In their study, myc-tagged versions of the different plant PEX11 proteins have been established and analyzed in cell suspension cultures. They observed that both the N- and C-termini of myc-tagged versions of AtPEX11B, -C, -D and -E proteins are facing the cytosol, whereas the N- and C-termini of AtPEX11A are facing opposite sides of the membrane (Lingard and Trelease 2006). All five plant PEX11 proteins remained attached to the peroxisomal membrane in the presence of harsh alkaline conditions (such as 0.1MNa<sub>2</sub>CO<sub>3</sub>). Under these conditions peripheral membrane proteins are normally released, indicating that all plant PEX11 proteins are integral membrane proteins (Fujiki et al. 1982).

Concerning PEX11 proteins found in other species, it was shown that in yeast and human cells the endogenous PEX11 proteins localize to the peroxisomal membrane. For example, Marshall et al. (1995) and Rottensteiner et al. (2003) reported the localization of the three yeast PEX11 proteins at peroxisomal membranes. The ScPEX11 (former name Pmp27) protein could be extracted from peroxisomal membranes by high pH, suggesting that the protein is a peripheral peroxisomal membrane protein (Marshall et al. 1995). Rottensteiner et al. (2003) characterized the two remaining yeast PEX11 proteins, ScEX25 and ScPEX27, which also were found in association with the peroxisomal membrane in yeast cells.

Studies on mammalian PEX11 proteins revealed, that the HsPEX11 $\alpha$  protein localizes to the peroxisomal membrane (Schrader et al. 1998). Localization to the peroxisomal membrane was also observed for EGFP-HsPEX11 $\alpha$  and EGFP-HsPEX11 $\beta$  fusion proteins in human HEK293T cells (Koch et al. 2010).

However, so far it was not analysed whether PEX11 proteins from organism such as yeast or human would be targeted to peroxisomal membranes in evolutionary distant cells such as plant cells. For this I performed transient expression experiments by agrobacterial transfection of leaves. Yeast or human YFP-PEX11 fusions were expressed and their intracellular distribution analyzed. All PEX11 fusion proteins from all three organisms (yeast, human and *Arabidopsis*)

localize to structures surrounding the peroxisomal matrix (see chapter B2. Figure 12). A cross-species study performed in co-operation with the laboratories of Andreas Hartig and Cecile Brocard (MFPL, University of Vienna) was conducted. The overexpression of yeast, human and plant EGFP-PEX11 fusion proteins in human embryonic kidney cells (HEK293T) revealed a similar result like observed for the expression of the YFP-PEX11 fusion proteins in epidermal leaf cells of *N. benthamiana*. All PEX11 fusion proteins from all three kingdoms were able to localize to peroxisomal membranes in human cells (Koch et al. 2010).

Based on the result, that all tested PEX11 fusion proteins are found in association to the peroxisomal membrane in plant cells as well as in human kidney cells, we suggest that the targeting of PEX11 proteins to peroxisomes is evolutionarily conserved.

### C.3. Overexpression of PEX11 proteins leads to peroxisome proliferation and cluster formation

In general it is thought that PEX11 proteins are key components of the peroxisome (PX) proliferation pathway and that their function in plants equals that of other organisms. By analyzing yeast cells lacking *ScPEX11* (*pex11Δ*) it has been shown that *ScPEX11* is a key player in the division and fission process during PX proliferation (Erdmann and Blobel, 1995; Marshall et al. 1995). These mutant cells contain only one or two large PX, and are unable to utilize oleate, whereas overexpression of *ScPEX11* results in a significant increase of the peroxisomal number per cell. In mouse and human cell cultures it was shown that the overexpression of *HsPEX11α* induces PX proliferation (Li and Gould, 2002) and Koch et al. (2010) found supporting evidence for a participation of the human PEX11 in the early steps of PX proliferation. However, to confirm this notion in plants and to evaluate the changes imposed by PEX11 proteins on PX number, size and shape, we performed a quantification study considering the size, number and average area of PX. We could show that in transient overexpression studies all yeast, human and plant PEX11 fusion proteins induces PX clustering and/or proliferation in various amounts in epidermal leaf cells of *N. benthamiana*. To exclude the possibility that the observed cluster formation of the PX was a byproduct of the dimerization activity of the used YFP-marker, we generated an AtPEX11D fusion protein without a tag under the control of the strong 35S promoter. As shown in chapter B.2. (Figure 12\_B6) cluster formation of PX, visualized with a peroxisomal matrix protein in red (mCherry-SKL), can be observed for the AtPEX11D protein. This test allowed us to confirm that the effects imposed by PEX11 on PX shape and numbers are independent of the YFP dimerization activity.

One interesting observation was that particularly strong changes on PX size and number were observed by the expression of the heterologous yeast ScPEX27 or the human HsPEX11y fusion proteins. Both PEX11 proteins induced a significant increase of PX number as well as area (chapter B.3.1., Figure 13). In contrast significant smaller PX were observed for nearly all plant PEX11 proteins after the ectopic expression of the fusion construct in epidermal leave cells. An exception was *AtPEX11B*, which did not induce any significant changes concerning the size of PX. Also the number of PX was increased due to expression of *AtPEX11B*, *AtPEX11C*, and *AtPEX11D*. The significance of the observed changes was confirmed by analyzing a high number of as well as by biometrical computer-assisted measurements (ImageJ) of the intracellular fluorescence distribution. Beside the changes in size and number of PX per cell a significant shift of all PEX11 fusion proteins towards the formation of peroxisomal clusters was observed.

Our data are at least to some degree inconsistent with published data. Lingrad and Trelase (2006) have observed in cell suspension cultures that *AtPEX11B* leads to PX aggregation without changes in PX abundance or length. In our experiments in different cell types suggest a significant increase in PX number induced by *AtPEX11B*. However, I could not detect elongation of PX as describe for *AtPEX11A*, *AtPEX11C* and *AtPEX11D* by Lingrad and Trelase (2006) in our transient expression studies. This discrepancy might be explained by the usage of different expression levels or use of cell systems. The authors used a cell suspension culture whereas we used a transient expression system (agro-infiltration) of epidermal leave cells of *N. benthamian* plants. In addition, Lingrad and Trelase (2006) expressed myc-tagged N-or C terminal *AtPEX11* proteins, whereas we used N-terminal tagged YFP-PEX11 fusion proteins.

To evaluate the effect of PEX11 proteins on PX appearance, we established stable transgenic *Arabidopsis thaliana* Col0 lines constitutively expressing the YFP fusion proteins driven by a 35S promoter. By this means we could confirm our results from the transient expression experiments, showing that all yeast, human and plant PEX11 fusion proteins associate to peroxisomal membranes in plant cells and induce the formation of peroxisomal clusters.

Our results are consistent with the observations reported by Orth et al. (2007) during the time I performed the studies. The authors show that all plant PEX11 fusion proteins (CFP-PEX11) localize to PX. In addition the Class I members *AtPEX11C*, *AtPEX11D* and *AtPEX11E* led to the formation of PX clusters and an increase of PX number, like shown in our own studies. Only in few cases elongation of PX could be observed in transgenic *A. thaliana* lines overexpressing *AtEX11A*, *AtPEX11B* and *AtPEX11D* in plants showing a weaker fluorescence.

However, in general we could confirm these published data and showed that the five plant PEX11 proteins are involved in the early steps of PX proliferation. We suggest that the observed peroxisomal cluster formation represent an incomplete fission and/or separation step in the process of PX proliferation due to a hyperproliferation of peroxisomes. This in turn, results in an imbalance in the proliferation machinery process, leading to insufficient separation and therefore to the formation of the observed cluster.

On a molecular level, members of two protein families might play a role in the observed cluster formation and reduced separation.

It is believed that in *Arabidopsis*, besides PEX11, two additional components are involved in the division and fission process of peroxisomes: a member of the dynamin-like protein (DRPs) family, DRP3A, and a member of the FISSION1 (FIS1) protein family, FIS1B.

A study by Lingard and Trelase in 2008 revealed evidence that all five *Arabidopsis* PEX11 homologs interact with the FIS1B, but not with FIS1A, both homologs to the yeast and mammalian FIS1 protein. FIS1 has been previously reported to anchor a dynamin-like protein DLP1 in mammals (Koch et al. 2003) or a dynamin-like protein VPS1 in yeast (Hoepfner et al. 2001) to the peroxisomal membrane, thereby leading to membrane fission in yeast and mammalian cells.

In *Arabidopsis*, two dynamin-related proteins, DRP3A and DRP3B, have been identified as playing a role in the fission process of peroxisome (Zhang and Hu 2009; reviewed in Kaur et al. 2009). A study by Lingard and Trelase (2008) suggested that PEX11 recruits FIS1B to the peroxisomal membrane, which in turn interacts with DRP3A, localizing it to the peroxisomal membrane and thereby initiating the fission step of PX replication in dividing *Arabidopsis* cell suspension culture. Zhang and Hu (2009) revealed evidence that not only DRP3A, but also DRP3B, as well as FIS1A are involved in the fission steps in PX and that PEX11 is not actually necessary for the recruitment of FIS1A or FIS1B to the peroxisomal membrane. They suggest that the different roles of FIS1A and FIS1B observed by Lingard and Trelase (2008) may be due to the analyses of FIS1 in cell-cycle-associated PX divisions in cell suspension culture, compared to PX division in *Arabidopsis* plants (Zhang and Hu 2009).

However, both studies showed the two protein families: FISSION1 (FIS1) and DYNAMIN-RELATED PROTEIN 3 (DRP3) are involved in PX division in *Arabidopsis* plants.

The observed cluster formation upon overexpression of the plant PEX11 fusion proteins could maybe lead to an inhibition of PX division due to the unattainability of PX localised in these

clusters and/or the saturation of the fission system by abundant PEX11 proteins. The endogenous produced FIS1 might be limited or unable to bind to the peroxisomal membrane and therefore also not recruit DRP3 to the membrane, which is necessary for an appropriate initiation of the fission step.

Since the over-expression of each one of the PEX11 family members from yeast, human and plant affected the PX appearance in human kidney cells (Koch et al. 2010) and in plant cells, they seem to be functional in both plant and human cells. This suggests that one or more common elements must exist in the PEX11-proteins of the three kingdoms.

To get a better insight into the functional conservation of the various PEX11 proteins, a functional complementation assay in the yeast *S. cerevisiae* was performed by Anja Huber, a member of our collaborating group of Andreas Hartig (MFPL, University of Vienna). Like shown in previous studies by Erdmann and Blobel (1995) yeast cells lacking PEX11 (*pex11Δ*) contain only a few large PX and lack the ability to utilize oleate as a carbon source. Therefore all eleven PEX11-proteins from yeast, human and plant have been expressed in *pex11Δ*-cells, and the consumption of oleate on agar-plates was analyzed as well as the number and size of PXs (Anja Huber et al.; manuscript submitted). Our collaborators could show that plant AtPEX11E can compensate for both defects (low number of PX as well as no utilization of oleat), whereas the human HsPEX11y and the plant AtPEX11A did not complement any of these defects. The remaining heterologous PEX11 proteins were able to compensate only one of the two defects of *pex11Δ* yeast cells (manuscript in preparation). In these assays AtPEX11B could only partially and AtPEX11C, -D, and -E could rescue the *pex11* oleat consumption deficit.

Similar assays were performed by Orth et al. (2007). Complementation assay of *S. cerevisiae pex11* null mutants with the five *Arabidopsis* PEX11 proteins, showed that *pex11* yeast transformants expressing AtPEX11C and AtPEX11E grew significantly better in liquid media supplemented with oleic acid compared to *Sc pex11* null mutants. At the same time immune electron-microscopy showed that the mutants contain a high percentage of enlarged and giant PX. This phenotype can be partially rescued upon expression of AtPEX11E, leading again to mainly small or only enlarged PX, similar to the situation observed in wild type cells (Orth et al. 2007). The remaining three plant PEX11 proteins AtPEX11A, AtPEX11B and AtPEX11D were not able to rescue the observed *pex11* phenotype (Orth et al. 2007).

A standard protein BLAST search, similar to the one performed by Orth et al. (2007), using the ScPEX11 protein (YOL147c) as a query showed that the *Arabidopsis* AtPEX11E homologue had



the highest similarity to ScPEX11 ( $E = 0.67$ ), followed by AtPEX11C ( $E=0.72$ ) and AtPEX11D ( $E=3.2$ ), whereas AtPEX11A and AtPEX11B, belonging to Class II seem to be to distantly related to be identified as similar. Also no high sequence similarities could be detected for any of the plant PEX11 proteins to the yeast ScPEX25 or ScPEX27 proteins, indicating a quite divergent sequence. This is in line with the strong clustering of PX upon expression of ScPEX11, as observed upon overexpression of the five plant PEX11 fusion proteins, while SCPEX25 and SCPEX27 overexpression causes less clustering.

The BLAST data together with the ability of AtPEX11C and especially AtPEX11E shown to rescue a *pex11* mutant phenotype by Orth et al. (2007) indicates that the plant PEX11 proteins C, D and E belonging to the Class I, could represent functional homologues of the yeast ScPEX11 protein. In addition this data indicate that the functionality of the plant PEX11 proteins may depend on the degree of sequence similarity, as AtPEX11E shows the highest rescue of the *pex11* mutant phenotype and the highest similarity to ScPEX11.

A correlation between a high sequence similarity and potential homologous function observed for the yeast ScPEX11 protein might also be found for the human PEX11 proteins. A default protein BLAST search with the human HsPEX11 $\alpha$  (NP\_003838), HsPEX11 $\beta$  (NP\_003837) and HsPEX11 $\gamma$  (NP\_542393) as a query was performed. The human HsPEX11 $\alpha$  showed only a relatively high similarity to AtPEX11B ( $E= 0.009$ ), whereas the other four seem to be too distantly related, to be identified as similar. In contrast, HsPEX11 $\beta$  showed high similarity to the plant Class II PEX11 proteins: AtPEX11A ( $E=0.012$ ) and AtPEX11B ( $E= 0.07$ ), whereas the plant Class I PEX11 proteins were more divergent AtPEX11D ( $E= 0.17$ ), AtPEX11E ( $E=1.2$ ) and AtPEX11C ( $E=2.4$ ). HsPEX11 $\gamma$  did not show any similarity to the plant PEX11 proteins.

This data suggest that the plant AtPEX11B is the most promising candidate for a functional homologue of the human protein HsPEX11 $\alpha$ , as it is the only one showing a significant sequence similarity. In addition, the Class II plant proteins AtPEX11A and AtPEX11B could represent a potential functional homologue to the human HsPEX11 $\beta$ , based on their higher sequence similarity compared to the Class I PEX11 proteins.

Despite low sequence similarities of HsPEX11 $\gamma$  to plant PEX11 proteins, this PEX11 member shows the most sever clustering among the three human PEX11 homologue in plants cells, but did not lead to a complementation of the the yeast *Sc pex11* mutant phenotype.

Our results taken together with the data available from our collaboration partners and the literature suggest that although the localisation to PX is conserved throughout the three kingdoms the individual PEX11 proteins may differ in their function.

### C.3.1. Overexpression of AtPEX11D led to a disintegration of ER membrane structures

An interesting aspect of our studies was the observation that some of the YFP-tagged PEX11 fusion proteins from all three kingdoms were found associated to a meshwork localized at the plant cell periphery. A closer look revealed that this netlike structure represent the endoplasmatic reticulum (ER). In transient over-expression assays nearly all PEX11 fusion proteins from all three organisms, except ScPEX25, ScPEX27 and HsPEX11 $\beta$  fusion proteins, were found in association with this ER-like structures.

Whereas the most PEX11 protein associated to the ER-like structures lead to a wide mashed ER pattern, only the overexpression of the AtPEX11D fusion protein led to the formation of aberrant ER membrane structures and induced a complete collapse of the ER already 48h *post* infiltration.

Recent studies suggest that some peroxisomal membrane proteins (PMPs group I) as well as ascorbate peroxidase (APX), after being translated in the cytosol, can travel through the ER membrane towards a specialized region of the ER, the so called peroxisomal ER (pER). There nascent ER-vesicle are formed and released into the cytoplasm which are then probably transported and fused with pre-existing mature peroxisomes, delivering the PMPs as well as membrane lipids to the peroxisomes (reviewed in Mullen et al. 2001 an in Kaur et al. 2009).

It was proposed that key peroxins such as PEX2, PEX3 and PEX16 traffic to PX via the ER in yeast cells of *Yarrowia lipolytica* and *Sacharomyces cerevisiae* (Titorenko and Rachubinski 1998). In addition plant AtPEX16 was found to traffic via an intermediate compartment to pre-existing PX in cell suspension cultures of *Arabidopsis* (Karnik and Trelease 2007). In mammalian cells PEX16 was also found to localise to PX as well as to the ER in COS-7 cells co-expressing a PEX16-GFP (Kim et al. 2006).

This resembles the situation we observed after overexpression of some of the YFP-PEX11 fusion proteins, which partially co-localise with an ER marker in our agro-infiltration studies in *N. benthamiana*.

In a recent study Knoblach and Rachubinski (2010) suggest that the yeast PEX11 protein may also traffic to the ER in cells of *Sacharomyces cerevisiae*. The authors could show that the PEX11 protein is phosphorylated at positions Ser<sup>165</sup> and/or Ser<sup>167</sup> and that the wild type PEX11 protein can translocate between the ER and PX due to changes in the phosphorylation state, indicating trafficking of the PEX11 to the ER during the early steps of peroxisome biogenesis (Knoblach and Rachubinski 2010).

In addition a study by Saray et al. (2011) provided evidence that a member of the PEX11 protein family in *Hansenula polymorpha*, PEX25 together with Rho1, is required to reintroduce peroxisomes in peroxisome-deficient *pex3* in *H. polymorpha*.

In regard to available literature data, it is possible that the observed co-localisation of YFP-PEX11 fusion proteins with an ER marker in our infiltration studies in *N. benthamiana* indicates a connection between the various PEX11 proteins and the ER in plant cells. Maybe PEX11 proteins can also travel to peroxisomes via the ER as previously reported for other PMPs like PEX16 or traffic to the ER like proposed for the yeast PEX11 protein. High levels of especially AtPEX11D might disturb the ER integrity.

### C.4. Overexpression of PEX11 might cause a dominant negative effect on peroxisomes

To observe if the overexpression of the plant PEX11 fusion proteins and the observed cluster formation has any effect on the functionality of the peroxisomes, sugar and various hormone dependent assays were performed.

Fatty acid  $\beta$ -oxidation in peroxisomes (=glyoxysomes) of young seedlings is important for the production of sucrose from storage lipids during germination (see introduction Figure 2 and 3). A defect in this process leads to an insufficient supply of sucrose and therefore energy, which is necessary for the germination and growth of plants. By addition of sucrose into the growth medium, these effects can be partially compensated.

This effect was observed upon overexpression of several PEX11 proteins in transgenic *Arabidopsis* plants (see chapter B.5.4 Figure 26\_A and \_B). Plants overexpressing AtPEX11A, AtPEX11B and AtPEX11C showed a strong inhibition of root elongation when grown on ½ MS medium without sucrose compared to wild-type plants. In addition, overexpression of AtPEX11D led to slightly shorter roots, whereas no obvious difference was detected upon overexpression of AtPEX11E (see chapter B.5.4 Figure 26\_A). After addition of 3% sucrose to the growth medium in some instances partial or full rescue of the root elongation phenotype was observed for AtPEX11A, AtPEX11B, AtPEX11C, and AtPEX11D (see chapter B.5.4 Figure 26\_B), whereas no significant difference was observed after the overexpression of AtPEX11E.

A similar sugar dependence phenotype for growth was reported by Hayashi et al. (1998). They applied 2,4- dichlorophenoxybutyric acid (2,4-DB) to plants, which was believed to be converted

into 2,4-dichlorophenoxyacetic acid (2,4-D) by the  $\beta$ -oxidation pathway in peroxisomes (Wain and Wightman 1954). 2,4-D in turn is toxic for plants at high levels and lead to a strong inhibition of root elongation and growth in *Arabidopsis* plants (Estelle and Sommerville 1987).

By an *Arabidopsis* mutant screen several so called *ped* (*peroxisomes defective*) mutants have been identified, showing a similar inhibition of root elongation with 2,4-DB (Hayashi et al. 1998), indicating that these plants have a defect in the fatty acid  $\beta$ -oxidation. These *ped* mutants are suggested to be inhibited in the conversion of 2,4-DB into 2,4-D indicating an impaired fatty acid  $\beta$ -oxidation pathway. This was supported by the fact that post-germinative growth of these mutants requires sucrose, circumventing the need for peroxisomal  $\beta$ -oxidation to supply energy for growth (Hayashi et al. 1998).

The root growth defect of plants overexpressing AtPEX11A to -D was also at least partially rescued by addition of 3% sucrose to the growth medium. Similar to the *ped* mutants this indicates an inhibited or at least slowed down fatty acid  $\beta$ -oxidation after overexpression of these PEX11 proteins. Based on the fact that PEX11 proteins are membrane and not matrix proteins this is probably an indirect effect on  $\beta$ -oxidation.

In contrast to our results Orth et al. (2007) observed no sucrose dependency of PEX11-overexpression plants (CFP<sub>p35</sub>-PEX11). They report slightly longer hypocotyls of overexpression plants on sucrose free medium compared to control plants, suggesting that glyoxysomes function properly.

In addition, RNAi silencing lines targeting single *PEX11* mRNAs showed a significant decrease in PX abundance but did not reveal a sugar depended phenotype (Orth et al. 2007). This suggests that the reduced PX abundance does not affect glyoxysomal function and that the five AtPEX11 proteins are to some part redundant.

A second study by Nito et al. (2007) failed to detect any morphological changes in single mutant knockdown plants as observed by Orth et al. (2007). At the same time, they could show that double and triple RNAi knockdown mutants like *pex11a/11b* and *pex11c/11d/11e* with a 20 and 31% decrease of gene expression, led to significantly larger PX (1.5 $\mu$ m and 2.4 $\mu$ m), compared to PX in wild type plants (approx. 1 $\mu$ m). However, both mutants did not require sucrose for post-germination growth and were sensitive to 2,4-DB, indicating a sufficient peroxisomal fatty acid  $\beta$ -oxidation. Again a functional redundancy was suggested (Nito et al. 2007).

However, we observed a growth phenotype (short roots) in the different PEX11 overexpression plants as well as a partial rescue of this defect by sucrose. The discrepancy between the inhibitory effects on elongation observed in some of our overexpression plants compared to no significant inhibition in the overexpression plants by Orth et al. (2007) might be explained by looking at the fluorescently tagged fusion proteins on a cellular level. The main difference is that I observed extreme cluster formation with hardly any free PXs, while Orth et al. (2007) observed less dense clusters in plants and more well separated as well as elongated PXs. We suggest that the clusters observed after the overexpression of the YFP-PEX11 fusion proteins are probably formed due to an insufficient fission and separation process during proliferation and may have a negative effect on the proper function of these PXs. Due to the fact that all plant PEX11 proteins are transmembrane proteins, the extreme overexpression of the PEX11 fusion proteins might lead to an overaccumulation of PEX11 at the PX membrane, thus having a negative effect on other membrane based mechanisms like fatty acid import or translocation of fatty acid degrading enzymes into PX. In addition, the observed cluster formation in our overexpression plants means that the PX inside the cluster do not face the cytosol and therefore are probably impaired in efficient uptake of fatty acids. So the actual PX surface that might be functional is much higher in the overexpression plants of Orth et al. (2007) who still observed many free PX. This might explain why PX are functionally inhibited or at least reduced in our overexpression lines compared to overexpression plants studied by Orth et al. (2007).

Taken together the dominant negative effect of PEX11 could be based on the observed proliferation and clustering of PX in the overexpression lines.

In the future it will be necessary to establish mutant plants in which all five PEX11 genes are completely disrupted to gain new insights into the role of the *PEX11* gene family during peroxisome proliferation as well as the fatty acid  $\beta$ -oxidation. This could further confirm the role of PEX11 proteins in PX biogenesis. In addition a 2,4-DB screen similar to the screen performed by Hayashi et al. (1998) with our AtPEX11 overexpression lines would be necessary, to confirm disrupted fatty acid  $\beta$ -oxidation and further support our data obtained by the sugar dependent growth assay. Also YFP-PEX11 protein should be expressed driven by its native promoter to study their dynamics and whether similar cellular structures such as the ER can be tagged by the PEX11 members.

### C.5. Overexpression of *AtPEX11A* causes growth defects

The established transgenic *A. thaliana* *PEX11* overexpression lines not only confirm our results from the transient expression assays, but also allowed us to analyze possible developmental phenotypes, which may occur due to the overexpression of the *PEX11* proteins.

As shown in chapter B.5.1 the overexpression of the plant *AtPEX11A* led to a dwarfed phenotype of the plants compared to control wild type Col0 or mCherry-SKL expressing plants (harbouring the peroxisomal matrix protein PTS1). Also, the rosette leaves were curved upwards and sometimes bleaching was observed. In addition, overexpression of the *AtPEX11C* fusion protein led to a delay in plant development, but without any further effects on plant morphology. Plants overexpressing the remaining three plant *PEX11* proteins, *AtPEX11B*, -E and -D did not display any obvious growth or pigmentation changes.

In contrast, Orth et al. (2007) did not observe a significant developmental phenotype after overexpression of the plant *PEX11* proteins. As discussed in the previous chapter this might be due to a higher amount of free and elongated PX versus clustering PX in our plants.

*Arabidopsis pex6* mutant plants have a defect in peroxisomal matrix protein import (Zoleman and Bartel 2004). The *pex6* mutant was isolated based on the inhibitory effects of indole-3-butyric acid (IBA), a naturally occurring auxin in some plant species, on root elongation in *Arabidopsis* (Zolman et al. 2000).

*Arabidopsis pex6* mutants show severe seedling defects in root and hypocotyl elongation when grown on medium without sucrose (Zolman and Bartl, 2004). The defects can be partially complemented when sucrose is added, indicating an inhibition of the fatty acid  $\beta$ -oxidation. In addition, development was also disturbed at later stages, leading to smaller rosettes, fewer leaves, shorter siliques as well as a shorter inflorescence stems.

A very similar phenotype can be observed in our transgenic plants overexpressing *AtPEX11A*. Plants grown on growth medium without sucrose showed a severe inhibition of root elongation compared to wild type Col0 plants. The supplementation of 3% sucrose led to a partial rescue of the phenotype, but roots were still shorter than in wild type plants. Adult plants overexpressing *AtPEX11A* resemble adult *pex6* plants: they are generally smaller, with smaller rosette leaves and shorter inflorescence stems. In addition only few siliques per inflorescence developed (see chapter B.5.1. Figure 20).

Zoleman and Bartel (2004) suggested that PEX6 plays a role in the peroxisomal matrix protein import in recycling of PEX5 to the cytoplasm. The insufficient recycling of PEX5 in the *pex6* mutants would then lead to a decreased fatty acid  $\beta$ -oxidation and the observed sucrose dependency. In addition, studies by Delker et al. (2007) revealed that PEX6 also plays a role in wound-induced synthesis of jasmonic acid and confirms the role of peroxisomal fatty acid  $\beta$ -oxidation in the biosynthesis of jasmonic acid. They suggested that *pex6* mutants are affected in the conversion of a precursor substrate OPDA, synthesised in chloroplast, into JA in peroxisomes. The *pex6* mutant plants show a significantly lower amount of jasmonic acid compared to wild type plants. The observed phenotype for the *pex6* mutant plants could therefore also be partially induced by an insufficient fatty acid  $\beta$ -oxidation involved in the JA biosynthesis.

While the growth phenotype of YFP-AtPEX11A on MS medium was only partially rescued by sucrose, the addition of 10 $\mu$ M methyl jasmonate (MJ) led to a complete rescue of the observed dwarf phenotype (see chapter B.5.4. Figure 26 A to B), again indicating a negative effect of *PEX11A* overexpression on PX function.

The strong expression of YFP-AtPEX11A could lead to the production of less amounts of JA, due to cluster formation, and thereby to negative effect on energy recovery from storage lipids. Both processes depend on fatty acid  $\beta$ -oxidation, which is probably highly affected in these plants.

In contrast to the other *PEX11* overexpression plants *AtPEX11A* plants might show a phenotype, because no increase in PX numbers was detected in our agro-infiltration studies (see chapter B.3.1. Figure 13 and Figure 14) compared to plants overexpressing the four other *PEX11* fusion. This means that the same amount of PX is present as in wild-type plants, but these are now clustered and their membranes are overloaded with AtPEX11A. This could lead to less cytosol-facing PX membrane surface available for import of matrix proteins than in the other overexpression plants and therefore could maybe lead to the observed phenotype.

Regarding the developmental delay observed for plants overexpressing the plant AtPEX11C fusion protein as well as the human HsPEX11y fusion protein, are also probably due to the observed strong PX cluster formation. The observed developmental delay after overexpression of the yeast ScPEX27 fusion protein remains unclear, as the observed cluster formation is not that dominant as observed for the other *PEX11* fusion proteins leading to a phenotype after overexpression of some of the *PEX11* fusion proteins.



### C.6. Some hormones affect *PEX11* overexpression plants

Another interesting aspect was the observation that the supplementation of a synthetic auxin (1 $\mu$ M NAA) into the growth medium ( $\frac{1}{2}$  MS with 3% sucrose) lead to a complete rescue of the observed root phenotype (shorter roots compared to wild type plant) in overexpression lines of *AtPEX11A* and *AtPEX11C* when grown on MS medium without sucrose, whereas *AtPEX11B*, *AtPEX11D* and *AtPEX11E* remained unaffected.

Several studies have implicated a role of peroxisomes in the biosynthesis of the endogenous auxin indole-3-acetic acid (IAA). It was suggested, that indole-3-butyric acid (IBA) is converted into IAA, by a  $\beta$ -oxidation pathway similar to the fatty acid  $\beta$ -oxidation occurring in peroxisomes (Fawcett et al. 1960, reviewed in Kaur et al. 2009).

An *Arabidopsis* mutants screen led to the identification of so called IBR-resistant (*ibr*) plants, due to the inhibitory effect of IBA on the root elongation. Mutant plants showing a resistance to the inhibitory effect of IBA on root elongation, but remaining sensitive to indole-3-acetic acid (IAA), where thought to have a defect in the  $\beta$ -oxidation pathway (Zolmann et al. 2000). This was supported by the finding that some of these IBA-resistant mutants also showed a sucrose dependent growth phenotype as well as a 2,4DB-resistance, indicating lower fatty acid  $\beta$ -oxidation efficiency (Zolman et al. 2000). This implicates that the conversion of IBA to IAA was also disrupted in these mutants (Hayashi et al. 1998; Zolman et al. 2000).

This suggest that the impaired  $\beta$ -oxidation in plants overexpressing *AtPEX11A* and *AtPEX11C* also may have an effect on the conversion of IBA into IAA, leading to reduced level of IAA in these plants, thereby leading to shorter roots compared to wild type plants on  $\frac{1}{2}$  MS medium without sucrose. The observed root elongation rescue by the addition of NAA can therefore probably be explained by the compensation of the low levels of IAA, by the exogenous addition of the syntetic auxin (NAA).

Interestingly, the addition of ABA into the growth medium led to a complementation of the root-length phenotype in lines overexpressing *AtPEX11A* and has a positive effect on root growth in plants overexpressing *AtPEX11D* and *AtPEX11E*, even though no data are available connecting the biosynthesis of ABA to peroxisomes.

However, it was reported that ABA is a key inducer of H<sub>2</sub>O<sub>2</sub> production in plant cells upon water stress and that exogenous applied ABA lead to an increase of H<sub>2</sub>O<sub>2</sub> in plant cells (Hu et al. 2006). It was shown that exogenous application of H<sub>2</sub>O<sub>2</sub> can induce *PEX* genes in plant and animal cells

upon a direct response to H<sub>2</sub>O<sub>2</sub> (Lopez-Huertas et al 2000). Therefore the application of ABA could lead to an increase of the H<sub>2</sub>O<sub>2</sub> level in the plant cells affecting the expression of endogenous *PEX* genes, which in turn could maybe compensate the observed growth deficiency in the transgenic *AtPEX11A* lines on MS medium.

In contrast, the addition of GA did not have any effects on the root elongation of plants overexpressing *AtPEX11A-D*, and only a slight increase of root length was observed for *AtPEX11E*, suggesting no positive or negative effect of GA.

A recent study in by Mitsuya et al. (2010) revealed that salt stress induces *AtPEX11E* expression and peroxisome proliferation. At the same time overexpression of *AtPEX11E* does not increase salt resistance as reported by Mitsuya et al. (2010). We could confirm this, with our own experiments, showing that *AtPEX11E* overexpression plants grown on  $\frac{1}{2}$  MS supplemented with 100mM NaCl did not contain shorter or longer roots compared to wild-type plants. In general, addition of NaCl leads to reduced root growth in all plants, also the Col0 control. Summarized this suggests that presence of high NaCl concentrations has no effect on root elongation and growth in our *PEX11* overexpression lines.

### C.7. A minimal promoter region sufficient for the expression of the *AtPEX11D* gene as well as the search for potential regulatory factors

The design of five different *AtPEX11D* promoter deletion constructs allowed us to find a promoter fragment sufficient for expression of *AtPEX11D*, which can be used as a bait region for a Yeast One Hybrid Screen. The screen should reveal possible regulatory factors binding to the promoter of *AtPEX11D*. To identify regions that might be of interest, an *in silico* analysis of the *AtPEX11D* promoter (see chapter B.6.1. Figure 27) was performed. This approach predicted several regulatory motifs such as Y patches or regulatory elements (REG) (source: <http://www.ppdb.gene.nagoya-u.ac.jp>; Yamamoto and Obokata 2008). According to this analysis various deletion constructs were made and fused to a GUS/GFP reporter system (EGFP-GUS, pKGWFS7, Karimi 2002) and transgenic *A. thaliana* plants were established. By this means I could follow the *in situ* expression pattern and quantity by GUS staining and measurements (Jefferson et al. 1987).

The results from the GUS expression assays revealed a short DNA region from - 424bp to -165bp upstream the ATG start codon of *AtPEX11D*, further referred to as minimal promoter region. The *AtPEX11D* promoter did not show any GUS activity after the deletion of this area (see chapter: B.6.2. Figure 28). This indicates, that this promoter region is necessary and sufficient for expression of *AtPEX11D* (At2G45740) in most tissues.

An additional *in silico* analysis of the *AtPEX11D* promoter region revealed the localization of one *cis*-regulatory site (source: ATTED-II database <http://atted.jp>, Obayashi et al. 2008) in the minimal promoter region of *AtPEX11D* (Figure 44 below). *Cis*-regulatory elements are DNA fragments where transcription factors can bind, leading to regulation of the expression of nearby genes (Davidson, 2006). This *in silico* data further proposed the minimal promoter as a necessary region for sufficient expression and regulation of the *AtPEX11D* gene.

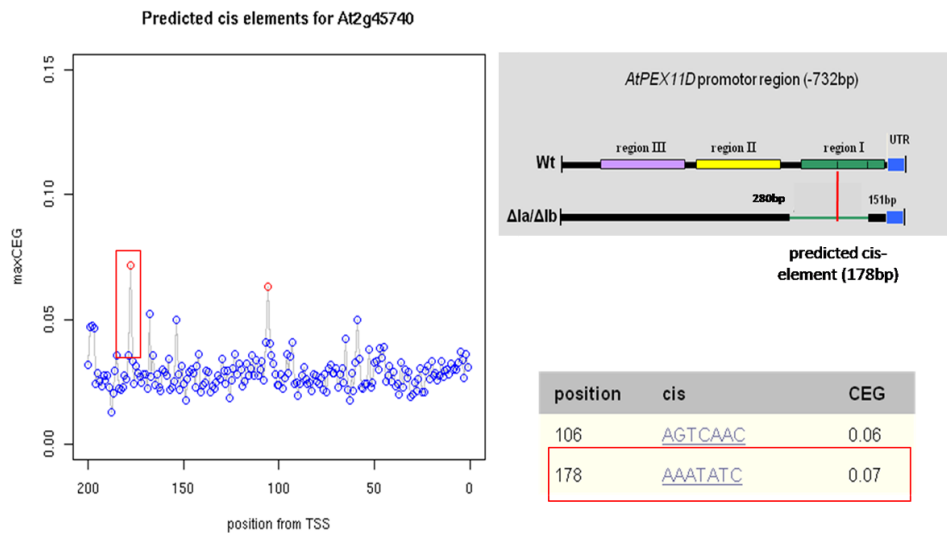


**Figure 44: Predicted *cis*-regulatory elements for the *AtPEX11D* promoter by the ATTED-II database (<http://atted.jp>; Obayashi et al. 2008).**

The *cis*-element 178bp upstream of the UTR is located in the minimal promoter region of *AtPEX11D*. **CEG value** = correlation between *cis*-element appearance and relative expression of genes. **TTS**: transcription start site. **Wt**: full-length promoter of *AtPEX11D*. **Δla/Δlb**: minimal promoter region of *AtPEX11D*.

Our results from GUS expression assays revealed a promoter fragment (424bp to 161bp upstream the ATG) sufficient and necessary for the expression of the gen, which can be used as a bait for the Yeast One hybrid screen.

## **C.8. Tissue specific regulatory elements are present upstream of the minimal promoter**

Our *in situ* GUS assays of seedlings not only allowed us to search for a minimal promoter region but also enabled us to analyze the tissue specific expression of the *AtPEX11D* gene. Our results revealed that the full-length promoter drives expression of the GUS reporter in cotyledons, young leaves, the hypocotyl and primary root in 7 day old seedlings (Figure 28\_B). In contrast, the construct including only the minimal promoter region led to an obvious increase in the GUS expression in young leaves and a slight increase in the primary root (see chapter: C6.2. Figure 28), whereas no expression could be observed in the root tip of plants, carrying only the minimal promoter region.

Cross section of various plant organs and a closer analysis of the tissue specific GUS expression were performed to further analyse the observed differences.

On the one hand the promoter region (715bp to 424bp) upstream of the minimal promoter seemed to be essential for an appropriate GUS expression in the apical differentiation/division zone of the root tip, (no GUS expression with the minimal promoter region alone) as well as for a sufficient expression in the ovules. On the other hand, the same area seems to act as a suppressor for GUS expression in the vasculature of young leaves and in mesophyll cells, where GUS expression was increased with the minimal promoter, in comparison to the full-length promoter. In addition an expression could also be observed in the parenchymatic cortex of the elongation and differentiation zone of the primary root, and sometimes also in the root vasculature.

On one hand these results suggest the potential presence of a suppressor sequence for young leaves and the primary root upstream in the minimal promoter region. On the other hand the upstream sequence appeared to drive expression in the root tip and partially also in ovules.

Summarized we conclude that the minimal promoter region (424bp to 161bp upstream the ATG) is essential for expression of the whole gen, whereas distinct tissue specific regulatory sequences seem to be present in both the upstream region of the *AtPEX11D* promoter (715bp to 424bp) and in the minimal promoter region.

### C.9. The expression of *AtPEX11D* seems to be light but not heat induced.

Based on online data (eGFP bar.utoronto.ca/ status 2011) a light induced expression of the *AtPEX11D* gen was predicted with the strongest expression between 8 and 12 hours after light exposure (Figure 45).

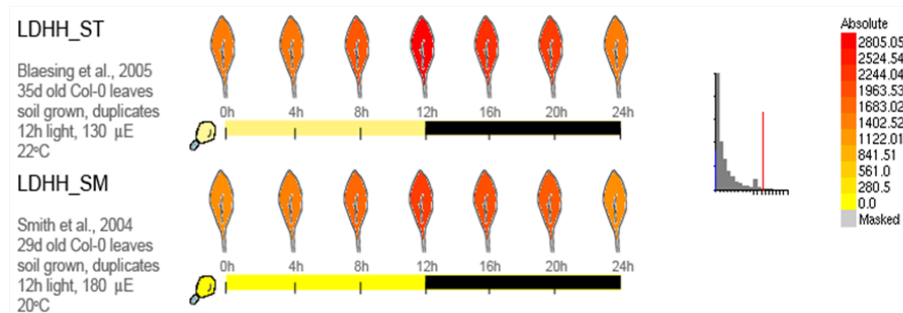


**Figure 45: Microarray data from eFP Browser at bar.utoronto.ca/ (Winter et. al., 2007 Plos One 2(8):e718 Status from 2011) indicate a light dependent expression of the *AtPEX11D* (*At2G457450*) gen. Leaves from 35 days or 29 days old Col0 plants grown on soil at 22°C and 12h light.**

Our results (see chapter B.6.3. Figure 29) are in agreement with the predicted light cycle dependent expression pattern of the *AtPEX11D* gene. We could observe the highest expression level after 10 hours of light exposure, under standard growth conditions (16h light cycle). In contrast, a lower GUS expression level was observed after 3h of light exposure and a slight decrease of the expression could be detected after 12h. A similar result was obtained for GUS expression under the control of the minimal promoter region (see supplemental Figure S2). Again the highest GUS expression was observed 10h after light exposure, even though the general expression was higher compared to the full length promoter (see chapter B.6.3. Figure 29) and no expression was detected in the root tip.

In addition, light experiments of *N. benthamiana* leaves infiltrated with a GUS reporter system under the control of the minimal promoter region, as well as the GUS vector without a promoter region were performed 24h post infiltration (see supplemental Figure S3). GUS staining showed that even though the expression was very weak a slight increase after 8h of light exposure compared to 2h light exposure was detected. No expression was observed after 11h of light exposure.

Beside our light cycle dependent experiments, shading experiments have been performed, indicating a negative effect of shading on the expression level of the *AtPEX11D* gene. Due to a small amount of samples (1 experiment with two biological measurements), these results are only preliminary, and the experiment has to be repeated to confirm this effect.

In contrast, the predicted heat induced expression of *AtPEX11D* (Abiotic Stress by Kilian et. al., 2007, [bar.utoronto.ca/](http://bar.utoronto.ca/) Status 2011) seemed not to take place. We were not able to observe any significant differences between plants exposed to 37°C for 4 hours compared to plants grown under control conditions (22°C) (see chapter B. Figure 35\_A). This suggests that *AtPEX11D* is either not heat induced as suggested, or that potentially other stress conditions are altering the expression such as salt stress or light stress.

### C.10. The transcription factor SOL1 affects *AtPEX11D* expression in plant cells

So far only very little is known about factors regulating the expression of genes involved in peroxisome proliferation in plant cells, compared to yeast and human systems.

In yeast three proteins, ADR1, OAF1, and PIP2, have been identified to act as transcription factors binding to a conserved upstream activation sequence (UAS1) and an oleat responsive element (ORE) localized in the promoter region of some genes encoding peroxisomal proteins such as the *POX1* gene, encoding a peroxisomal acyl coenzyme A oxidase or the yeast *ScPEX11* gene (Karpichev et al. 1997, Gurvitz et al. 2001). It was shown that OAF1 and PIP2 are forming a heterodimer before binding to the ORE of peroxisomal genes. The presence of oleic acid induces the formation of the PIP2/OAF1 dimer, which then together with ADR1 binds to the overlapping area of the UAS1 and the ORE in the promoter region of *ScPEX11*, thereby activating peroxisome proliferation (Figure 46; modified after Kaur and Hu 2009).

In mammalian cells, ligand-dependent transcription factors, the so-called peroxisome proliferator activator receptors (PPARs) have been identified, regulating peroxisomal genes by binding to a peroxisome proliferator response element (PPREs) (Berger and Moller 2002; reviewed in Kaur and Hu 2009). So far three isoforms of PPAR have been identified: PPAR $\alpha$ , PPAR $\beta$  and PPAR $\delta$ , each of them interacting with a retinoid X receptor (RXR), thereby forming a heterodimer which binds to the PPRE (Figure 46, modified after Kaur and Hu 2009, Berger and Moller 2002).

Whereas in yeast cells, the only function of the OAF1/PIP2 dimer is regulating PX, the PPARs in mammalian cells show additional functions in stress, inflammation or immune response (Berger and Moller 2002).

A various number of PPAR activating ligands have been identified such as the natural ligands oleic, palmetic or linoleic acid activating PPAR $\alpha$  or PPAR $\delta$ . In addition synthetic ligands like thiazolidinedione (TZD) or clofibrate (CFB) are shown to increase the activity of PPAR $\alpha$  (Berger and Moller 2002).

A recent study by Desai and Hu (2008) in *Arabidopsis* plants showed that *Arabidopsis* null mutant plants of phytochrom A (phyA) have decreased *AtPEX11B* expression levels. In addition they could show that the transcription factor LONG HYPOCOTYL5 HY5 HOMOLOG (HYH), a regulator of photomorphogenesis, can bind to light-response elements (LREs) located in the promoter region of *AtPEX11B*. This indicates that far red light can induce peroxisome proliferation via phyA and up-regulation of *AtPEX11B* see Figure 46 (modified after Kaur and Hu 2009 and Desai and Hu 2008).

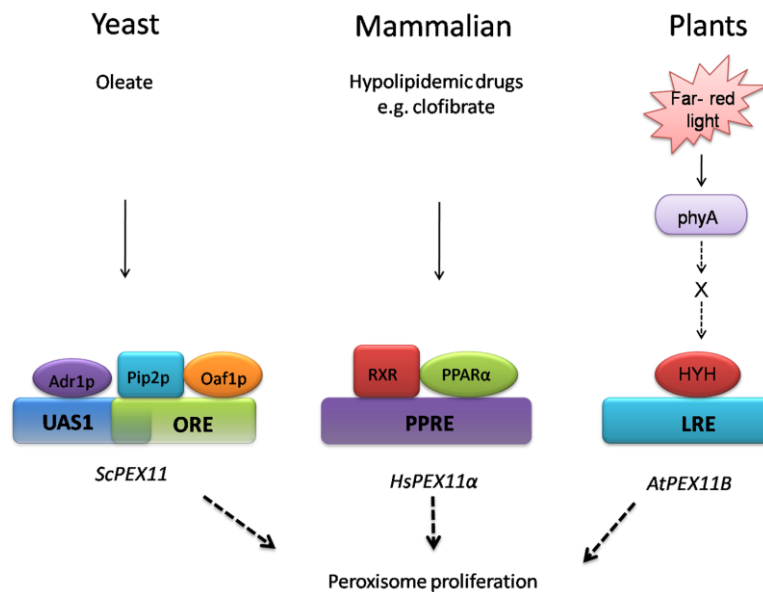


**Figure 46: Comparative model of the regulation of a member of the *PEX11* gene family in yeast (*ScPEX11*), in human (*HsPEX11 $\alpha$* ) and in plant (*AtPEX11B*) modified after Kaur and Hu 2009 and Desai and Hu 2009.** In yeast the presence of oleic acid induces the formation of the OAF1/PIP2 dimerization complex, which then together with Ardp1 binds to the overlapping area of the upstream activation sequence 1 (UAS1) and the oleat response element (ORE) in the promoter region of *ScPEX11*, thereby activating peroxisome proliferation. In mammals, the peroxisome proliferator-activated receptor alpha (PPAR $\alpha$ ) interacts with the retinoid X receptor (RXR), forming a heterodimer complex, which now can bind to the peroxisome proliferator response element (PPRE) in the human *HsPEX11 $\alpha$*  promoter, induced by the addition of clofibrate. In plants, far red light induces the expression from the *AtPEX11B* promoter via



the light receptor phytochrom A (phyA) and a direct binding of the bZIP transcription factor HY5 HOMOLOG (HYH) to suggested light-response elements (LREs) predicted to be located in a promoter region 200bp upstream the TTS site.

Despite intensive database searches no orthologues to the mammalian PPARs or the yeast OAF1/PIP2 could be identified so far in the plant genome (Kaur and Hu 2009). In addition, LONG HYPOCOTYL5 (HY5), a homolog of the *AtPEX11B* promoter binding HY5 HOMOLOG (HYH), has more than 3000 chromosomal binding sites in *Arabidopsis* promoters, suggesting that HYH might also bind to wide range of promoters, making it a rather unspecific transcription factors (Lee et al. 2007).

Thus we decided to perform a yeast one-hybrid screen to search for potential transcription factors binding to the *AtPEX11D* promoter and potentially regulating *AtPEX11D* expression. This particular *PEX11* gene was selected as it showed the strongest effect upon overexpression regarding PX shape and number in transient assays as well as a strong effect on membrane structures. Also *AtPEX11D* has a relative simple promoter region arrangement and the gene shows high tissue specific expression levels.

In our Yeast One Hybrid screen we could identify a promising candidate transcription factor binding to the minimal promoter of *AtPEX11D*. The isolated clone carried the full-length cDNA sequence encoding the transcription factor SOL1 (TSO1-Like, also called TCX3 for TSO1-like CXC).

I could show that SOL1 increases the relative GUS activity regulated by the full-length promoter of *AtPEX11D* in protoplasts from *A. thaliana* (see chapter B.9. Figure 43). This confirms an effect of SOL1 on the *AtPEX11D* promoter in *A. thaliana* cells and indicates that SOL1 might be a positive regulator of *AtPEX11D* expression.

In line with this is the effect of transient overexpression of YFP-SOL1 in epidermal leaf cells of *N. benthamiana*, which increased the number of peroxisomes per cell. In addition peroxisomes showed clustering. Two control constructs, YFP-TCTP, which is a false positive 1 hybrid clone, and YFP-KNAT1, a homeodomain transcription factor, had no effect on peroxisome numbers or clustering (see chapter B.8. Figure 43). This indicates that SOL1 is able to bind to the endogenous promoters of *N. benthamiana* *PEX11* orthologous genes, thereby inducing their expression. This in turn could cause the observed clustering of PX.

These results suggest that the transcription factor SOL1 positively regulates *AtPEX11D* expression, leading to higher *AtPEX11D* protein levels. This, in turn, induces peroxisome

proliferation, which results in higher peroxisome numbers and clustering of peroxisomes in plant cells.

*SOL1 (TSO1-Like)* and *SOL2 (TSO2-Like)* are both *Arabidopsis* paralogs of the *TSO1* gene, identified by a database research by Hauser et al. (2000). A protein sequence alignment of *TSO1* with *SOL1* and *SOL2* showed a significant sequence conservation throughout their lengths, especially in two cysteine-X-cysteine (CXC) motifs shaded in gray in Figure 47 below (taken from Hauser et al. 2000). In addition an arginine-glycin-aspartate (RGD) sequence was identified in *TSO1* (see red box in Figure 47), which is suggested to be sufficient for binding receptors that mediate attachment between cells or the extracellular matrix, so called integrins (Hauser et al. 2000). No RGD domain could be detected in *SOL1* and *SOL2*.

```

SOL2 MDTPOKSTI.QIGTPISKSRFEDSPVFNYINLSPIRPVRSIPNPQFSSLNFTSPSPSVF
TSO1 MDKSKQNPSTQIGTSTPKSKFEDSPVFNYISNLSPIESVKISISTAQTFSSLSFTSPSPSVF
SOL1 MDTPEKSET.QIGTPVSKLKVEDSPVFSYICNLSPIKTIKPIPIITCPLSSLNYSPPSPSVF
100
SOL2 TSPHLTSSHKESRFFKTHNSSSDPTNSVESQEDESTSHEEVPAEGD.TKGLNIDDCMR
TSO1 TSPHVI.SHRESRFFRCHN..SVDRSKHLESLDGSVKGVEVVPLVEDLNKEASLED..E
SOL1 TSPHAV.SHKESRF.....RSQKDVSAKSEV.....GE
SOL2 EEASVETNLD.....DSVA.....SPCGNTTDLSLVPA.PTRGEDG.SCEDNGMEL
TSO1 EETSVETSSSLPQILKFDSQTSEHSDSPC...TEDVVEIASSDPH.RGD.NGSSSEEDVTMGL
SOL1 EEALV..GSEPEQSYKNCNTPRVLN.....DVK.....DNGC.....GKDL
200
SOL2 QKMHNDVQGGKTETPDWESLIADASELLIFDSPDASEAFRCFMMQRASNSEARFRNGVEKQ
TSO1 QNMLVVRREG.NDTPGCGRLISDATELLVFRSPNDSEAFRC.LVDKISSSERRFCAGV.KS
SOL1 QVMDNDVKKKSDTPDWETLIAATTE.LIYGSPRESEAFSC.LLKKTSNSEARLRGSIT.A
SOL2 TMQHDSNKE.PESANAIPYEVNSGV.ISQAVSLHR.GIRRRCLDFEMPGNK.....Q
TSO1 TKRPDINKDIPANGSSNENQPLAVLPTNESVFNLRHGMRRRCLDFEMPGKRKDIIVDDQ
SOL1 TSVAVTNTDVTNNNESESV.....DALSLHR.GVRRRCLDFEVKGN.....
300
SOL2 TSSENNTAACESSRVCVPSIGLHLNAILMSSKCKTNVTQDYSCSANIQVGLQRSISTL
TSO1 QSVCDNNVAGESSSCVVPGLHLNNAVAMSAKDSNISVIHGYSISGEIQKSFSGSTTPI
SOL1 ....NQQTLESSSCVVPISIGLHLNTIAMSSKDK..NVANEYSFSGNIKVGVSSTLPV
400
SOL2 ...QDSDLQDEN.EIREDADQDVPVEPALQELNLSPPKKKS.....
TSO1 ..QSQDVTQETSD.QAENEPVEEVPKALVFPPELNLGSLKKMRKSEQAGEGE.SCKRCNC
SOL1 LHSQHDIVRENESGKDSGQIEVVPKSLASVDLTPISPKKKRRKSEQSGEGDSSCKRCNC
SOL2 .....YCECFAAGVYCIIEPCSCIDCFNKPIHEDVVLATRKQIESRNPLAFAPKVIRN
TSO1 KKSCKLKYCECFAAGVYCIIEPCSCIDCFNKPIHEETVLATRKQIESRNPLAFAPKVIRN
SOL1 KKSCKLKYCECFAAGVYCIIEPCSCIDCFNKPIHKDVVLATRKQIESRNPLAFAPKVIRN
SOL2 SDSVQETGDDASKTPASARHKRGKCNCKKSNCLKKYCECYQGGVGCSSINCRCEGCKNAPGR
TSO1 ADSIMEASDDASKTPASARHKRGKCNCKKSNCKMKYCECYQGGVGCSSMNCRCGCTNVFGR
SOL1 SDSIIEVGEDASKTPASARHKRGKCNCKKSNCLKKYCECYQGGVGCSSINCRCEGCKNAPGR
SOL2 KDGS.SIDMEAEQEENETSEKSRKTAQSQNTQEV..MRKDMSSALPTTPTPIYRPELVQ
TSO1 KDGSLLVIMESKLEENQETYEK.RIAKIQHNVESKEVEQNPSDQSTPLPPYRHLVVH
SOL1 KDGSLSF.....EQDEENETSGTPGTTKQTNVLFKP.....AAPSTPIP.FRQPLAQ
600
SOL2 LPFSSSKNRMPPQSLGSGSSSGIFNSQYLRKPDISLSQSRIEKS.FETVAVDGAEQMP
TSO1 QPF.LSKNRLPPTQFFLTGSSS.....FRKPNSDLAQSQNEKKPLETVTEKTEIMP
SOL1 LPISSNNRLLPQSHFHGAIGSSSSGIYNIRKPDMSL...LSHSRIETITD.IDDMS
SOL2 EILIHSPINIKSVSPNGKRVSPPHMSSSSSGSILGRRNGGRKLILQSIPSPSLTPQH
TSO1 EILLNSPIANIKAISPNKRVSPPPGSSSESGSILRRRNGRKLILRSIPAPPSLNPNQ
SOL1 ENLIHSPIT...TLPNSKRVSLSHLDSPES.TPWRNNGEGRNLI.RSFPTFPLSTPHH

```

Figure 47: Protein sequence alignment of *TSO1* with *SOL1 (TSO1-Like)* and *SOL2 (TSO2-Like)* proteins. A high similarity throughout the whole protein sequence can be observed. Two extremely conserved cysteine-X-cysteine (CXC) motifs can be detected (shaded in gray), whereas the arginine-glycin-aspartate (RGD) (red box) identified in *TSO1* is missing in *SOL1* and *SOL2*. Figure taken from Hauser et al. 2000.

It was shown that the CXC domain in tesmin/*TSO1*-like proteins binds zinc *in vitro*, indicating a binding function of this domain towards DNA, RNA, proteins, or small molecules (Andersen et al. 2007). In addition a recent study provided evidence that the CXC domain actually represent a DNA binding domain of the male-specific lethal 2 (*MSL2*) gene in *Drosophila* (Fauth et al. 2009).

The *TSO1* gene is involved in the cytokinesis and cell expansion as well as in male and female fertility in *Arabidopsis* plants, whereas the function of *SOL1* and *SOL2* is not known (Hauser et al., 2000; Andersen et al., 2007).

RNA quantification experiments of *TSO1* and its paralog *SOL1* by Hauser et al. (2000) showed similar levels of mRNA in nearly all organs examined, except for rosette leaves where *SOL1* levels are higher than *TSO1* transcript levels (Hauser et al. 2000). In RNA *in situ* experiments levels of both genes are highest in flowers, especially in microspores and ovules, whereas the *SOL1* transcript is more abundant than *TSO1* in sepals (Hauser et al. 2000). Despite their sequence and expression pattern similarity *SOL1* and *TSO1* proteins are not redundant as *SOL1* does not complement the *tso1* mutation (Hauser et al. 2000).

Regarding the expression pattern of the *AtPEX11D* gene compared to the *SOL1* gene as detected by Hauser et al. (2000) shows some overlaps in several tissues. The *AtPEX11D* promoter is highly active in cotyledons, cauline, adult, senescent leaves as well as in sepals and *SOL1* mRNA was detected in rosette leaves and sepals. Online microarray data ([bar.utoronto.ca/](http://bar.utoronto.ca/), status 2011) indicate low expression of *SOL1* in the protophloem as well as in the columella of roots, where the *AtPEX11D* promoter also drives GUS expression.

At the same time, *SOL1* mRNA levels are highest in ovules and especially pollen, where only very low or no *AtPEX11D* promoter activity was detected. This suggests that *SOL1* might need at least in some tissues co-factors regulating the *AtPEX11D* expression see model Figure 48.

In addition our GUS expression experiments indicate the presence of a tissue specific regulatory sequence for young leaves and the primary root upstream of the minimal promoter region of the *AtPEX11D* promoter (see Figure 48). The same promoter region might be important for binding of a transcription factor other than *SOL1*, activating *AtPEX11D* expression in the root tip, as the minimal promoter does not drive GUS expression in this region.

This indicates that *SOL1* is not the only transcription factor driving *AtPEX11D* expression.

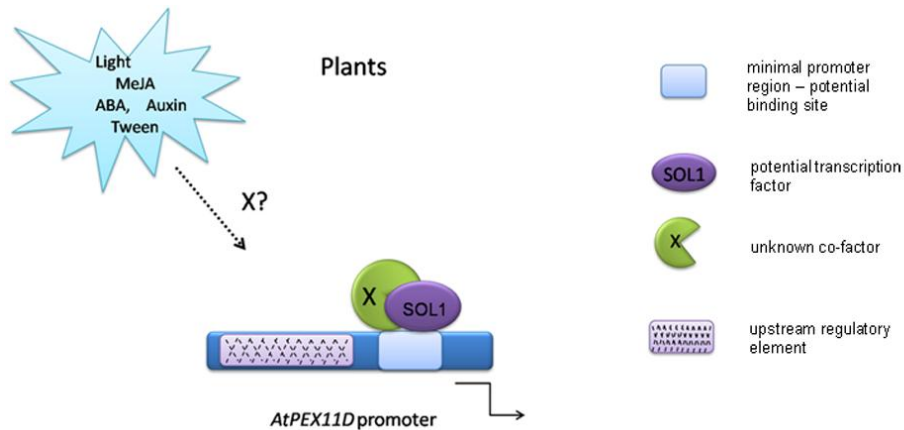


**Figure 48: A model of the regulation of the *AtPEX11D* promoter.** Light, MeJA, ABA, Auxin and Tween upregulated the *AtPEX11D* promoter activity in our GUS expression analysis. SOL1 together with an unknown co-factor might be involved in the regulation of the *AtPEX11D* gene by directly binding to the minimal promoter region. In addition, based on our GUS expression experiments, a potential regulatory element was predicted upstream of the minimal promoter region.

To further confirm the positive regulation of the *AtPEX11D* expression by SOL1, like observed in the infiltration studies in *N. benthamiana*, transgenic *Arabidopsis* plants expressing a SOL1 fusion protein together with a peroxisomal matrix protein would be necessary to be establish and further analysed. In addition, binding of SOL1 to the *AtPEX11D* promoter can be further confirmed by an Electrophoretic Mobility Shift Assay (EMSA) and a Chromatin Immunoprecipitation (CHIP).

In co-operation with the service group of the Gregor Mendel Institute (GMI) Borries Lubracki and Stefan Ferscha already tried to express the *SOL1* gene from a various number of gen-expression vectors (plasmid service group pSG1, pSG7 and pSG8) for further analysis via an EMSA assay. So far from none of the tested vectors SOL1 was successfully express.

In addition a comparative promoter analysis of all five *AtPEX11* genes would show whether SOL1 and/or HYH are also regulating promoters other than *AtPEX11D* and *AtPEX11B* respectively.

## C.11. Conclusions

Taken together I could show that:

- all tested PEX11 fusion proteins from yeast, human and plant are found in association to the peroxisomal membrane in plant cells as well as in human kidney cells (shown by Johannes Koch), suggesting that the targeting of PEX11 proteins to peroxisomes is evolutionarily conserved throughout the three kingdoms.
- based on the different effects upon overexpression of the various PEX11 fusion proteins on the size, number and morphology of peroxisomes in plant cells, it seems that even though the localisation is conserved throughout the three kingdoms, the individual PEX11 proteins may differ in their function.
- most of the PEX11 proteins show a connection to the ER or ER-like structures, indicating that PEX11 maybe also travel to peroxisomes via the ER as previously reported for other PMPs like AtPEX16 or traffic to the ER like proposed for the yeast PEX11 protein. High levels of especially AtPEX11D might disturb the ER integrity.
- the overexpression of *PEX11* might cause a dominant negative effect on peroxisomes, based on the observed proliferation and clustering of PX in the overexpression lines, thereby indirectly affecting the  $\beta$ -oxidation pathway.
- the identified minimal promoter region (424bp to 161bp upstream the ATG) is essential for expression of the *AtPEX11D* gene, whereas distinct tissue specific regulatory sequences are present in both the upstream region of the *AtPEX11D* minimal promoter region (715bp to 409bp) as well as in the minimal promoter region itself.
- light and the addition of the hormones MeJA, ABA, Auxin as well as Tween lead to an upregulation of the *AtPEX11D* promoter activity in our GUS expression analysis.
- SOL1 together with an unknown co-factor might be involved in the regulation of the *AtPEX11D* gene by directly binding to the minimal promoter region.



## D. Materials and Methods

### D.1. Bacteria

#### D.1.1. Bacterial strains

The electro or chemical competent *Escherichia coli* strains TOP10 or DH5 $\alpha$  were used for standard cloning procedures as well as the electro competent DB3.1 *E. coli* strain for propagation of vectors containing toxic ccdB genes. The electro competent *Agrobacterium tumefaciens* strain AgL1 was used for plant transformation.

#### D.1.2. Bacterial stock

Mix 500 $\mu$ l of dense bacterial overnight culture with 500 $\mu$ l of 50% glycerol. Store at -80°C.

#### D.1.3. Bacterial media

##### *Luria-Bertani (LB) medium/ 1l*

- 10g tryptone
- 5g NaCl
- 5g yeast extract
- for LB plates add additionally 10g agar
- store at 4°C until use

Antibiotics were added after cooling to approximately 55°C. The following concentrations of antibiotics were prepared as 100x stocks:

- Carbenicillin as Ampicillin substitute: 100mg/ml in water.
- Chloramphenicol: 34mg/ml in ethanol.
- Kanamycin: 50mg/ml in water.
- Spectinomycin: 100mg/ml in water.
- Zeocin: 50mg/ml in water, use in LB pH = 7,5 (light sensitive)

##### *SOC medium*

- 2% w/v bacto tryptone
- 0.5% w/v yeast extract
- 10mM NaCl
- 2.5mM KCl



- 10mM MgCl<sub>2</sub>
- 10mM MgSO<sub>4</sub>
- 20mM D-glucose

### D.1.4. Preparation of electro competent *E. coli* TOP10, DH5α or DB3.1 cells

A 3 ml LB over night culture was inoculated. The next day a 1:100 dilution with the appropriate antibiotic was grown to an OD<sub>600</sub> of 0.8-1.2. Afterwards the cells were harvested by centrifugation at 5.800 rcf for 12 minutes at 4°C and washed 3 times with ice cold ddH<sub>2</sub>O. The last washing step was performed with ice cold 10% glycerol. The pellet was then resuspended in 1 ml ice cold 10% glycerol and shock frozen with liquid nitrogen. The cells were then stored at -80°C until use.

### D.1.5. Transformation of electrocompetent *E. coli* and *A. tumefaciens* cells

For the transformation 100-500µg of plasmid DNA together with 50µl of competent cells were transferred into dry and sterile electroporation cuvettes. For the electroporation a Gene Pulser<sup>TM</sup> from BioRad was set to 1.7kV (*E. coli*) or 0.85kV (Agro), 15µF and 200Ω. Afterwards 500µl LB or SOC medium was added and incubated at 37°C (*E. coli*) or 28°C (Agro) for 1 hour and plated on LB media with the appropriate antibiotic.

### D.1.6. Transformation of chemically competent *E. coli*

Approximately 1µg of plasmid DNA was gently mixed with 25µl of chemically competent TOP10 cells (Invitrogen) and incubated on ice for 10min. Afterwards the cells were heat shocked at 42°C for 45sec. 250µl LB or SOC medium was added and incubated for 1 hour at 37°C before plating on LB containing the necessary antibiotics.

### D.2. Yeast

#### D.2.1. Yeast strains

**YM4271:** MATa, *ura3-52, his2-200, ade2-101, ade5, lys2-801, leu2-801, leu2-3;112, trp1-901, tyr1-501, gal4D, gal8D, ade5::hisG*.

**W303-1B:** MAT $\alpha$  {*leu2-3,112 trp1-1 can1-100 ura3-1 ade2-1 his3-11,15*}.

**Screen strain 8.1:** The minimal promoter region ( $\Delta$ III/ $\Delta$ II) of AtPEX11D (see chapter B.6.2.) was introduced via a gateway reaction into a modified integrative yeast YIplac204 vector. For this, first a gateway cassette was cloned into the multiple cloning sites (MCS) of the original YIplac204 vector, via HindIII and XbaI restriction sites (Figure 49\_A and 49\_B). Afterwards the lacZ reporter system was replaced by a His interaction marker. For this, the His3 reporter gen was amplified with the following primer pair (*GCG TCT AGA ATG ACA GAG CAG AAA GCC C*) and (*CGC GGC GCC TCA CAT AAG AAC ACC TTT G*) introducing XbaI and NarI restriction sites for a standard cloning into the modified YIplac204 vector (Figure 49\_C). This newly created vector allows now screening of potential transcription factors binding to the minimal promoter region with the help of a His interaction marker. This vector was then transformed into the YM4271a yeast strain.

In addition the not active promoter region ( $\Delta$ Ia/ $\Delta$ Ib, see chapter C.6.2.) was introduced into the modified integrative yeast YIplac211 vector (Figure 46\_D) with a LacZ interaction marker: A gateway cassette was cloned via HindIII and XbaI restriction sites into the YIplac211 yeast vector and afterwards a gateway reaction was performed, introducing the  $\Delta$ Ia/ $\Delta$ Ib region. The modified YIplac211 vector was then transformed into the W303-1B $\alpha$  yeast strain.

Both plasmids were then combined in a new yeast strain by mating the YM4271 yeast strain (harbouring the plasmid with the minimal promoter region of AtPEX11D) and W303 strain (harbouring the plasmid with the not active promoter of AtPEX11D). This yeast strain was used for the Yeast One Hybrid Screen and will further be referred to as screen strain 8.1. Interaction partners of the minimal promoter can now be identified by His selection, whereas false positives can be identified and excluded by not active promoter via the LacZ interaction marker.

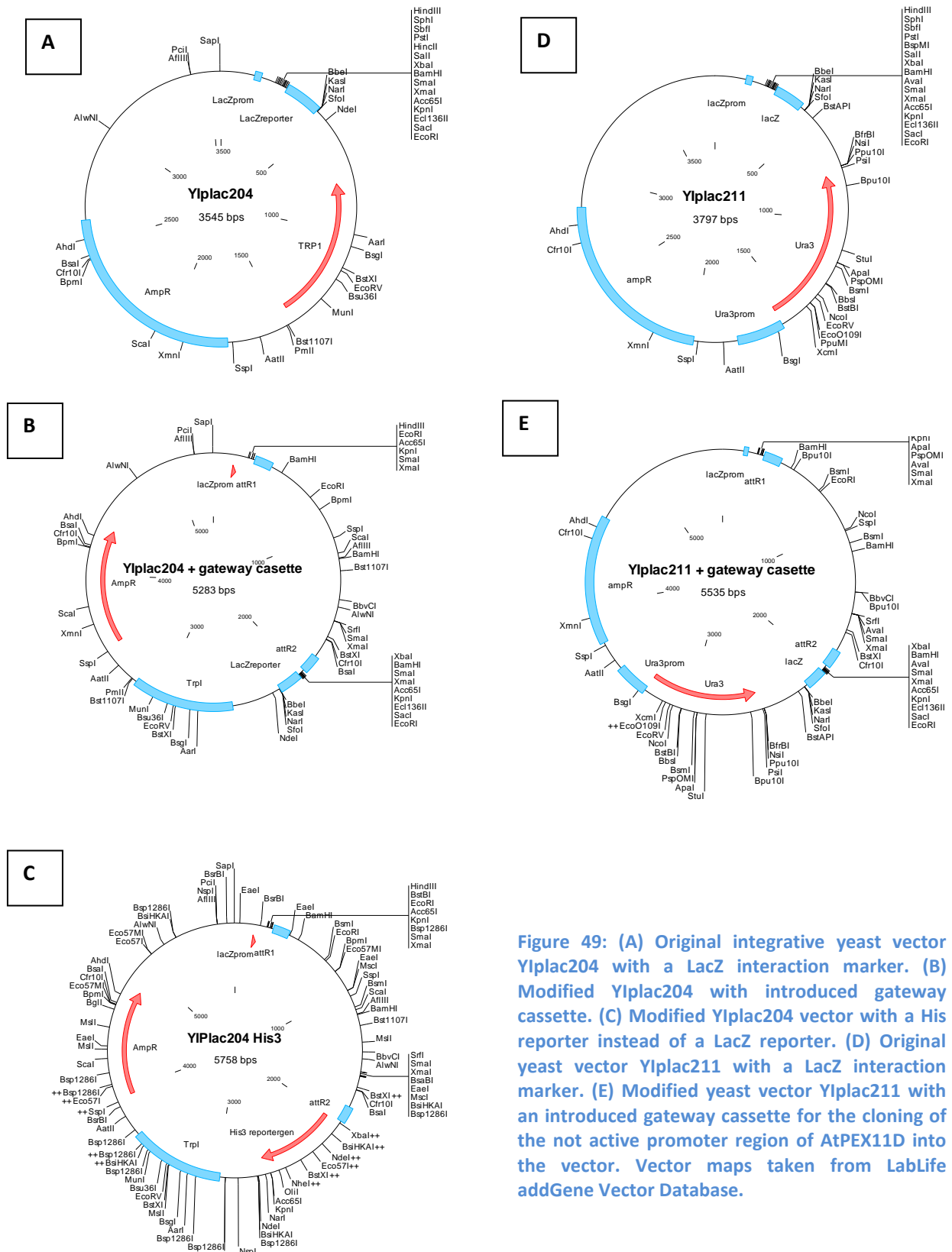


Figure 49: (A) Original integrative yeast vector YIplac204 with a LacZ interaction marker. (B) Modified YIplac204 with introduced gateway cassette. (C) Modified YIplac204 vector with a His reporter instead of a LacZ reporter. (D) Original yeast vector YIplac211 with a LacZ interaction marker. (E) Modified yeast vector YIplac211 with an introduced gateway cassette for the cloning of the not active promoter region of AtPEX11D into the vector. Vector maps taken from LabLife addGene Vector Database.

**Delta 6/1 LacZ strain:** In addition a yeast strain was constructed by introduction of the minimal promoter region into the modified yeast YIPlac211 vector (Figure B1-E). This vector was then transformed into the YM4271 yeast train. The newly created vector will be referred to as delta 6/1 LacZ. Potential candidates can now be additionally analysed with the LacZ marker via a liquid  $\beta$ -gal assay.

### D.2.2 Yeast media

#### *Yeast extract peptone dextrose (YPD)*

- 2% difco peptone
- 1% yeast extract
- 2% glucose- include in plates,
- add fresh before use to liquid medium
- 2% agar for plates

#### *SC-medium*

- 6,7g YNB
- 20g Glucose
- 55mg Tyrosin
- 55mg Adenin
- 20-30g Agar
- For selective media appropriate AS have been added.

### D.2.3. One step yeast transformation

Take approximately 50 $\mu$ l stationary yeast cells from a plate and resuspend them in 200 $\mu$ l transformation buffer. Add 1g plasmid DNA and 10 $\mu$ g heringsperm DNA and vortex it for 30 seconds. Incubate the cells at 45°C for 45min with light shaking. Afterwards spin the cells down (30sec at 1000g) and resuspend the pellet in 100 $\mu$ l water. Plate it on selective medium and incubate the plates for two to four days at 30°C.

#### *Transformation buffer*

- 0,2N lithium acetate
- 40% polyethylene glycol (PEG) 3350 pH 5.0
- 100mM dithiothreitol (DTT)

### D.2.3. High efficiency yeast transformation

A high efficiency yeast transformation was performed like described by Gietz and Schiestl (2007).

Inoculate 30ml o/n culture in YPD. Dilute it then to an OD of 0.2 to 0.3 in 300ml YPD and let it grow until an OD of 0.8 (4-5 hours). When the cells reach this density, wash them 3 times by centrifugation (10min at 2500rpm) and resuspension in 50 ml distilled water. Wash the cells afterwards 1 time with 1x TE/LiOAc (10min, 2500rpm) and resuspend them in 1ml of 1xTE/LiOAc. Incubate the cells for 30min at RT. In the meanwhile heat a water bath to 42°C and boil the single stranded carrier DNA (heringsperm 10mg/ml stock; Sigma) at 95°C for 5min and transfer it immediately to ice until use. Now add 10-50µg plasmid DNA (cDNA library A or B) to the yeast pellet, as well as 200µl carrier DNA and 6ml of a PRG/LiOAc /TE mixture and incubate for 30min at 30°C. Afterwards add 700µl of fresh DMSO and incubate for 20min in a 42°C water bath. Harvest the cells by centrifugation (5min at 2500rpm) and resuspend them in 8ml 1xTE buffer. Plate 1.5ml on SC-Ura-Leu-Trp-His plates containing 3mM ATZ (Gietz and Schiestl 2007).

### *Solutions for high efficiency yeast transformation*

- YPD medium
- Selection medium:
  - SC-Ura-Leu-His-Trp +3mM ATZ
- Lithium acetate (LiOAc) (1.0 M):
  - 10.2 g of lithium acetate in 100 ml of water.
- PEG MW 3350 (50% w/v):
  - 50 g of PEG 3350 in 30 ml of distilled/deionized
  - filter sterilized using a Nalgene filter unit and a vacuum pump
- Single-stranded carrier DNA (2.0 mg ml<sup>-1</sup>, stock 10mg/ml, Sigma)
- 6 ml PEG/ LiOAc /TE mixture: 8ml PEG 3350 50% (w/v)/1ml 10x TE/1ml 10xLiOAc

### D.2.4. Plasmid isolation from yeast

Inoculate yeast cells from plate in an appropriate selection medium (SC) and grow them over night. Dilute the cells afterwards to an OD of 0.2 and grow them in YPD to an OD of 0.8. Centrifuge the cells for 10min at 3000rpm and resuspend them in 600µl lysis buffer and add 300µl glass beads and 600µl phenol:chloroform:isoamyl alcohol (25:24:1). Break the cells up in a fast beater for 2min at full speed and harvest them by centrifugation for 2min (full speed). Transfer the supernatant into a new 2ml microcentrifuge tube and add 800µl 70% EtOH. Harvest

the plasmids by centrifugation at full speed for 15min. Wash the pellet with 500µl 70% EtOH, centrifuge for 2min (full speed) and resuspend it after drying in 50µl 1xTE.

### *Lysis solution:*

- 0,5 ml 10% SDS
- 1ml TritonX-100 10%
- 1 ml NaCl, 5M
- 0,5 ml tris, pH8, 1M
- 100µl EDTA, 0,5M, pH 0,8
- Ad 50ml dh2O

### D.2.5. Filter Lift Assay

Colonies are grown on a cellulose nitrate membrane (Whatman, pore size 8µm) placed on YPD medium for 2 days. Colonies on the membrane are broken up by two freeze and thaw cycles in liquid N<sub>2</sub>. The membrane is placed on two layers of Whatman 17 Chr paper (0,92mm) soaked in Z buffer and incubated in the dark.

### *Z-buffer:*

**10x Buffer A:** 600mM Na<sub>2</sub>HPO<sub>4</sub>,  
400mM NaH<sub>2</sub>PO<sub>4</sub>.

**10x Buffer B:** 100mM KCl,  
10mM MgSO<sub>4</sub>.

Mix buffer A and B to 1x concentration and add 0,24µl β-mercaptoethanol and 1,74% X-gal solution (5-bromo-4-chloro-3-indolyl- beta-D-galactopyranoside, 20mg/ml stock in DMF).

### D.2.6. Liquid β-galactosidase assay

An overnight culture (50ml) was grown to an OD600 between 0,5 and 1. Afterwards cells were harvested by centrifugation (2500 rpm) for 2 minutes and washed with ice cold water. The pellets were then stored at -80°C. They were resuspended in 200µl bufferA and 200µl glass beads were added. The cells were broken up by using a vibrax for 20 minutes at 4°C. The cell debris were removed by centrifugation (10 min at full speed) at 4°C. Afterwards 10-20µl of the protein containing supernatant was used to measure the protein concentration at 280nm. The same amount of protein was used for the liquid β-gal assay. 1 ml of Z-buffer was added to the

proteins as well as 200µl of ONPG buffer to start the reaction. The reaction was stopped with 500µl 1M Na<sub>2</sub>CO<sub>3</sub> after the colorless liquid changed to yellow. The β-gal activity was measured at an OD<sub>420nm</sub>.

**Formula used for β-gal unit calculation:**  $(1700 + \text{sample volume in } \mu\text{l}) \times A_{420} / (0,0045 \times \text{time in min} \times \text{sample volume}) / \text{protein OD}_{420}$ .

### Solutions for liquid β-gal assay

**BufferA\_1:** 20% glycerin

0,1M Tris-Cl pH 8

**Buffer Z :**      **BufferA\_2**                      **BufferB**

60mM Na<sub>2</sub>HPO<sub>4</sub>

10mM KCl

40mM NaH<sub>2</sub>PO<sub>4</sub>

1mM MgCl<sub>2</sub>

Mix BufferA\_1 with BufferB and add 2-mercaptoethanol (50mM).

**30ml ONPG buffer:** 120mg o-Nitrophenyl-β-D-galactopyrosid

add 1,5 ml 1M KH<sub>2</sub>PO<sub>4</sub>

add 28,5 ml H<sub>2</sub>O

## D.3. Plant

### D.3.1. Growth medium

#### *½ Murashige and Skoog Medium (MS) / 1l*

- 0,5g MES
- 4g Murashige and Skoog medium including vitamins
- 6g plant agar for plates
- Adjust pH to 5,7 with KOH
- Antibiotics:
  - Hygromycin 20mg/l
  - Kanamycin 50mg/ml
  - BASTA 25mg/ml



- BASTA for spraying: 200mg

### D.3.2. Growth condition

Two soil mixes were used: First, 70l autoclaved soil (Erde/Spezialsubstrat "Max Planck Institut", Stender) containing 2g Confidor diluted in 10l of water and 75g Osmocote "Start".

Second, soil containing 70l of N3 Humin Substrat N3 (Neuhaus) and 1 part perlite sand together with 0.3g Triatum-P (Koppert biological Syst.), 180µl Companion G (Loeffler) in 2l water and 225g Osmocote.

*A. thaliana* and *Nicotiana benthamiana* plants were cultivated in climate chambers with a light intensity of 800 to 1000 µmol.m<sup>-2</sup>.s<sup>-1</sup> and a temperature of 22°C and 16h of light (for *Arabidopsis*) and 12h (for *Nicotiana*). Osram Lumilux Cool white fluorescent tubes were used as light source and mounted approximately 40cm above the shelves.

### D.3.3. Sterilization of *Arabidopsis thaliana* and *Nicotiana benthamiana* seeds.

1 ml of sterilization solution (10mg/ml bayrochlor tablets, 100µl dH<sub>2</sub>O and 900µl EtOH per ml) was mixed with the seeds and incubated for 10 min. The supernatant was discarded and the seeds were washed in 1ml EtOH three times. The seeds were then dried over night.

### D.3.4. Transient expression in *N. benthamiana* leaves

*N. benthamiana* plants were grown on soil in a greenhouse at 22°C-25°C, with 16 hours of light. Six-week old plants were used for leaf infiltration experiments. Agrobacterial solutions harbouring the relevant binary plasmids were grown in LB medium supplemented with the appropriate antibiotic. For single expression studies the OD<sub>600</sub> was 0.15 or for equally mixed cultures a final OD<sub>600</sub> of 0.3 for double expression was used. Afterwards the cells were harvested by centrifugation (10min, 3500g) and the bacteria were resuspended in 2ml infiltration medium, incubate 2h up to 1 week. Afterwards a 1ml syringe was used to gently infiltrate the bottom side of young and healthy *N. benthamiana* leaves and then they were rinsed with water to remove excess bacteria. Place the infiltrated plants under a plastic bag and keep them out of strong light for 24h. Infiltrated plants were then kept under standard growth conditions until used. The expression can be analysed after 24h-72h.

For estradiol-mediated expression estradiol (final concentration of 10 $\mu$ M, stock 50mM in ethanol, Sigma) was added to the infiltration solution.

Infiltration medium 50ml:

- 500 $\mu$ l 1M MgSO<sub>4</sub> (autoclaved)
- 500 $\mu$ l 1M MES (sterile filtered)
- 75 $\mu$ l 100mM acetosyringone

### D.3.5. Floral Dip of *A. thaliana* plants

#### B.3.5.1. Culture preparation

Grow an overnight culture of *A. tumefaciens* cells harboring the plasmid of interest in LB with the appropriate antibiotics at 30°C. Dilute it in 200ml LB with antibiotics and grow until an OD<sub>600</sub> of approximately 0.8. Spin the culture down (30min, 3000g) and resuspend it in 200ml 0.5x MS with 5% saccharose. Add 0.01% Silwet L-77 and mix well.

5x MS medium for dip: 3.25M sorbitol

325mM MES

pH 5.5

#### D.3.5.2. Plant preparation

Grow *A. thaliana* under long day conditions until flowering and remove the open flowers and siliques. The above-ground parts of plant are dipped into the *A. tumefaciens* solution for 20s with gentle agitation. Place the dipped plants under a plastic bag for 1day and keep them out of direct light. Afterwards return them to the growth chamber. Selection of the transgenic plants on growth medium supplemented with the appropriate selection marker, depending on the used vector construct for transformation.

### D.3.6. Isolation of genomic DNA from plants

Put plant material into 2ml microcentrifuge tube with 2 steel beads and freeze in liquid N<sub>2</sub>. Homogenize in a cooled TissueLyser (Qiagen) with two runs of 30s each at 30 oscillations/s and add 700 $\mu$ l extraction buffer and vortex shortly. Centrifuge for 1min at 16000g. Transfer the supernatant into a new microcentrifuge tube and add 600 $\mu$ l isopropanol. Vortex briefly and

centrifuge for 10min at 16000g. Wash the pellet with 70% and 100% ethanol and dry it at 60°C and dissolve in 150µl water.

### *Extraction Buffer for genomic DNA isolation*

- 200mM tris pH 8,8
- 250mM NaCl
- 25mM EDTA
- 0,5% SDS

### **D.3.6. Protoplast isolation of *A. thaliana***

About 4 weeks old *Arabidopsis* leaves or 9 days old seedlings (0.5 - 1.0 g) are cut into 1-2 mm strips and transferred into 10 ml of digestion buffer in a Petri dish. The samples are then vacuum infiltrated for 30 min and placed in the dark for 6 hours at room temperature (25 °C). Afterwards 10 ml of W5 buffer is added to the Petri dish and the protoplast suspension is filtered into a 50 ml tube through a 100 µm nylon mesh. The protoplasts are harvested by centrifugation at 100×g for 3 min (no brake) and washed two times in 10 ml of W5 buffer. Then the protoplasts are resuspended in 10 ml of W5 solution and kept at 4 °C for 30 min. The protoplast are again collected by centrifugation at 100×g for 3 min (no brake) and washed in 5 ml of MMg solution. The protoplast pellet is resuspended in 5 ml MMg solution and stored at 4°C until use (Sheen 2002).

### *Buffers for protoplast isolation*

#### **Digestion buffer:**

- 1%(w/v) cellulase from *Tricoderma viride* (Serva 1,10U/mg)
- 0.25%(w/v) pectinase from *Aspergillus niger* (Fluka 1.32 U/mg)
- 0.4 M mannitol
- 20 mM MES (pH 5.7)
- 20 mM KCl
- 10 mM CaCl<sub>2</sub>

#### **W5 buffer:**

- 154 mM NaCl
- 125 mM CaCl<sub>2</sub>
- 5 mM KCl
- 2 mM MES (pH 5.7)

### MMg solution:

- 0.4 M mannitol
- 15 mM MgCl<sub>2</sub>
- 4mM MES (pH5.7)

### D.3.7. Protoplast transformation of *A. thaliana*

Use about 5µg plasmid for each transformation reaction. Add 100µl of isolated protoplasts into each tube (2ml) and mix by ticking against the tube. Add immediately 300µl PEG solution and mix gently. Incubate the mixture for 12-15 min at room temperature in the dark. Remove the PEG by adding 1.5ml 0.275M (Ca(NO<sub>3</sub>)<sub>2</sub>) and mix by inverting the tub a few time. Spin for 7 min at 800rpm (no brake) and remove the supernatant. Add 300-500µl of B5-0.34M GM and keep the tubes on a dark place. Check the fluorescence 24hours later (Sheen 2002).

0.275M Ca(NO<sub>3</sub>)<sub>2</sub>: 64.94g/l Ca(NO<sub>3</sub>)<sub>2</sub> x 4 H<sub>2</sub>O

### PEG solution:

- PEG 6000                      60g
- Mannitol                      16.4g
- Ca(NO<sub>3</sub>)<sub>2</sub> x 4 H<sub>2</sub>O              4.7g
- in 200ml H<sub>2</sub>O (pH: 9.0 with KOH)

### B5\_0.34M GM:

- B5 Powder (growth medium, Duchefa)
- 96g/l sucrose
- pH 5.5 with KOH
- cool to 4°C before use

### D.2.8. Fluorometric GUS measurements of *A. thaliana* protoplasts

Collect protoplasts by centrifugation 3 min at 800rpm (no brake) and add 500µl of GUS extraction buffer to the transformed protoplasts and vortex the mixture briefly. Centrifuge at 13000rpm for 15min at 4°C. Transfer the supernatant to a new tube and use a small aliquot to measure the protein concentration via the Bradford assay.

Incubate the rest for 24hours at 37°C and stop the reaction with 1ml Na<sub>2</sub>CO<sub>3</sub>solution. Measure the fluorescence using the following parameters: For GUS measurements the excitation

wavelength was 355nm, whereas the emission wavelength was 460nm. For YFP measurements the excitation wavelength was 510nm and the emission wavelength was 530nm.

### 2ml GUS extraction buffer:

1.1ml	4-MUG in sodiumphosphat (stock 0.004g in 5.7 ml sodiumphosphatbuffer pH: 7)
40µl	0.5M EDTA (pH 8)
20µl	10% SDS
20µl	10% Triton
13.8µl	β-mercaptoethanol
807µl	dH <sub>2</sub> O

### Bradford measurement OD<sub>420</sub>:

- 500µl Bradford solution (1:5 diluted with dH<sub>2</sub>O) with 5µl supernatant after extraction.
- BSA (0.1, 0.5, 1, 2 and 5 mg/ml) used for calibration of the protein measurements (mg/ml).

Formula for calculation of protein content:  $=0,05 \cdot \text{EXP}(x \cdot \text{OD}_{595})$ .

Calculation of relative activity protein/GUS (mg/ml):  $\text{GUS}_{(355/460)} / \text{protein (mg/ml)}$

### D.3.8. GUS staining

The plant material was collected after 8-10 hours light exposure and vacuum infiltrated in 80% acetone for 15 min and incubated for 1 hour at -20°C. The material was then washed twice with 100mM sodium phosphate buffer and afterwards transferred into the GUS staining solution and vacuum infiltrated for 20 minutes (Hemerly et al. 1993). The samples were incubated at 37°C in a light protected environment over night. Afterwards, the GUS staining solution was replaced by 10%, 30%, 50% and 70% EtOH for 20 minutes and afterwards cleared with a 1:1 mixture of acetic acid and EtOH over night. Store in 70% EtOH (based on Hemerly et al 1993, Vitha et al. 1995).

### Beta-glucuronidase (GUS) staining solution

According to Hemerly et al. (1993) and Vitha et al. (1995).

Mix before use:

- 50mM sodium phosphat buffer ph 7,2
  - 2mM potassium ferrocyanide:  $K_4Fe(CN)_6$  [100mM stock]
  - 2mM potassium ferricyanide:  $K_3Fe(CN)_6$  [100mM stock]
  - 2mM 5-bromo-chloro-3-indolyl- $\beta$ -glucurinic acid (X-Gluc in DMSO, fresh)
  - 0,1% Triton-X100
  - 2mM X-Gluc [dissolve 20mM in DMSO]
- **Pipes Buffer [100mM]**
  - 37,86g Pipes
  - 3,804g EGTA
  - 0,241g  $MgSO_4$
  - Add 800 ml ddH<sub>2</sub>O
- **Clearing solution**

Mix acetic acid and EtOH(absolute) in a ratio 1:1.

### D.3.9. Paraffin Embedding

The GUS stained plant material was transferred into embedding cassettes and the cassettes were put into a tissue processing machine (Thermo Shandon Tissue Excelsior) following a standard embedding protocol over night.

Afterwards the material was manually infiltrated by liquid paraffin in the embedding Thermo Electron Shandon Histocenter3. After about 30 min of cooling, the paraffin blocks were removed

For cutting, the paraffin blocks were trimmed and the dispensable wax has to be removed before sectioning. Depending on the plant material 10-40 $\mu$ m thick sections were produced with the help of a rotary microtom (Micron HM 500 OM). The samples (paraffin sections) were placed on a preheated glass slide covered with a dH<sub>2</sub>O:EtOH mixture. Afterwards the slides were dried at 42°C-45°C for at least 3 hours and afterwards stored at 4°C until further use. The glass slides were dewaxed 2 times with Neo-Clear (Xylolersatz, Merck) for 10 min, air dried and afterwards mounted and sealed with Entellan (Mercke).

### D.3.10. Cyro-cuttings of agarose embedded samples

Before usage add 1% DMSO to the fixative (PFA solution) to improve the penetration of the plant tissue. Pour 2.5% PFA into vials and collect your samples into them while they are on ice. Put the vials with the samples into a vacuum pump for about 30 min and let them then shake at 4°C over night. Exchange the 2.5% PFA solution gradually with fresh 1% PFA solution containing raising sucrose concentration of 10%, 20% and finally 30%, each for 30min. Prepare 7% low melting point agarose by dissolving it in water in a microwave at 90Watt for about 15 minutes. Prepare a small Petri dish for each and pour the low melting agarose into it. Take your samples out of the fixative, dry it for few seconds on a paper and then immediately put them into the liquid agarose. Use forceps and tooth picks to orient your sample properly.

For slicing of the tissue we used a Leica 2000 microtome with a freezing facility. We have found that for *Arabidopsis* samples the best longitudinal sections are 20 micron thick for vegetative stage and 25 micron for reproductive stage. Transverse sections should be 35-40 microns for vegetative and 40-50 microns for reproductive stage. Before slicing the block with the tissue should be cut out of the gel and placed at a desired angle at the microtome stage, then tissue-tek (Hartenstein) is used to fix the block to the stage. For freezing dry ice is used. An antifade reagent was added to preserve the GFP/YFP fluorescence up to one week.

**10xPBS:** 1.3M NaCl

0.07M Na<sub>2</sub>HPO<sub>4</sub>

0.3M NaH<sub>2</sub>PO<sub>4</sub>

#### **2.5 % PFA solution pH7.4:**

- 12,5 gr. of PFA in 200 ml of H<sub>2</sub>O at 60°C
- Add NaOH until solution gets clear.
- Add 50ml of 10xPBS
- Cool down to 4°C
- Fill volume to 500ml with ddH<sub>2</sub>O
- Adjust pH to 7.4

#### **Materials and equipment:**

- Paraformaldehyde (PFA)(Sigma P-6148),
- Agarose LM-GQT (Conda, Pronadisa, Cat# 8088)
- Leica microsystems Sliding Microtome SM-2000 with freezing facility.
- Tissue- tek® O.C.T Compound (Cat #62550-01)



- Glass slides(25x75x1mm Menzel-Glaser, Super Frost® Plus, Art No J1800AMNZ)
- ProLong® Gold antifade reagent (Invitrogen, Molecular Probes TM Cat # P36934)

### D.4. DNA

#### D.4.1. Buffers and solutions

##### *10xPBS*

1.3M NaCl

0.07M Na<sub>2</sub>HPO<sub>4</sub>

0.3M NaH<sub>2</sub>PO<sub>4</sub>

10xPBST

PBS + 0.05% v/v Tween-20

##### *1xTBE*

89mM Tris

89mM boric acid

2.5mM EDTA disodium salt

pH 8.2 (with HCl)

##### *TBS(T)*

50mM Tris

150mM NaCl

(0.05% v/v Tween 20)

##### *TE*

10mM Tris

1mM EDTA disodium salt

pH 7.7 with HCl

### D.4.2. Polymerase chain reaction (PCR)

The standard PCR reaction was as following:

10x buffer	5µl
dNTPs	1µl
Enzyme	0,5µl
Primer F	1µl
Primer R	1µl
DNA	1µl
MQ	40,5µl

PCRs were performed utilizing either a Primus (HVD life Science) Cyclor or a RobocyclerGradient96 (Stratagen) with the following standard PCR program:

	° C	Time	
Denaturation	94°C	2`	
Denaturation	94°C	30``	
Annealing	x °C	30`	Cycles 30-35
Elongation	72°C	y`	
Final Elongation	72°C	10`	

X depends on the primers use, y on the length of the insert. PCR products were analyzed with standard gel electrophoresis as described below.

### D.4.3. Agarose gel electrophoresis

Agarose gel electrophoresis was performed to separate DNA fragments due to their different size. 1% agarose gels were used if not stated otherwise. The agarose was mixed with 1xTAE buffer and heated in a microwave until completely dissolved. After cooling to approximately 55°C add 5% (v/v) ethidiumbromide solution (10mg/ml) and pour into the gel casting equipment.

Allow the gel to solidify for at least 30 min. Mix DNA with 20% loading dye. Run gels in 1xTAE at 100V constant voltage.

### 1% agarose

- 1g agarose
- 100ml 1x TAE buffer
- 5µl 10mg/ml etidiumbromid solution in aqua

### Loading dye

- 4M Urea
- 50% (w/v) sucrose
- 50mM EDTA
- 0,1% bromphenole blue

### 50x TAE

- 242g Tris base
- 57,1ml acetic acid
- 100ml 0,5M ethylenediaminetetracetic acid (EDTA) pH 8,0

### D.4.4. Restriction digest

Digests were performed according to the manufacturer's instruction unless otherwise stated. All restriction enzymes and corresponding buffers were purchased from Roche, Fermentas or New England BioLabs. Digests are normally incubated at 37°C for 1 to 2h.

#### ***Digestion reaction with an end volume of 20µl:***

- 2µl DNA of a Quick and dirty mini or 1µl of a kit mini
- 2µl of restriction enzyme buffer 10x
- 0,2µl of enzyme
- add water to a volume of 20 µl

#### ***Digestion reaction with an end volume of 50µl:***

- 1µl of a clean DNA (kit)
- 5µl of restriction enzyme buffer 10x
- 1µl of enzyme
- add water to a volume of 50 µl

### D.4.5. Ligation

To achieve the optimal ligation rate different ratios (4:1 - 1:2) of vector: insert have been used. In addition 1 µl of a 10x ligase buffer, 0.2µl DNA ligase (NEB) and water to a final volume of 10µl were added. The whole reaction was incubated over night at 16°C.

### D.4.6. Clean plasmid isolation from bacteria with a kit

The Wizard Plus SV 96 Plasmid DNA Purification System (Promega) is used for small scale plasmid isolation (mini prep). All steps, except elution are performed according to manufacturer's instruction. DNA is eluted twice in 25-50µl of water (depending on concentration required) from the column by centrifugation.

### D.4.7. Quick and Dirty plasmid isolation from bacteria

Isolated plasmids are only used for restriction digests to identify bacterial colonies containing the desired plasmid. Harvest the 3ml o/n culture by centrifugation for 1min and resuspend in 300µl P1 buffer. Add 300µl P2 buffer and invert the tube 4 times. Add 300µl P3 buffer and mix again by inverting the tube 2 times. Centrifuge for 10min at RT at 14000rpm and transfer the supernatant into a fresh tube (850ul). Add 650ul isopropanol and mix it gently. Incubate for 10 min at RT and centrifuge for 15min at 14000rpm at 4°C. Wash the pellet 2x with 70% EtOH and dry it, afterwards resuspend it in 50ul ddH<sub>2</sub>O.

#### *P1: Resuspension buffer*

- 50mM Tris HCl pH 7.5
- 10mM EDTA disodium salt pH: 8
- 100µg/ml RNase A

#### *P2: Lysis buffer*

- 200mM NaOH
- 1% w/v sodium dodecyl sulfat SDS

#### *P3: Neutralisation buffer*

- 3M KOAc
- pH 5 with HCl

### D.4.8. DNA purification from an agarose gel

The DNA was purified from agarose gels with a Wizard SV Gel and PCR Clean-Up System or an QIAquick Gel Extraction Kit according to manufacturer's instructions.

### D.4.9. Gateway® cloning

The gateway® technology provided by Invitrogen was used to create various yeast, human and plant PEX11-fusion proteins. The tag (N-terminal YFP) is part of the destination vector, while the protein of interest is coded in the entry vector pENTR4 or pDONORzeo. Both vectors contain so called att-sites. The entry vectors contain attL sites, whereas the destination vector possesses attR sites. With the help of an enzyme, called clonase, a recombination reaction takes place, where the gene of interest, previously located in the entry vectors is placed in frame with the tag in the destination vector. This product is called expression vector. With this technique we were able to create various numbers of expression vectors by using the same entry vectors as a starting point. This recombination reaction is defined as LR-reaction (Early et al. 2006).

The standard mixture and conditions for an LR-reaction used are:

- vector:insert ratio (1:1 or 3:1)
- 0.5µl clonase enzyme mix
- 1µl 10x clonase buffer
- add water to 10µl end volume
- incubate o/n to improve the recombination efficiency.
- treat with Proteinase K (10', 37°C),
- transform into electro competent TOP10 E. coli

Beside the LR-reaction, it is also possible to use a PCR product flanked by attB recombination sites and recombine it directly into a donor vector (pDONORzeo ) containing attP recombination sites. This recombination gives than rise to an entry vector with attL sites. This new entry vector is now harboring the protein sequence of interest and can be used in an LR-recombination reaction like described above. The resulting binary vectors allow 35S promoter -driven expression of N-terminal tagged YFP-PEX11 fusion proteins in planta(Early et al 2006).

### Entry Gateway Cloning vectors:

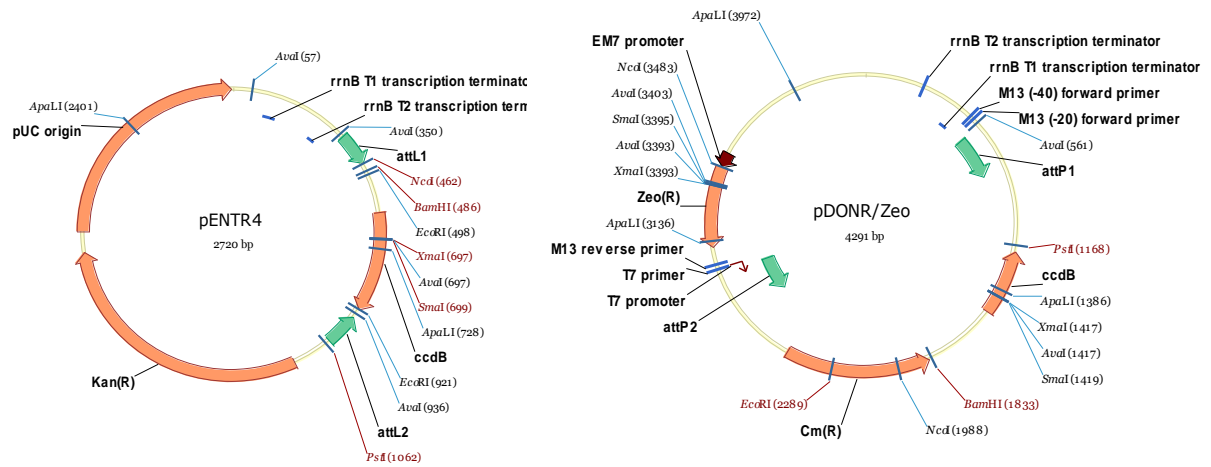


Figure 50: Maps of the Entry Gateway Vectors used in this study, pENTR4 and pDONOR<sup>zeo</sup>.

### Destination Gateway cloning vectors:

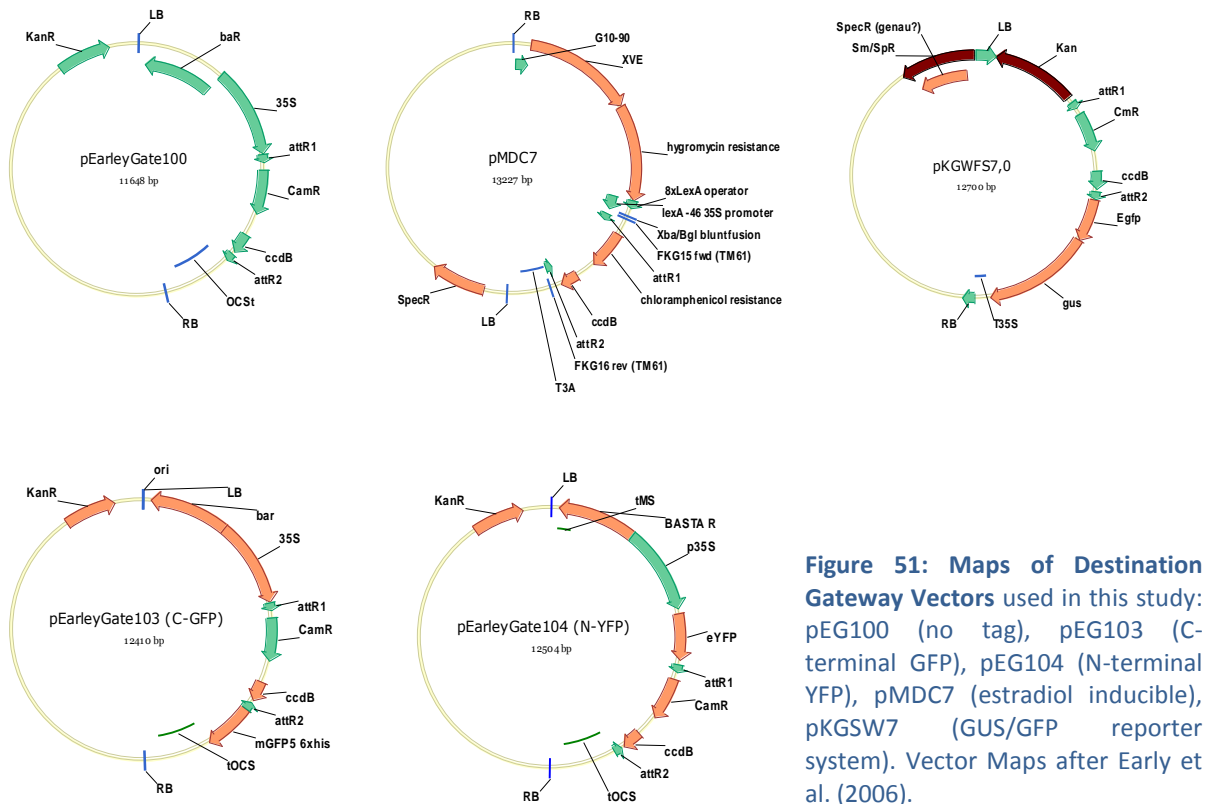


Figure 51: Maps of Destination Gateway Vectors used in this study: pEG100 (no tag), pEG103 (C-terminal GFP), pEG104 (N-terminal YFP), pMDC7 (estradiol inducible), pKGW7 (GUS/GFP reporter system). Vector Maps after Early et al. (2006).

### D.4.10. TOPO-TA cloning

TOPO TA Cloning Kits are designed for a rapid and easy cloning of PCR products, directly from a PCR reaction. In this study the Dual Promoter TOPO TA Cloning Kit pCR II-TOPO Vector (Invitrogen) was used. For a standard cloning reaction 2µl of a purified PCR-product together with 0.5µl salt solution, 0.5µl of the pCR II-TOPO vector and 2µl sterile water (all components provided in the kit) have been used. The reaction is then gently mixed and incubated at RT for 5 minutes.

### D.4.11. Cloning of PEX11 fusion proteins from yeast, human and plant

The coding regions of the *ArabidopsisAtPEX11A* (At1g01820), *AtPEX11B* (At3g47430), *AtPEX11C* (At1g47750), *AtPEX11D* (At2g45740) and *AtPEX11E* (At3g61070) as well as the human *HsPEX11α* (NP\_003838), *HsPEX11β* (NP\_003837), *HsPEX11γ* (NP\_542393) and the yeast *ScPEX11* (YOL147C), *ScPEX25* (YPL112C) and *ScPEX27* (YOR193W) were amplified using the primers in Table 6.

The purified cDNAs from *AtPEX11C*, *AtPEX11E* and *AtPEX11D* were directly cloned into the pENTR4 gateway vector with the help of the XhoI and NcoI sites and checked by PstI digestion. The cDNA from *AtPEX11A* and *AtPEX11B* were first cloned into a pCRII-Topo TA vector and checked with a PvuI digest before transferring them into a pENTR4 gateway vector. The resulting pENTR4-PEX11 entry plasmids from yeast, human and plants were sequenced and used for a Gateway recombination reaction into the binary plant expression vector pEarlyGate104 (Earley et al. 2006).

In addition a non-tagged version of the *AtPEX11D* was designed using an estradiol inducible pMDC7 binary vector (Curtis and Grossniklaus 2003).



Oligonucleotides	Sequence (5'-3')	Description
Pex11A-Hs-5	CCATGGACGCCTTCACCCG	Fwd-HsPEX11 $\alpha$ in pENTR4 (NcoI)
Pex11A-Hs-6	CTCGAGCTAACGGGTCTTCAGCTTCATCTGAGG	Rev-HsPEX11 $\alpha$ in pENTR4 (XhoI)
Pex11B-Hs-5	CCATGGACGCCTGGGTCCG	Fwd-HsPEX11 $\beta$ in pENTR4 (NcoI)
Pex11B-Hs-6	CTCGAGTCAGGGCTTGAGTCGTAGCCAGG	Rev-HsPEX11 $\beta$ in pENTR4 (XhoI)
Pex11G-Hs-1	TGGATCCGGATGGCGTCGCTGAGCGGCCTGG	Fwd-HsPEX11 $\gamma$ in pENTR4 (BamHI)
Pex11G-Hs-2	CTCGAGTCAGGGGGTAGTGGCCTCGGCCT	Rev-HsPEX11 $\gamma$ in pENTR4 (XhoI)
Pex11-y-6	GGATCCGGCTTAAGTGGACTGG	Fwd-ScPEX11 in pENTR4 (BamHI)
Pex11-y-7	CTCGAGTCAATCTTTTGAAGAGCAAAGTGACCT	Rev-ScPEX11 in pENTR4 (XhoI)
Pex25-y-6	GGATCCGGCTTAAGTGGACTGG	Fwd-ScPEX25 in pENTR4 (BamHI)
Pex25-y-7	CTCGAGTCAATCTTTTGAAGAGCAAAGTGACCT	Rev-ScPEX25 in pENTR4 (XhoI)
Pex27-y-9	GGGGACAAGTTTGTACAAAAAGCAGGCTGCACCATGACATCC GATCCTGTTAAT	Fwd-ScPEX27 in pDONOR
Pex27-y-10	GGGGACCACTTTGTACAAGAAAGCTGGGTTCAAACAGCGCTTGT ATGTTT	Rev-ScPEX27 in pDONOR
Pex11-ARA-1	CGGCCATGGGTACCCCTTGAGACCACAAG	Fwd-AtPEX11-1 in pENTR4 (NcoI)
Pex11/1-ARA-11	GCG CTC GAG TCA GAC CAT CTT GGA CTT GGG	Rev-AtPEX11-1 in pENTR4 (XhoI)
Pex11-ARA-3	CGGCCATGGCTACACTAGATTTGACCAGAG	Fwd-AtPEX11-2 in pENTR4 (NcoI)
Pex11/2-ARA-12	GCG CTC GAG TCA AGG TGT CTT CAA CTT GGG G	Rev-AtPEX11-2 in pENTR4 (XhoI)
Pex11-ARA-5	CGGCCATGGCTACGAAAGCTCCAGAGAAA	Fwd-AtPEX11-3 in pENTR4 (NcoI)
Pex11/3-ARA-13	GCG CTC GAG TCA ACA AGA GAT CCA GTT CTT ATG	Rev-AtPEX11-3 in pENTR4 (XhoI)
Pex11-ARA-7	CGGCCATGGCTTTGGACACTGTGGACAAAC	Fwd-AtPEX11-4 in pENTR4 (NcoI)
Pex11/4-ARA-14	GCG CTC GAG TCA CGA TGG CCA GTT CCT ATA C	Rev-AtPEX11-4 in pENTR4 (XhoI)
Pex11-ARA-9	CGGCCATGGGGACGACGTTAGATGTATCA	Fwd-AtPEX11-5 in pENTR4 (NcoI)
Pex11/5-ARA-15	GCG CTC GAG TCA GGG TGT TTT GAT CTT GGG	Rev-AtPEX11-5 in pENTR4 (XhoI)
FK304	GGGG ACA AGT TTG TAC AAA AAA GCA GGC TGC GTC GAC ATG GTG AGC AAG GGC GAG GAG	Fwd-mCherry-SKL BP cloning in pDONOR <sup>Zeo</sup> (Sall/XbaI)
FK463	GGGG AC CAC TTT GTA CAA GAA AGC TGG GTC TAG A TTA CAG TTT GGA CTT GTA CAG CTC GTC CAT G	Rev-mCherry-SKL BP cloning in pDONOR <sup>Zeo</sup>

Table 6: Primers used for the amplification of the various PEX11 gen members from yeast, human and plant.

As a control, a red fluorescent peroxisomal marker protein PST1 (mCherry-SKL) was produced via a BP Gateway reaction into the pDONOR plasmid (Invitrogen). The donor vector was then used for an LR gateway recombination into the estradiol inducible pMDC7 binary expression vector (Curtis and Grossniklaus 2003).

### D.4.11. Mutagenesis of the full length AtPEX11D promoter

In the Figure 52 below, the full-length promoter sequence of the *AtPEX11D* (AT2G45740) promoter is shown (sequence obtained from TAIR-database) as well as a scheme, showing the exact position of the primers to clone the various deletion constructs.

#### **Full lenght promotor sequence of AtPEX11-5 (AT2G45740): 732bp large**

gagactgcagttatgtttggttagtttcagttctgattacaaataaagtgaatggcggattagtaagtaaaacccctaactacacgactaaagggtttgtc  
ggttaataaagagcggtttaaattgtaataattaaggccaaggtagagccatttaggtgaaacattattggccttaagagtgtattgccccaaat  
aaatgtaaaaaatccacgtggaattcaatctgtgtcctagatatgtgtgccacgtggtggagcgcgcaaatatcctcaactccgaaagcaga  
gtgggagaggatgatccaatgtggtgtacacagtacacataaaaaagagtaacatgatcaacggcttagaatgaaagattgaagagatgagtgc  
gttgacccaacgacgtgtttgtctgttatcggaacgaagatgaccaaacaagccctatctcgattacacacacaatcaaaagaagatcaag  
ccaaaaacagaggcattgcgaatttaattgatcactctctctctatctgttcacacatctctccaaagggtatttcgaatcgaaattctttgattctt  
ctatgattgtttacatttttcgtggtgtcttgattttttcttgatcaaaactagtagaaatttccaatttcgtcctgccttgtagtagtagatatttgaa  
tttgattagtaggtagaagaag

ΔIII oligo : red-green	ΔII oligo: green-blue
ΔIa oligo: blue-violet	ΔIb oligo : violet-gray
ΔIa/Ib oligo: blue-gray	ΔIII/II oligo: red-blue

**Figure 52: Full-lenght promotor sequence of *AtPEX11D* and the localisation of the primer pairs used for the cloning of the deltion constructs.**

The primers used for the in vitro mutagenesis of the *AtPEX11D* promoter are listed in Table 6.

The obtained PCR fragments are carrying a BP cloning site for recombination into a pDONR vector, followed by LR gateway cloning into the pKGWs7 gateway vector (Gateway cloning: Figure 13).

Oligonucleotides	Sequence (5'-3')	Description
FK520	gagactgcagttatgtgccccaaataaatg 76, 6 °C	promotor studies AtPEX11-5, mutagenesis delta III oligo fw
FK521	catttatttggggcacataactgcagtctc 76, 6 °C	promotor studies AtPEX11-5, mutagenesis delta III oligo rev
FK522	tgccccaaataaatggaggatgatccaatg 76, 6 °C	promotor studies AtPEX11-5, mutagenesis delta II oligo fw
FK523	cattggatcatcctccatttatttggggca 76, 6 °C	promotor studies AtPEX11-5, mutagenesis delta II oligo rev
FK524	gaggatgatccaatgagatgaccaaacaag 76, 6 °C	promotor studies AtPEX11-5, mutagenesis delta Ia oligo fw
FK525	cttgtttggtcatctcattggatcatcctc 76, 6 °C	promotor studies AtPEX11-5, mutagenesis delta Ia oligo rev
FK526	agatgaccaaacaagacatctctcccaaag 76, 6 °C	promotor studies AtPEX11-5, mutagenesis delta Ib oligo fw
FK527	ctttgggagagatgtcttgtttggtcatct 76, 6 °C	promotor studies AtPEX11-5, mutagenesis delta Ib oligo rev
FK528	Gaggatgatccaatgacatctctcccaaag 77, 9°C	promotor studies AtPEX11-5, mutagenesis delta Ic olig fw
FK529	ctttgggagagatgtcattggatcatcctc 77, 9°C	promotor studies AtPEX11-5, mutagenesis delta Ic olig rev
FK530	gagactgcagttatggaggatgatccaatg 77, 9°C	promotor studies AtPEX11-5, mutagenesis delta III + II oligo fw
Fk531	cattggatcatcctccataactgcagtctc 77, 9°C	promotor studies AtPEX11-5, mutagenesis delta III + II oligo rev

Table 7: Primers used for the cloning of the five different deletion constructs of the *AtPEX11D* promoter.

## D.5. RNA

### D.5.1. RNA isolation with TRIzol from plant material

Homogenize 100-200mg plant tissue without thawing and add 500µl TRIzol per 100mg and vortex vigorously. Incubate for 5min at room temperature and centrifuge 10min, at 4°C with 16000g. Transfer the supernatant into a fresh tube and add 100µl chloroform per 100mg tissue, vortex vigorously. Centrifuge for 15min at 4°C with 16000g and transfer upper, transparent phase into fresh tube. Add 1µl DNase (1U) and 1µl RNasin and vortex. Incubate for 15min at room temperature. Add first 300µl TRIzol then 50µl chloroform and vortex after each step. Centrifuge for 5min at 4°C with 16000g and transfer upper, transparent phase into fresh tube. Precipitate RNA with 1 volume isopropanol (-20°C) and 3M sodium acetate pH 5,5. Invert the tube three times and incubate 10min at -20°C. Centrifuge for 30min at 4°C with 16000g and remove supernatant. Wash the pellet twice with 0,5ml 80% ethanol (-20°C) and centrifuge (5min, 4°C, 16000g). Wash the pellet again with 0,5ml 99% ethanol (-20°C), centrifuge (5min,

4°C, 16000g). Remove the ethanol completely and dry the pellet. Dissolve it in 10-25µl DEPCwater. Run the RNA on an agarose gel to estimate RNA concentration. Prepare a 2% agarose gel in TBE (89mM tris, 2mM EDTA, 89mM boric acid) and load 1µl RNA .

### **D.5.2. Reverse transcriptase (RT) reaction**

For a standard RT reaction 2µg RNA together with 20pM 3' or polyT primer are used and filled up to final volume of 12,5µl with DEPC water. Incubate then 10min at 70°C and add following components to the reaction:

- 2µl 10mM dNTPs
- 4µl 5x RT buffer (Promega)
- 0,5µl RNAsin (Promega)

Incubate for 5min at 37°C and add 1µl reverse transcriptase (AMV-RT fromPromega). Incubate for 1,5h at 42°C and add 1µl reverse transcriptase. Incubate again for 1,5h at 42°C and afterwards for 10min at 70°C. Add 1µl RNaseA and store at 4°C for up to two weeks. For a PCR reaction 2µl are used.

## **D.6. Microscopy and photography**

### **D.6.1. Stereo microscopy**

Samples were analyzed using the Zeiss Discovery V12 Stereo-microscope and documented with the AxioCamMRc5 Zeiss color camera or with the LeicaEL600 microscope and pictures were taken with the LeicaDFC300FX colure camera.

### **D.6.2. Light microscopy**

GUS stained plant parts and cross sections were analyzed using the ZEISS Axio Imager M1 upright microscope. Pictures were taken using an AxioCamMRc5 Zeiss colore camera and AxioVision software.

### D.6.3. Confocal microscopy of plant peroxisomes

#### Sample preparation

For the analyses and quantification of peroxisomes, infiltration experiments in *N. benthamiana* were performed. The infiltrated leaf parts were removed 48h after infiltration and incubated in 500µl of a 100µM F-actin depolymerizing Cytochalasin D (Sigma, in DMSO) solution for 0.5 hours. This treatment led to immobile but otherwise normal PX (Mathur et al. 2002) and therefore allows high resolution imaging of the epidermal plant cells and peroxisomes (Koch et al 2010).

#### Settings

All confocal images of plant cells were acquired with a LeicaTCS SP microscope utilising a Kr/Ar laser and the following settings: The excitation of YFP and cherry-SKL were performed at 476nm/568nm and detected at 500-535nm/ 600-635nm, respectively. The auto fluorescence of chloroplasts was detected at 665-795nm. The pinhole was set to 1.5 Airy Units (AU) and the detector gain and amplifier offset was adjusted to avoid clipping (Koch et al. 2010).

### D.6.4. Statistical analyses

To evaluate the total number of peroxisomes we included free and clustered peroxisomes from at least three independent infiltration experiments per construct. In each infiltration experiment at least 10 expressing epidermal cells were scanned. All images were processed using ImageJ (Collins 2007). Usually, images were despeckled (radius 1.0) and converted to 8-bit. To highlight the peroxisomal associated fluorescence a “Maximum Entropy” threshold was set using the “Multithresholder”.

To measure all fluorescently tagged peroxisomes in epidermal cells we performed 20µm deep z-stack projections (6 z-scans, distance 4 µm). The particle analysis feature of ImageJ was used to count the number and average size of peroxisomes and clusters in pixel<sup>2</sup>. These data set has been used to calculate the average size of PX in µm<sup>2</sup> (using following calculation: pixel<sup>2</sup> x 0,0596044775390625). The actual size (diameter) of peroxisomes was calculated with the formula:  $d = 2 \times (\text{square root } A/\pi)$  ( $\pi = 3,141596$ ). Peroxisomes have been divided into six categories concerning their size and area: I (very small PX), II (small PX), III (normal PX), IV (large PX), A (small cluster) and B (large cluster) see table 8 below.

	Category I	Category II	Category III	Category IV	Category A Small cluster	Category B Large cluster
Diameter [ $\mu\text{m}$ ]	0.0-0.5	0.51-0.87	0.88-1.9	1.91-2.75	2.76-6.16	6.17-27.55
Area [ $\mu\text{m}^2$ ]	0-0.21	0.21-0.59	0.59-2.98	2.98-5.96	5.96-29.80	29.80-596.04

**Table 8: Six categories of peroxisomal size were assigned:** Category I and II for very small and small peroxisomes (0.0-0.87 $\mu\text{m}$  in diameter), Category III for normal sized peroxisomes (0.88-1.9 $\mu\text{m}$ ) and categories IV for enlarged peroxisomes (1.91-2.75 $\mu\text{m}$ ). The categories A and B represents small (2.96-7.16 $\mu\text{m}$ ) and large peroxisomal cluster (6.17-27.55 $\mu\text{m}$ ) formed after over-expression of the different PEX11 fusion proteins.

To evaluate the total number of peroxisomes we have to include the peroxisomes located in small and large clusters (category V and VI). Therefore we used high resolution scans (63x or 100x Objective, single xy scans) to measure the diameter of peroxisomes within clusters. The resulting average peroxisomal diameter allowed us to calculate the number of peroxisomes within clusters using the average area of clusters ( $AK = d^2 * \pi/4$ ).

An example is shown below in Figure 15 for the human HsPEX11 $\gamma$  fusion protein.

- A single peroxisome is 1.1 $\mu\text{m}$  in diameter =  $d^2 * \pi/4$  (evaluated by 5 individual high resolution images of PX clusters).
- $AK = d^2 * \pi/4$ :  $(1.1^2 * 3.14159)/4 = 0.9\mu\text{m}^2$
- The total area of the cluster is 59  $\mu\text{m}^2$  (calculated by the ImageJ program).
- Therefore the total number of peroxisomes in the cluster is 65:  $59\mu\text{m}^2 / 0.9\mu\text{m}^2 = 65$

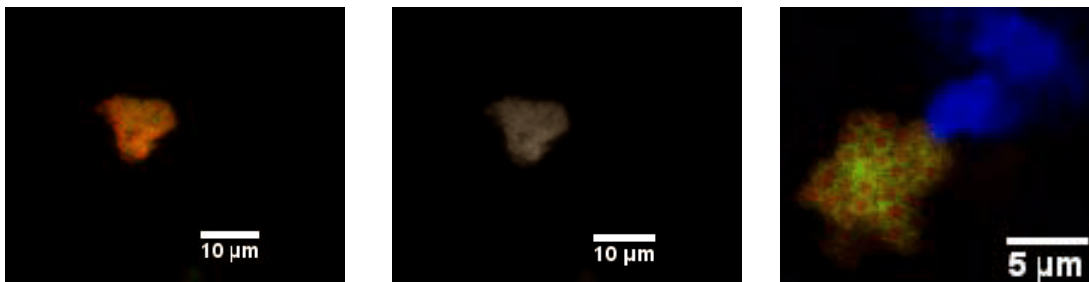


**Figure 53: A high-resolution image of the human HsPEX11 $\gamma$  fusion protein for.**

#### D.6.5. Digital photography

All photographs were taken using the digital camera Olympus E-410 carrying the objectives Olympus Zuiko Digital (35mm 1:3.5 Macro,  $\emptyset$  52) or the Olympus Digital (14-42mm 1:3.5-5.6).

## Supplemental

A

Average area covered by peroxisomes per cell:

	control	ScPEX11	ScPEX25	ScPEX27	HsPEX11α	HsPEX11β	*n/d	HsPEX11γ	AtPEX11A	AtPEX11B	AtPEX11C	AtPEX11D	AtPEX11E
Average	27,54939	12,60371	42,1991	104,2875	24,05842			052,03374238	16,31454451	25,35912013	16,72562218	18,98414833	13,04230996
StDev	9,845874	4,053475	13,42035	31,92961	10,80095			034,93608802	5,39403751	8,885207741	6,766582513	6,138126102	5,863481451
StErrMeans	1,392417	0,71656	2,45021	5,829522	1,825694			06,378427827	0,91175875	1,622209569	1,1437612	1,120663376	0,991109259

Average number of peroxisomes per cell:

	control	ScPEX11	ScPEX25	ScPEX27	HsPEX11α	HsPEX11β	*n/d	HsPEX11γ	AtPEX11A	AtPEX11B	AtPEX11C	AtPEX11D	AtPEX11E
Average	25,45906	23,27341	30,98818	74,84547	29,28359			059,69709384	18,12461435	58,75035211	50,66942287	52,77477376	28,72993653
StDev	3,641077	7,4418	7,982154	18,39942	10,19508			025,10276923	6,008461538	20,48063077	18,04458462	14,29230769	12,91561538
StErrMeans	0,664767	1,358681	2,439342	3,359258	3,914756			04,583076923	1,096989974	3,739234488	3,294461538	2,609406441	2,358057963

B

B													
	control	ScPEX11	ScPEX25	ScPEX27	HsPEX11α	HsPEX11β	HsPEX11γ	AtPEX11A	AtPEX11B	AtPEX11C	AtPEX11D	AtPEX11E	
Sum I-IV	83,06866	2,396829	50,4725	52,46959	11,52682	0	12,27691	3,945272	4,091217	0,842621	0,682398	1,38543	
StErrorMeans	2,610499	0,230096	1,757436	1,512655	1,067859	0	0,793972	0,358189	0,198544	0,080639	0,05118	0,111647	
Category A	16,93134	56,94115	49,5275	52,46959	51,63751	0	46,46959	47,36121	53,63905	50,81851	61,75507	44,63093	
StErrorMeans	2,127027	4,233484	4,70274	4,488259	2,137455	0	6,008608	4,500648	2,233624	4,204051	4,038043	4,105951	
Category B	0	40,66202	0	0	36,83567	0	41,2535	48,69352	42,26973	48,33887	37,56253	53,98364	
StErrorMeans	0	1,869998	0	0	4,27491	0	6,910112	4,927955	2,258793	3,689693	2,75041	4,338697	

Figure S1: Data set used for the statistical analysis of peroxisome (PX) abundance and area as well as the amount of PX localised in clusters.

(A) Summarized Data of 3 independent infiltration experiments peroxisome (PX) abundance and area 48h post infiltration per cell: Average area of all peroxisomes per cell in  $\mu\text{m}^2$ . Average number of peroxisomes per cell. Calculation of Standard error of means; n: representing approximately 190 cells. \*n/d = not determined.

(B) Summarized Data of 3 independent infiltration experiments counting the peroxisomes localised in the different categories in percentage % per cell:

Sum I-IV: all PX localised in the categories I to IV, representing small to large PX which are not clustered. **Category A:** Percentage of PX located in small clusters. **Category B:** percentage of PX located in large clusters; Calculation of Standard error of means; n= represent approximately 190 cells, n/d\* = not determined.

Definition of Categories see materials and methods chapter D.6.3, Table8.



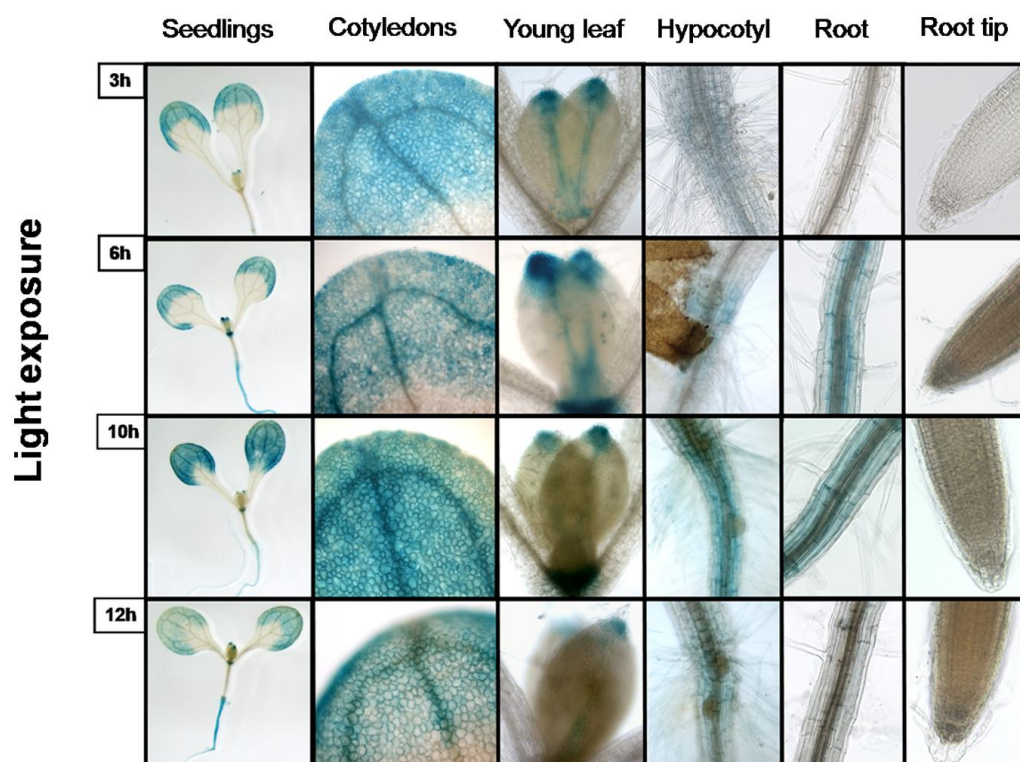


**Figure S2: Light exposure experiment of transgenic *A. thaliana* plants harbouring the minimal promoter of *AtPEX11D* driving a GUS reporter system.** 7days old seedlings were grown on ½ MS medium with 3% sucrose at 22°C and standard light conditions (16h light/ 8h dark). The GUS expression of these seedlings was analysed at 4 different light exposure time points (3h, 6h, 10h and 12h) and following plant organs have been analysed: overview of seedlings, cotyledons, young leaf, hypocotyls, root and root tip.

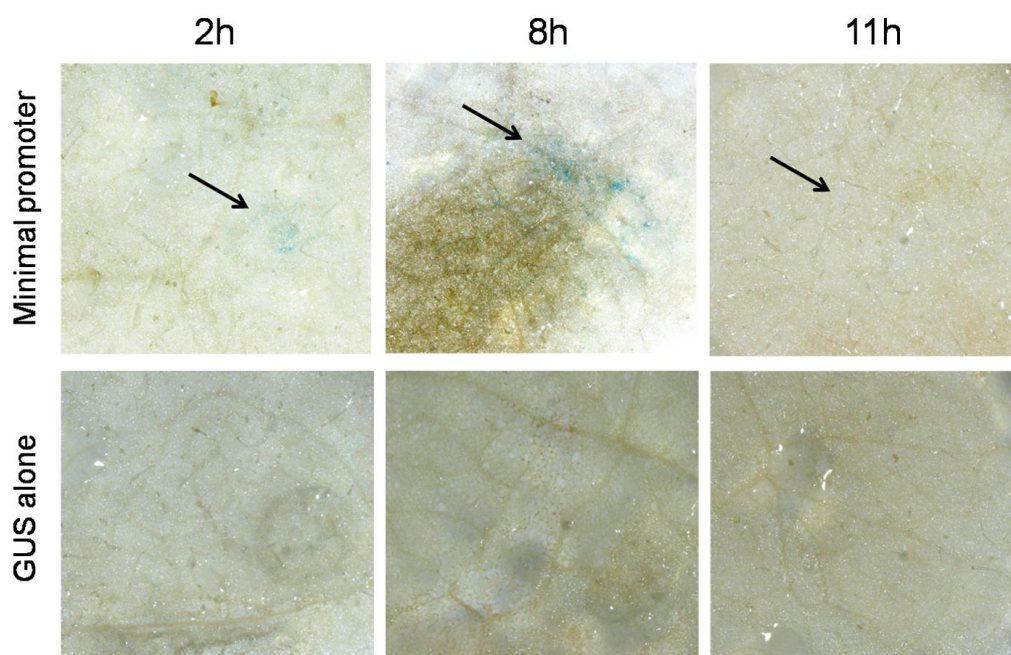


**Figure S3: Light exposure experiment of infiltrated *N. benthamiana* harbouring the minimal promoter of *AtPEX11D* driving a GUS reporter system.** A GUS staining of *N. benthamiana* leaves 24h *post* infiltration has been performed together control plants infiltrated with the GUS vector alone. The light exposure time points were 2h, 8h and 11h. No background activity of the GUS staining was observed in the plants infiltrated with the GUS vector alone, whereas a slight increase in the GUS expression after 8h of light exposure compared to 2h of light exposure could be observed. No GUS expression was detected after 11h of light exposure.

LIB-A					
ID	Results	ATG-Number	Orientation	AD-fusion	ORF
A76	Arabidopsis thaliana WAK2; ATP binding / calcium ion binding / protein kinase/	<a href="#">AT1G21270</a>	reverse	no AD fusion	no ORF, Frame 3: 1528-2161bp
A336	empty vector pGAD10	<a href="#">36574</a>			
A411	tubulin9	<a href="#">AT4G20890</a>	forward	AD fusion	ORF, 910bp until STOP
A447	empty vector pGAD10	<a href="#">36574</a>			
A451	empty vector pGAD10	<a href="#">36574</a>			
A537	splicing factor fragment/pGAD10	<a href="#">36574</a>	reverse		no ORF
A538	photosystem I subunit D	<a href="#">AT1G03130.1</a>	forward		
A541	empty vector pGAD10	<a href="#">36574</a>			
A546	CAB1 chlorophyll binding protein 1	<a href="#">AT1G29830</a>	reverse	no AD fusion	
A547	TCTP (translationally controlled tumor protein)	<a href="#">AT3G16640</a>	reverse	no AD fusion	ORF1: full length CDS of TCTP
A548	unknown protein	<a href="#">AT4G13630</a>	forward	no AD fusion	no ORF
A550	malate dehydrogenase	<a href="#">AT1G79750</a>	reverse	no AD fusion	no ORF only 30 bp until first STOP
A564	ATP ADP antiporter	<a href="#">AT3G08580</a>	reverse	no AD fusion	
A569	empty vector pGAD10	<a href="#">36574</a>			
A574	empty vector pGAD10	<a href="#">36574</a>			
A581	empty vector pGAD10/ used for negative control	<a href="#">36574</a>	reverse	no AD fusion	
A592	Arabidopsis thaliana MAM1 (METHYLTHIOALKYLMALATE SYNTHASE 1); 2- isopropylmalate synthase/ methylthioalkylmalate synthase (MAM1) mRNA, complete cds	<a href="#">AT5G23010</a>	forward		
A595	empty vector pGAD10	<a href="#">36574</a>	reverse	no AD fusion	no ORF, Frame 3 704-870bp aligns with full length CDS ORF 1: very short sequence until STOP, ORF3 full length CDS of MSS
A600	Fbox protein	<a href="#">AMG08098</a>	reverse	no AD fusion	
A602	MSS3 (multicopy suppressors of snf4 deficiency in yeast3)	<a href="#">AT2g43290</a>	reverse	no AD fusion	
A622	Arabidopsis thaliana ribulose biphosphate carboxylase small chain 2B / RuBisCO small subunit 2B (RBCS-2B) (ATS2B) (AT5G38420) mRNA, complete cds	<a href="#">AT5G38420</a>	forward		
A623	Arabidopsis thaliana SDH3-2; succinate dehydrogenase (SDH3-2) mRNA, complete cds	<a href="#">AT4G32210</a>	reverse	no AD fusion	
A625	16sRNA	<a href="#">ATCG00920</a>	reverse	no AD fusion	
A639	TCTP translational D tumor protein/ Arabidopsis thaliana TCTP (TRANSLATIONALLY CONTROLLED TUMOR PROTEIN) (TCTP) mRNA, complete cds	<a href="#">AT3G16640</a>	reverse	no AD fusion	no ORF, Frame 3
A644	Arabidopsis thaliana 60S ribosomal protein L31 (RPL31B) (AT4G26230) mRNA, complete cds	<a href="#">AT4G26230</a>	reverse	no AD fusion	
A645	Arabidopsis thaliana ribulose biphosphate carboxylase small chain 3B / RuBisCO small subunit 3B (RBCS-3B) (ATS3B) (AT5G38410) mRNA, complete cds	<a href="#">AT5G38410</a>	forward		
A650	unknown protein Blast NCBI pGAD10 vector	<a href="#">AT1G30190.1</a>	reverse	no AD fusion	no ORF, only 10bp alignment
A651	plant U-box 9, PUB9	<a href="#">AT3G07360</a>	forward	AD fusion	only 100bp very short sequence until first STOP, 1295-1348bp
A653	GRP-3	<a href="#">AT2G05520</a>	reverse	no AD fusion	Frame 3: 323-490
A655	Arabidopsis thaliana putative fatty acid elongase 3-ketoacyl-CoA synthase 1 (At1g01120) mRNA, complete cds	<a href="#">AT1g01120</a>	forward		ORF1 ORF1, gegen CDS align von 1135-1920bp
A657	radical SAM, TRAM protein domain	<a href="#">AMG36390</a>	reverse	no AD fusion	ORF1, ORF2 180-423 and then again from 451-1025bp
A658	integral membrane protein/ Arabidopsis thaliana integral membrane family protein (AT1G78620) mRNA, complete cds	<a href="#">AT1G78620</a>	forward	no AD fusion	
A659	empty vector pGAD10, based on PCR	<a href="#">36574</a>			
A669	GDSL-motif lipase/hydrolase family	<a href="#">AT4G18970</a>	reverse	no AD fusion	no ORF with no Frame no alignment with full CDS at all
A670	chloroplast-encoded 23S	<a href="#">ATCG01180</a>	forward		
A671	LHCA4 (LIGHT-HARVESTING CHLOROPHYLL-PROTEIN COMPLEX I SUBUNIT A4); chlorophyll binding (LHCA4) mRNA general regulatory factor 3 GRFGRF3, RC1   GRF3 (GENERAL REGULATORY FACTOR 3); ATP binding / protein binding / protein phosphorylated amino acid binding	<a href="#">AT3G47470</a>	forward		
A680	tRNA-Thr	<a href="#">AT5G38480.1</a>	reverse	no AD fusion	no ORF no alignment with CDS at all
A681	chloroplast DNA	<a href="#">ATCG00390.1</a>	reverse	no AD fusion	no ORF
A682	empty pGAD10 vector	<a href="#">ATCG01180</a>			
A683	empty pGAD10 vector	<a href="#">36574</a>			
A684	empty pGAD10 vector	<a href="#">36574</a>			
A685	transcription factor SOL1 (-TSO1-like)	<a href="#">AT3G22760</a>	forward	no AD fusion	no ORF, Frame 3 aligns with full length CDS from 293-1301bp 1-231bp, full length 231bp, full length CDS
A686	unknown protein	<a href="#">36574</a>			
A687	empty vector pGAD10, based on PCR	<a href="#">AT2G01021</a>	forward		ORF about 500bp before stop
A688	unknown protein, RNA repeat unit				
A689	empty vector pGAD10, based on PCR				
A690	empty vector pGAD10, based on PCR				
A691	4F5 protein-related, unknown protein	<a href="#">AT4G13615</a>	forward	AD fusion	ORF until Stop 291bp, full length protein from database 366bp
A692	PSAK (photosystem I subunit K)	<a href="#">AT1G30380.1</a>	forward		
A694	chloroplast-encoded 23S	<a href="#">ATCG01180.1</a>	reverse	no AD fusion	no ORF
A695	peroxidase putative	<a href="#">AT5G64120</a>	forward	no AD fusion	no ORF
A696	empty vector pGAD10	<a href="#">36574</a>			
A697	empty vector pGAD10, based on PCR	<a href="#">36574</a>			
A698	empty vector pGAD10, based on PCR	<a href="#">36574</a>			
A699	CP29, poly(U) binding	<a href="#">AT3G53460</a>	forward	AD fusion	ORF only 156bp until Stop
A701	empty vector pGAD10, based on PCR	<a href="#">36574</a>			
A704	empty vector pGAD10, based on PCR	<a href="#">36574</a>			

LIB-A					
ID	Results	ATG-Number	Orientation	AD-fusion	ORF
A705	empty vector pGAD10, based on PCR	<a href="#">36574</a>			
A706	empty vector pGAD10, based on PCR	<a href="#">36574</a>			
A707	rev FK726/pGAD 10	<a href="#">36574</a>			
A708	empty vector pGAD10, based on PCR	<a href="#">36574</a>			
A709	empty vector pGAD10, based on PCR	<a href="#">36574</a>			
	GUN5, magnesium chelatase/Arabidopsis thaliana GUN5 (GENOMES UNCOUPLED 5); complete cds				
A713		<a href="#">AT5G13630</a>	reverse	no AD fusion	no ORF, 3458-4077bp alingnt with CDS full lenght 4146bp
A714	40s, ribosomal protein S4	<a href="#">AT2G17360</a>	forward		no ORF
	Arabidopsis thaliana PSAE-1 (PSAE1 KNOCKOUT); catalytic (PSAE-1) mRNA, complete cds	<a href="#">AT4G28750</a>	reverse	no AD fusion	no ORF
A716	empty vector pGAD10, based on PCR	<a href="#">36574</a>			
A719	empty vector pGAD10, based on PCR	<a href="#">36574</a>			
A720	empty vector pGAD10, based on PCR	<a href="#">36574</a>			
A722	unknown protein	<a href="#">AT5G48480</a>	forward	no AD fusion	no ORF, no alignmet with CDs at all, only 30bp until first STOP
A724	sequence very bad		reverse		
A726	LHC82.2, LHC82   LHC82.2; chlorophyll binding	<a href="#">AT2G05070</a>	reverse	no AD fusion	no ORF
A731	TCTP	<a href="#">AT3G16640</a>	reverse	no AD fusion	no ORF
A733	Arabidopsis thaliana (AT3G41768) rRNA	<a href="#">AT3G41768</a>	forward		
A735	pGAD10 vector	<a href="#">36574</a>			
A741	RRN23S.2   chloroplast-encoded 23S ribosomal RNA	<a href="#">ATCG01180</a>	forward		
	MT2Bmethionin 2B/Arabidopsis thaliana MT2B (METALLOTHIONEIN 2B); copper ion binding				
	(MT2B) mRNA, complete cds.				
A743		<a href="#">AT5G02380</a>	forward	Ad fusion	ORF3: 1-121bp full lenght 234bp
A745	Gluthation transferase, ATGSTU20	<a href="#">AT1G78370.1</a>	reverse	no AD fusion	no ORF
A746	empty vector pGAD10	<a href="#">36574</a>	forward		
A747	putative photosystem I	<a href="#">AT1G55670</a>	reverse	no AD fusion	no ORF
	thioredoxin 3 ATTRX3/Arabidopsis thaliana ATTRX3 (THIOREDOXIN 3); oxidoreductase, acting on sulfur group of donors, disulfide as acceptor (ATTRX3)mRNA, complete cds.				
A752		<a href="#">A5G42880</a>	reverse	no AD fusion	ORF2: 1-223 (full lenght 501bp) sequence has a lot of punct mutation
	eukaryotic tranArabidopsis thaliana eukaryotic translation initiation factor SUI1 family protein (AT5G11900) mRNA, complete cdsslation factor SUI1/	<a href="#">AT5G11900</a>	reverse	no AD fusion	no ORF, ATG 1-492bp alingnt with CDS, full length 597bp
A753	Arabidopsis thaliana eukaryotic translation initiation factor SUI1 family protein (AT5G11900) mRNA, complete cds	<a href="#">AT5G11900</a>	reverse	no AD fusion	no ORF
A755		<a href="#">AT5G11900</a>	reverse	no AD fusion	no ORF, 1163-1405 full length 1887bp
A757	Symbols: VSR-2   VSR-2; calcium ion binding	<a href="#">AT2G14720.2</a>	reverse	no AD fusion	no ORF 3; Frame 2 1-289bp full lenght CDS 663bp
A767	serine-rich protein related	<a href="#">AT5G25280</a>	forward	no AD fusion	
A771	unkown protein, sequence very bad, looks like pGAD10	<a href="#">36574</a>			
A772	pGAD10 vector	<a href="#">36574</a>			
A780	Arabidopsis thaliana DJ-1 family protein / protease-related (AT3G02720)	<a href="#">AT3G02720.1</a>	reverse	no AD fusion	Frame 1: 949-1168bp; full length 1167bp
A784	Arabidopsis thaliana ATL5 (A. THALIANA RIBOSOMAL PROTEIN L5); 5S rRNA binding / structural constituent of ribosome (ATL5)mRNA, complete cds	<a href="#">AT3G25520</a>	forward		no ORF
LIB-B					
ID	Results	ATG-Number	Orientation	AD-fusion	ORF
B79	Arabidopsis thaliana LHC83 (LIGHT-HARVESTINGCHLOROPHYLLB-BINDING PROTEIN 3); structural molecule (LHC83) mRNA, complete cds	<a href="#">AT5G54270</a>	reverse	no AD fusion	
	Arabidopsis thaliana RBCS1A (RIBULOSE BISPHOSPHATE CARBOXYLASE SMALL CHAIN 1A); copper ion binding / ribulose-bisphosphate carboxylase (RBCS1A) mRNA, complete cds	<a href="#">AT1G67090</a>	reverse	no AD fusion	
B85	empty vector pGAD10	<a href="#">36574</a>	reverse		
B111	empty vector pGAD10	<a href="#">36574</a>	reverse		
B162	empty vector pGAD10	<a href="#">36574</a>	reverse		
	Arabidopsis thaliana leucine-rich repeat family protein (AT2G17440) mRNA, complete cds	<a href="#">AT2G17440</a>	forward	no AD fusion	no ORF, 1253-1578bp, only STOP missing at the end,
B197		<a href="#">36574</a>	reverse		
B227	empty vector pGAD10	<a href="#">36574</a>	reverse		

**S4: Sequencing data of all yeast one hybrid candidates re-grown on SC-drop out medium. Orientation:** orientation of the inserted fragment (candidate) in the pGAD10 vector. **AD-fusion:** are the candidates in an ORF with the promoter. **ORF:** open reading frame.

### Abbreviations

**ABA** abscisic acid

**AMS** aberrant membrane structures

**ER** endoplasmic reticulum

**JA** jasmonates

**GA** gibberellic acid

**HEK** human embryonic kidney

**MeJA** methyl jasmonate

**MS-medium** Murashig and Skoog medium

**ORE** oleate-responsive element

**PMP** peroxisomal membrane protein

**PPAR** peroxisome proliferator activated receptor

**PPRE** peroxisome proliferator responsive element

**PTS** peroxisomal targeting sequence

**ROS** reactive oxygen species

**RT** room temperature

**PX** peroxisome(s)

**PXC** peroxisomal cluster

**TMD** transmembrane domain

**SA** salicylic acid

**At** *Arabidopsis thaliana*

**Hs** *Homo sapiens*

**Sc** *Saccharomyces cerevisiae*

## Bibliography

- Abe I., and Fujiki Y. (1998). cDNA cloning and characterization of a constitutively expressed isoform of the human peroxin Pex11p. *Biochem. Biophys. Res. Commun.*, 252: 529-33.
- Andersen S.U., Algreen-Petersen R.G., Hoedl M., Jurkiewicz A., Cvitanich C., Braunschweig U., Schauser L., Oh S.A., Twell D., and Jensen E. (2007). The conserved cystein-rich domain of a tesmin/TSO1-like proetin binds zinc in vitro and TSO1 is required for both male and female fertility in *Arabidopsis thaliana*. *Journal of Experimental Botany*, 58(13): 3657-3670.
- Anton M., Passreiter M., Lay D., Thai T.P., Gorgas K., and Just W.W. (2000). ARF- and coatamer-mediated peroxisomal vesiculation. *Cell Biochem Biophys.*, 32:27-36.
- Ben-Tabou de-Leon S., Davidson E.H. (2007). Gene regulation: gene control network in development. *Annu Rev Biophys Biomol Struct*, 36: 191.
- Berger J., and Moller D.E. (2002). The mechanisms of action of PPARs. *Annu. Rev. ed.*, 53:09–35.
- Bliek A.M. (1999). Functional diversity in the dynamin family. *Trends in Cell Biology*, 9(3): 96-102.
- Brocard C., and Hartig A. (2006). Peroxisome targeting signal 1: is it really a simple tripeptide? *Biochim Biophys Acta.*, 1763(12): 1565-73.
- Brocard, C., and A. Hartig. (2007). Peroxins: A Proliferation Romance amongst Supposition and Disposition. *Dyn Cell Biol.*, 1: 1-11.
- Brown L.A. and Baker A. (2008). Shuttles and cycles: transport of proteins into the peroxisome matrix. *Mol Membr Biol.*, 25(5): 363-75.
- Bunkelmann J.R., and Trelease R.N. (2006). Ascorbate peroxidase. A prominent membrane protein in oilseed glyoxysomes. *Plant Physiol.*, 110: 589-598.
- Clay N.K., Aido A.M., Denoux C., Jander G. and Ausubel F.M. (2009). Glucosinolate metabolites required for an *Arabidopsis* innate immune response. *Science*, 323:95-01.
- Collins T.J. (2007). ImageJ for microscopy. *BioTechniques*, 43.
- Corpas F.J., Barroso J.B. and del Rio L.A. (2001). Peroxisomes as a source of reactive oxygen species and nitric oxide signal molecules in plant cells. *TRENDS in Plant Science* 6(4): 145-49.
- Cooper, T.G., and Beevers, H.J. (1969). Beta oxidation in glyoxysomes from castor bean endosperm. *J. Biol. Chem.*, 224: 3514-3520.
- Curtis M. and Grossniklaus U. (2003). A Gateway TM cloning vector set for high-throughput functional analysis of genes in plants. *Plant Physiology*, 133: 462-469.



- Davidson E.H. (2006). The Regulatory Genome: Gene Regulatory Networks in development and Evolution. Elsevier, 1–86.
- Davies P.J. (2004). Plant Hormones. Biosynthesis, Signal Transduction, Action! Book; Published by Springer, 1<sup>st</sup> edition.
- De Duve, C., and P. Baudhuin. 1966. Peroxisomes (microbodies and related particles). *Physiol Rev.*, 46: 323-57.
- Delker J.C., Zolman B.K., Miersch O., and Wasternack C. (2007). Jasmonate biosynthesis in *Arabidopsis thaliana* requires peroxisomal  $\beta$ -oxidation enzymes -Additional proof by properties of *pex6* and *aim1*. *Phytochemistry*, 68(12): 1642-650.
- del Río LR., Pastori G.M., Palma J.M., Sandalio L.M., Sevilla F., Corpas F.J., Jiménez A., López- Huertas E. and Hernández J.A. (1998). The Activated Oxygen Role of Peroxisomes in Senescence. *Plant Physiology*, 116(4): 1195-1200.
- Desai, M., and J. Hu. (2008). Light induces peroxisome proliferation in *Arabidopsis* seedlings through the photoreceptor phytochromeA, the transcription factor HY5 HOMOLOG, and the peroxisomal protein PEROXIN11b. *Plant Physiol.*
- Distel B., Erdmann R., Gould S.J., Blobel G., Crane D.I., Cregg J.M., Dodt G., Fujiki Y., Goodman J.M., Just W.W., Kiel J.A., Kunau W.H., Lazarow P.B., Mannaerts G.P., Moser H.W., Osumi T., Rachubinski R.A., Roscher A., Subramani S., Tabak F., Tsukamoto T., Valle J., van der Klei I., van Veldhoven P.P., and Veenhuis.(1996). A unified nomenclature for peroxisome biogenesis factors. *J Cell Biol.*, 135: 1-3.
- Earley K.W., Haag J.R., Pontes O., Opper K., Juehne T., Song K., Pikaard C.S. (2006). Gateway-compatible vectors for plant functional genomics and proteomics. *Plant* 45: 616–629.
- Erdmann, R., and Blobel G. (1995). Giant peroxisomes in oleic acid-induced *Saccharomyces cerevisiae* lacking the peroxisomal membrane protein Pmp27p. *J Cell Biol.*, 128: 509-23.
- Estelle M.A., and Somerville C. (1987). Auxin-resistant mutants of *Arabidopsis thaliana* with altered morphology. *Molecular and General Genetics*, 206(2): 200-206.
- Fagarasanu A., Fagarasanu M., and Rachubinsk R.A. (2007). Maintaining Peroxisome Populations: A Story of Division and Inheritance. *Annual Review of Cell and Developmental Biology*, 23: 321-344.
- Fang, Y., Morrell J.C., Jones J.M., and Gould S.J. (2004). *PEX3* functions as a *PEX19* docking factor in the import of class I peroxisomal membrane proteins. *J. Cell Biol.*, 164: 863–875.
- Fawcett C.H., Wain R.L., and Wightmann T. (1960). The metabolism of 3-indolylalkancarboxylic acids, and their amides, nitriles and methyl esters in plant tissues. *Proc R Soc Lond B Biol Sci.*, 152: 231-54.
- Foyer H., Bloom J., Queval G., and Noctor G., (2009). Photorespiratory Metabolism: Genes, Mutants, Energetics, and Redox Signaling. *Annual Review of Plant Biology*, 60: 455.



- Fujiki Y., Hubbard A.L., Fowler S., and Lazarow P.B. (1982). Isolation of intracellular membranes by means of sodium carbonate treatment: application to Endoplasmic ticulum. *JCB*, 93(1): 97-102.
- Fujiki Y. (2000). Peroxisome biogenesis and peroxisome disorders. *FEBS Letters* 476: 42-46.
- Gietz R.D. and Schiestl R.H. (2007). High-efficiency yeast transformation using the LiAc/SS carrier DNA/PEG method. *Nature Protocols*, 2(1): 31-34.
- Gould S.J., Keller G.A., Hosken N., Wilkinson J., and Subramani S. (1989). A conserved tripeptide sorts proteins to peroxisomes. *The Journal of Cell Biology*, 18: 1657- 664.
- Gurvitz A., Hiltunen J.K., Erdmann R., Hamilton B., Hartig A., Ruis H., and Rottensteiner H. (2001). *Saccharomyces cerevisiae* Adr1p Governs Fatty Acid  $\beta$ -Oxidation and Peroxisome Proliferation by Regulating POX1 and PEX11. *The Journal of Biological chemistry*, 276( 34): 31825–31830.
- Hauser B.A., He J.Q., Park S.O. and Gasser C.S. (2000). TSO1 is a novel protein that modulates cytokinesis and cell expansion in *Arabidopsis*. *Development* 127: 2219-2226.
- Hashimoto T. (1996). Peroxisomal  $\beta$ -Oxidation. *Enzymology and Molecular Biology*, 804: 86-98.
- Hayashi M., Toriyama K., Kondo M., and Nishimura M. (1998). 2,4-dichlorophenoxybutyric acid-resistant mutants of *Arabidopsis* have defects in glyoxysomal fatty acid  $\beta$ -oxidation. *The Plant Cell*, 10: 183-195.
- Hayashi M. and Nishimura M. (2006). *Arabidopsis thaliana*--A model organism to study plant peroxisomes. *Biochim Biophys Acta*, 1763(12): 1382-91.
- Hemerly A.S., Ferreira P., de Almeida Engler J., Van Montagu M., Engler G. and Inzé D., (1993). *cdc2a* expression in *Arabidopsis* is linked with competence for cell division. *Plant cell*, 5(12): 1711-1723.
- Hoepfner D., van den Berg M., Philippsen P., Tabak H.F., and Hettema E.H. (2001). A Role for Vps1p, actin, and the Myo2p motor in peroxisome abundance and inheritance in *Saccharomyces cerevisiae*. *Journal of Cell Biology*, 155(6): 979- 90.
- Hooft van Huijsduijnen R.A.M., Alblas S.W., De Rijk R.H. and Bol J.F. (1986). Induction by Salicylic acid of Pathogenesis-related Proteins and Resistance to Alfalfa Mosaic Virus Infection in Various Plant Species. *Journal of Genetic Virology*, 67: 2135-2143.
- Hinshaw J.E. (2000). Dynamin and its role in membrane fission. *Annual Review of Cell Development Biology*, 16: 483-519.
- Hu, J., Aguirre, M., Peto, C., Alonso, J., Ecker, J., and Chory, J. (2002). A role for peroxisomes in photomorphogenesis and development of *Arabidopsis*. *Science*, 297: 405–409.
- Hu J., Zhang A., Zhang J., and Jiang M. (2006). Abscisic Acid is a Key Inducer of Hydrogen Peroxide Production in Leaves of Maize Plants Exposed to Water Stress. *Plant cell Physiology*, 47(11): 1484-1495.

- Lazarow P.B., and Fujiki Y. (1985). Biogenesis of peroxisomes. *Annu Rev Cell Biol.* 1:489-530.
- Lopez-Huertas , Charlton W.L., Johnson B., Graham I.A. and Baker A. (2000). Stress induces peroxisome biogenesis genes. *The EMBO Journal*, 19: 6770 - 6777
- Jefferson R.A., Kavanagh T.A., and Bevan M.W., (1987). GUS fusions: beta-glucuronidase as a sensitive and versatile gene fusion marker, in higher plants. *EMBO J.*, 16(13): 3901–3907.
- Johnson T., and Olsen L.J. (2001). Building New Models for Peroxisome Biogenesis. *Plant Physiology*, 127:731-739.
- Karpichev I.V., Luo Y.I., Mariani R.C. and Small G.M. (1997). A Complex Containing Two Transcription Factors Regulates Peroxisome Proliferation and the coordinate Induction of  $\beta$ -Oxidation Enzymes in *Saccharomyces cerevisiae*. *Molecular and Cellular Biology*, 17(1): 69-80.
- Karpichev I.V., and Small G.M. (1998). Global Regulatory Functions of Oaf1p and Pip2p (Oaf2p), Transcription Factors That Regulate Genes Encoding Peroxisomal Proteins in *Saccharomyces cerevisiae*. *Molecular and cellular Biology*, 18(11): 6560–6570.
- Karnik S.K. and Trelease R.N. (2007). *Arabidopsis* peroxin 16 trafficks through the ER and an intermediate compartment to pre-existing peroxisomes via overlapping molecular targeting Signals. *Journal of Experimental Botany*, 58(7): 1677–1693.
- Kaur N., Reumann S. and Hu J. (2009). Peroxisome Biogenesis and Function. *The Arabidopsis Book*. The American Society of Plant Biologists: 1-41.
- Kaur N., and Hu J. (2009). Dynamics of peroxisomes abundance: a tale of division and proliferation. *Current Opinion in Plant Biology*, 12: 1-8.
- Kazan K., and Manners J.M., (2008). Jasmonate Signaling: Toward an Integrated View. *Plant Physiology*, 146(4): 1459–1468.
- Kim P.K., R.T. Mullen, U. Schumann, and J. Lippincott-Schwartz. 2006. The origin and maintenance of mammalian peroxisomes involves a de novo PEX16-dependent pathway from the ER. *Journal of Cell Biology*, 173: 521-32.
- Knoblauch B., and Rachubinski R.A. (2010). Phosphorylation-dependent Activation of Peroxisome Proliferator Protein PEX11 Controls Peroxisome Abundance. *J Biol Chem.* 6, 85(9): 6670-6680.
- Koch A., Thiemann M., Grabenbauer M., Yoon Y., McNiven M.A., and Schrader M. (2003). Dynamin-like Protein 1 Is Involved in Peroxisomal Fission. *The Journal of Biological Chemistry*, 278: 8597-8605.
- Koch A., Schneider G., Luers G.H., and Schrader M. (2004). Peroxisome elongation and constriction but not fission can occur independently of dynamin-like protein 1. *J Cell Sci.*, 117: 3995-4006.
- Koch A., Yoon Y., Bonekamp N.A., McNiven M.A., and Schrader M. (2005). A role for Fis1 in both mitochondrial and peroxisomal fission in mammalian cells. *Mol Biol Cell*, 16: 5077-5086.

- Koch J., Pranjić K., Huber A., Ellinger A., Hartig A., Kragler F., and Brocard C. (2010). PEX11 family members are membrane elongation factors that coordinate peroxisome proliferation and Maintenance. *Journal of Cell Science*, 123: 3389-400.
- Kornberg H.L., and Krebs H.A., (1957). Synthesis of Cell Constituents from C<sub>2</sub>-Units by a Modified Tricarboxylic Acid Cycle. *Nature*, 179: 988-991.
- Kragler F., Lametschwandtner G., Christmann J., Hartig A. and Harada J.J. (1998). Identification and analysis of the plant peroxisomal targeting signal 1 receptor NtPEX5. *PNAS*, 95: 13336–13341.
- Lazarow, P.B., and Y. Fujiki. 1985. Biogenesis of peroxisomes. *Annu Rev Cell Biol.*, 1: 489-530.
- Lee J., He K., Stolc V., Lee H., Figueroa P., Gao Y., Tongprasit W., Zhao H., Lee I., and Deng X.W. (2007). Analysis of Transcription Factor HY5 Genomic Binding Sites Revealed Its Hierarchical Role in Light Regulation of Development. *The Plant Cell*, 19: 731-749.
- Lemberger T., Desvergne B., and Wahli W. (1996). Peroxisome proliferator-activated receptors: a nuclear receptor signaling pathway in lipid physiology. *Annu Rev Cell Dev Biol.*, 12: 335-63.
- Leon J. (2008). Peroxisome proliferation in *Arabidopsis*. The challenging identification of ligand perception and downstream signalling closer. *Plant Signaling & Behavior*, 3(9): 671-673.
- Li X., Baumgart E., Morrell J.C., Jimenez-Sanchez G., Valle D., and Gould S.J. (2002a). PEX11 $\beta$  Deficiency Is Lethal and Impairs Neuronal Migration but Does Not Abrogate Peroxisome Function. *Mol Cell Biol.* 22(12): 4358–4365.
- Li X., Baumgart E., Dong G.X., Morrell J.C., Jimenez-Sanchez G., Valle D., Smith K.D., and Gould S. (2002b). PEX11 $\alpha$  Is Required for Peroxisome Proliferation in response to 4 Phenylbutyrate but Is Dispensable for Peroxisome Proliferator- Activated Receptor Alpha Mediated Peroxisome Proliferation. *Mol Cell Biol.*, 22(23): 8226–8240.
- Li X., and Gould S.J. (2002). PEX11 promotes peroxisome division independently of peroxisome metabolism. *JCB*, 156(4): 643-651.
- Li X., and Gould S.J. (2003). The dynamin-like GTPase DLP1 is essential for peroxisome division and is recruited to peroxisomes in part by PEX11. *Journal of Biological Chemistry*, 278(19): 17012-17020.
- Lindgard M.J., and Trelase R.N. (2006). Five *Arabidopsis* peroxin 11 homologs individually promote peroxisome elongation, duplication or aggregation. *Journal of Cell Science*, 119: 1961-1972.
- Lingard M.J., Gidda S.K., Bingham S., Rothstein, R.T. Mullen, and Trelase R. (2008). *Arabidopsis* PEROXIN11c-e, FISSION1b, and DYNAMIN-RELATED PROTEIN3A cooperate in Cell Cycle-Associated Replication of Peroxisomes. *The Plant Cell*, 20: 567–1585.
- Lipka V., Dittgen J., Bednarek P., Bhat R., Wiermer M., Stein M., Landtag J., Brandt W., Rosahl S., Scheel D., Llorente F., Molina A., Parker J., Somerville S., and Schulze-Lefert P. (2005). Pre- and postinvasion defenses both contribute to nonhost resistance in *Arabidopsis*. *Science*, 310: 1180-1183.

- Mano S, Nakamori C, Kondo M, Hayashi M, Nishimura M. (2004). An *Arabidopsis* dynamin related protein, DRP3A, controls both peroxisomal and mitochondrial division. *Plant Journal*, 38(3):487-98.
- Mano S., and Nishimura M. (2005). Plant peroxisomes. *Vitamins and Hormones*, 72: 111-154.
- Mano S., Nakamori C., Nito K., Kondo M., and Nishimura M. (2006). The *Arabidopsis* pex12 and pex13 mutants are defective in both PTS1 and PTS2-dependent protein transport. *Plant Journal*, 47(4): 604-18.
- Marshall P.A., Krimkevich Y.I., Lark R.H., Dyer J.M., Veenhuis M., and Goodman J.M. (1995). Pmp27 promotes peroxisomal proliferation. *J Cell Biol.*, 129:345-55.
- McConn M., Creelman R.A., Bell E., Mullet J.E., and Browse J., (1997). Jasmonate is essential for insect defense in *Arabidopsis*. *PNAS*, 94(10): 5473-5477.
- Mitsuya S., El-Shami M., Sparkes I.A, Charlton W.L., De Marcos Lousa C., Johnson B., and Baker A. (2010). Salt Stress Causes Peroxisome Proliferation, but Inducing Peroxisome Proliferation Does Not Improve NaCl Tolerance in *Arabidopsis thaliana*. *PLoS ONE* 5(2):.
- Mullen R.T., Lisenbee C.S., Miernyk J.A., and Richard Trelease N., (1999). Peroxisomal membrane ascorbate peroxidase is sorted to a membranous network that resembles a subdomain of the endoplasmic reticulum. *Plant Cell*, 11: 2167–185.
- Mullen R.T. and Trelease R.N. (2000). The sorting signals for peroxisomal membrane-bound ascorbate peroxidase are within its C-terminal tail. *J. Biol. Chem.*, 275: 16337–16344.
- Mullen R.T., Flynn C.R. and Trelease R.N., (2001). How are peroxisomes formed? The role of the endoplasmic reticulum and peroxins. *Trends in Plant Science*, 6(6): 256-261.
- Mullen R.T. and Trelease R.N. (2006). The ER-peroxisome connection in plants: Development of the “ER semi-autonomous peroxisome maturation and replication” model for plant peroxisome biogenesis. *Biochim Biophys Acta*, 1763(12): 1655-68.
- Nito K., Hayashi M., and Nishimura M. (2002). Direct interaction and determination of binding domains among peroxisomal import factors in *Arabidopsis thaliana*. *Plant Cell Physiol*, (4): 355-366.
- Nito K., Kamigaki A., Konfo M., Hayashi M. and Nishimura M. (2007). Functional Classification of *Arabidopsis* Peroxisome Biogenesis Factors Proposed from Analyses of Knockdown Mutants. *Plant Cell Physiology* 48(6): 763-774.
- Nayidu N.K., Wang L., Xie W., Zhang C., Fan C., Lian X., Zhang Q., Xiong L. (2008). Comprehensive sequence and expression profile analysis of PEX11 gene family in rice. *Gene*, 15; 412(1-2):59-70.
- Obayashi T., Hayashi S., Saeki M., Ohta H., and Kinoshita K., (2009). ATTED-II provides coexpressed gene networks for *Arabidopsis*. *Nucleic Acids Res.*, 37.
- Orth T., Reumann S., Zhang X., Fan J., Wenzl D., Quan S. and Hu J. (2007). The PEROXIN11 protein Family Controls Peroxisome Proliferation in *Arabidopsis*. *The Plant Cell*, 19: 333-350.

- Osteryoung K.W., and Nunnari J. (2003). The division of endosymbiotic organelles. *Science*, 302(5651): 1698-704.
- Pastori G.M., and Del Rio L.A. (1997). Natural Senescence of Pea Leaves (An ActivatedOxygen-mediated Function for Peroxisomes). *Plant Physiol*, 113: 411-418.
- Passreiter M., Anton M., Lay D., Frank R., Harter C., Wieland F.T., Gorgas K., and Just W.W. (1998). Peroxisome biogenesis: involvement of ARF and coatomer. *J Cell Biol.*, 141: 373-3.
- Pistelli L., De Bellis L. and Alp A. (1995). Evidences of glyoxylate cycle in peroxisomes of senescent cotyledons. *Plant Science*, 109: 13-21.
- Platta, H.W., and R. Erdmann. 2007. Peroxisomal dynamics. *Trends Cell Biol.*, 17: 474- 484.
- Ramón N.M. and Bartel B. (2010). Interdependence of the peroxisome-targeting receptors in *Arabidopsis thaliana*: PEX7 facilitates PEX5 accumulation and import of PTS1 cargo into peroxisomes. *Mol Biol Cell*, 21: 1263–1271.
- Reumann S., Ma C., Lemke S., and Babujee L. (2004). AraPerox. A Database of Putative *Arabidopsis* Proteins from Plant Peroxisomes. *Plant Physiology*, 136: 2587–2608.
- Rottensteiner, H., A.J. Kal, B. Hamilton, H. Ruis, and H.F. Tabak. (1997). A heterodimer of the Zn2Cys6 transcription factors Pip2p and Oaf1p controls induction of genes encoding peroxisomal proteins in *Saccharomyces cerevisiae*. *Eur J Biochem.*, 247: 776-83.
- Rottensteiner H., Stein K., Sonnenhol E., and Erdmann R. (2003). Conserved function of pex11p and the novel pex25p and pex27p in peroxisome biogenesis. *Mol Biol Cell*, 14:4316-28.
- Ruiz M.T., Voinnet O. and Baulcombe D.C. (1998). Initiation and maintenance of virus- induced gene silencing. *Plant Cell*, 10(6): 937–946.
- Sakai Y., Marshall P.A., Saiganji A., Takabe K., Saiki H., Kato N., and Goodman J.M. (1995). The *Candida boidinii* peroxisomal membrane protein Pmp30 has a role in peroxisomal proliferation and is functionally homologous to Pmp27 from *Saccharomyces cerevisiae*. *Journal of Bacteriology*, 177(23): 6773–6781.
- Saraya R., Krikken A.M., Veenhuis M., and van der Klei I.J. (2011). Peroxisome reintroduction in *Hansenula polymorpha* requires Pex25 and Rho1. *J. Cell Biol*, 193(5): 885–900.
- Schoonjans K., Staels B., and Auwerx J., (1996). The peroxisome proliferator activated receptors (PPARS) and their effects on lipid metabolism and adipocyte differentiation. *Biochim. Biophys. Acta*, 1302: 93–109.
- Schrader M., Reuber B.E., Morrell J.C., Jimenez-Sanchez G., Obie C., Stroh T.A., Valle D., Schroer T.A. and Gould S.J. (1998). Expression of PEX11beta mediates peroxisome proliferation in the absence of extracellular stimuli. *J. Biol. Chem.*, 273: 29607-29614.
- Sommerville C.R. and Ogren W.L. (1980). Photorespiration mutants of *Arabidopsis thaliana* efficient in serine-glyoxylate aminotransferase activity. *Proc. Natl. Acad. Science*, 77(5): 2684 -2687.

- Simon S., and Petrášek P. (2011). Why plants need more than one type of auxin. *Plant Science*, 180(3): 454-460.
- Sheen J. (2002) A transient expression assay using *Arabidopsis* mesophyll protoplasts. <http://genetics.mgh.harvard.edu/sheenweb/>
- Staswick P.E., Su W., and Howell S.H. (1992). Methyl jasmonate inhibition of root growth and induction of leaf protein are decreased in an *Arabidopsis thaliana* mutant. *PNAS*, 89: 837-6840.
- Stintzi A., and Browse J. (2000). The *Arabidopsis* male-sterile mutant, opr3, lacks the 12-oxophytodienoic acid reductase required for jasmonate synthesis. *PNAS*, 97(19): 10625- 10630.
- Swinkels B.W., Gould S.J., Bodnar A.G., Rachubinski R.A., and Subramani S. (1991). A novel, cleavable peroxisomal targeting signal at the amino-terminus of the rat 3-etoacyl-CoA thiolase. *Embo J.*, 10: 3255-62.
- Tam Y.C., Torres-Guzman J.C., Vizeacoumar F.J., Smith J.J., Marelli M., Aitchison J.D., and Rachubinski R.A. (2003). Pex11-related Proteins in Peroxisome Dynamics: A Role for the Novel Peroxin Pex27p in Controlling Peroxisome Size and Number in *Saccharomyces cerevisiae*. *Molecular Biology of the Cell*, 14: 4089–4102.
- Tanaka, A., Okumoto K., and Fujiki Y. (2003). cDNA cloning and characterization of the third isoform of human peroxin Pex11p. *Biochem Biophys Res Commun.*, 300:819-23.
- Teif V.B. (2010). Predicting gene-regulation functions: lessons from temperate bacteriophages. *Biophysical Journal*, 98 (7): 1247–56.
- Titorenko V.I., and Rachubinski R.A. (1998). The peroxisome orchestrating important developmental decisions from inside the cell. *JCB*, 164(5): 641-645:
- Titorenko V.I., and Rachubinski R.A. (2004). The peroxisomes: Orchestrating important developmental descicions from insdie. *The Journal of Cell Biology*, 164(5).
- Titorenko I., and Mullen R.T. (2006). Peroxisome biogenesis: the peroxisomal endomembrane system and the role of the ER (mini review). *Journal of Cell Biology*, 174(1): 11-17.
- Tolbert N.E. (1971). Microbodies-Peroxisomes and Glyoxysomes. *Annu. Rev. Plant. Physiol.* 22: 45-74.
- Tsien R. (1998). The green fluorescent protein. *Annu Rev Biochem.*, 67: 509–44.
- Veenhuis M., Mateblowski M., Kunau W.H. and Harder W. (1987). Proliferation of Microbodies in *Saccharomyces cerevisiae*. *Yeast*, 3(2): 77–84.
- Vijayan P., Shockey J., Levesque A.A., Cook R.J. and Browse J., (1998). A role for jasmonatein pathogen defense of *Arabidopsis*. *Proc. Natl. Acad. Sci.*, 95: 7209-214.
- Vitha S., Beneš K., Phillips J.P. and Gartland K.M.A., (1995). Histochemical GUSAnalysis. *Methods in Molecular Biology*. 44.

- Vizeacoumar F.J., Torres-Guzman J.C., Bouard D., Aitchison J.D., and Rachubinski R.A. (2004). Pex30p, Pex31p, and Pex32p Form a Family of Peroxisomal Integral Membrane Proteins Regulating Peroxisome Size and Number in *Saccharomyces cerevisiae*. *Mol Biol Cell*, 15(2): 665–677.
- Wang D., Visser N.V., Veenhuis M., and van der Klei I.J. (2003). Physical Interactions of the peroxisomal Targeting Signal 1 Receptor Pex5p, Studied by Fluorescence Correlation Spectroscopy. *The Journal of Biological Chemistry*, 278: 43340–3345.
- Wanders R.J., and. Waterham H.R. (2006). Peroxisomal disorders: the single peroxisomal enzyme deficiencies. *Biochim. Biophys. Acta*. 1763:1707–1720.
- Wasternack C. (2007). Jasmonates: An Update on Biosynthesis, Signal Transduction and Action in Plant Stress Response, Growth and Development. *Annals of Botany*, 100: 681–69.
- Wildermuth M.C., Dewdney J., Wu G., Ausubel F.M. (2001). Isochorismate synthase is required of synthesizing salicylic acid for plant defence. *Nature*, 414: 562–565.
- Woodward A.W., and Bartel B. (2005). Auxin: Regulation, Action, and Interaction. *Annals of Botany* 95:707–735.
- Xie, D.X., Feys, B.F., James, S., Nieto-Rostro, M., and Turner, J.G. (1998). COI1: An *Arabidopsis* gene required for jasmonate-regulated defense and fertility. *Science* 280: 1091–1094.
- Xu Y., Chang P.F., Liu D., Narasimhan M.L., Raghothama K.G., Hasegawa P.M. and Bressan R.A., (1994). Plant Defense Genes Are Synergistically Induced by Ethylene and Methyl jasmonate. *The Plant Cell*, 6(8): 1077–1085.
- Yamamoto Y.Y. and Obokata J. (2008). ppdb: a plant promoter database. *Nucleic Acids Research*, 36.
- Yan M., Rayapuram N., and Subramani S. (2005). The control of peroxisome number and size during division and proliferation. *Current Opinion in Cell Biology*, 17(4): 376–383.
- Zhang J.Z., Laudencia-Chingcuanco D.L., Comai L., Li M. and Harada J.J., (1994). Isocitrate Lyase and Malate Synthase Genes from *Brassica napus* L. Are Active in Pollen. *Plant Physiol.*, 104: 857–864.
- Zhang X., and Hu J.P. (2008). FISSION1A and FISSION1B Proteins Mediate the Fission of peroxisomes and Mitochondria in *Arabidopsis*. *Molecular Plant*, 1(6): 1036–047.
- Zhang X., and Hu J.P. (2009). Two small protein families, DYNAMIN-RELATED PROTEIN3 and FISSION1, are required for peroxisome fission in *Arabidopsis*. *The Plant Journal*, 57: 146–159.
- Zolman B.K., Yoder A., and Bartel B. (2000). Genetic Analysis of Indole-3-butyric Acid Responses in *Arabidopsis thaliana* Reveals Four Mutant Classes. *Genetics*, 156: 1323–337.



- Zolman B.K., and Bartel B. (2004). An *Arabidopsis* indole-3-butyric acid-response mutant defective in PEROXIN6, an apparent ATPase implicated in peroxisomal function. PNAS, 101(6):1786-1791.
- Zolman B.K., Martinez N., Millius A., Adham A.R., and Bartel B. (2008). Identification and Characterization of *Arabidopsis* Indole-3-Butyric Acid Response Mutants Defective in Novel Peroxisomal Enzymes. Genetics, 180(1): 237-251.
- Zu (2002). Salt and drought stress signal transduction in plants. Annual Review of Plant Biology, 53: 247-273.

## CURRICULUM VITAE

### PERSONAL DATA

---

**Name:** Mag. Kornelija Pranjić

**Date of birth:** 04.09.1980

**Birth place:** Vienna, Austria

**Nationality:** Austrian



### EDUCATION

---

- 10/2007** Start of my PhD thesis "The Role of PEX11 gene family in the proliferation machinery of *A. thaliana*."
- 09/2007** Successful PhD selection at the Max F. Peroutz Laboratoties (MFPL).
- 10/2004** Graduation to Magistra of Science in Botany.
- 06/2002** Start of my Diploma thesis in Botany/Plant Physiology "The ecology of carnivorous plants: The role of micro-organisms in the degradation process of prey in carnivorous plants."
- 1999–2001** Studies in biology, University of Vienna.
- 1990-1999** High School "Gymnasium und Realgymnasium der Armen Schulschwestern von Unserer Lieben Frau", Vienna.

### WORKING EXPERIENCE

---

- 2006-2007** Work on a scientific film about pollen tube growth in flowering plants.
- 2005** Scientific work on a project analysing the *Drosera* (sundew) population in different peat bogs in Austria.
- 2004-2006** Tutorial work at the University of Vienna: „The praxis of light and video-microscopy“, „Excursion to heavy metal contaminated sites in Slovakia“ , „Introduction into general biology“ and „Functional Cytology“.

### INTERNATIONAL EXPERIENCE

---

#### Indiana, Louisville / 2006

Scholarship at the University of Indiana South East, in the lab of Prof. Douglas W. Darnowski, where I was working on the metabolomics of carnivorous plants, especially *Drosera* and *Utricularia*.

**Venezuela / 2006**

Ecophysiological and microbiological investigations on *Heliamphora*, a carnivorous plant at their natural sites (Tepuis Roraima).

**Bonn, Deutschland / 2005**

Training course in GFP-transformation of *Drosera* plants.

**Portugal / 2004**

Ecophysiological investigations on *Drosophyllum*, a carnivorous plant at their natural sites in Portugal and Spain.

---

**ORAL PRESENTATION**

- 2010**      **Pranjić K.**, Koch J., Huber A., Hartig A., Brocard C. and Kragler F. An evolutionary study on the role of PEX11 as a key player in peroxisomal proliferation in plant cells. Oral Presentation at the 8. ATSPB Tagung, Illmitz, Austria
- 2006**      **Pranjić K.**, Adlassnig W., Lichtscheidl I.K. Carnivorous Plants. Some New Insights into the Ecophysiology. Invited Lecture at: University of Indiana Southeast, Department of Biology
- 2005**      **Pranjić K.**, H Daims, K Stoecker, W Adlassnig, M Wagner and IK Lichtscheidl. "The mucilage of *Drosera*, a carnivorous plant: habitat or battlefield for bacteria" XVII International Botanical Congress in Vienna, Austria

---

**PUBLICATIONS**

- 2010**      Koch J., **Pranjić K.**, Huber A., Ellinger A., Hartig A., Kragler F., and Brocard C. PEX11- family members are membrane elongation factors that coordinate peroxisome proliferation and maintenance. *Journal of Cell Science* 123: 3389-3400.
- 2010**      Adlassnig W., **Pranjić K.**, Mayer E., Steinhauser G., Hejjas F. and Lichtscheidl I.K. The Abiotic Environment of *Heliamphora nutans* (Sarraceniaceae): Pedological and Microclimatic Observations on Roraima Tepui. *Brazilian archives of biology and technology*. Book chapter Vol.53, n. 2: 425-430.
- 2008**      Peroutka M., Adlassnig W., Lendl T., **Pranjić K.** & Lichtscheidl I. K.. Functional biology of carnivorous plants. - In: Teixeira da Silva J. A. (Ed.), *Floriculture, Ornamental and Plant Biotechnology. Advances and Topical Issues*, 266 - 287. - Isleworth.
- 2006**      **Pranjić K.**, Adlassnig W., Peroutka M., Pois W., Mayer E. & Lichtscheidl I.K.: Flora and ecology of the ombrogenic fen "Schwarzes Moos" *Verhandlungen der Zoologisch-Botanischen-Gesellschaft in Österreich*, 143.

## Acknowledgments

### A BIG THANK YOU TO:

*Fritz Kragler* for giving me the opportunity to work in his group and for his support during the last years.

*Daniela Fichtenbauer* for her great friendship and help and an always open ear!

*Eva Klopff, Nikola Winter  
and Gregor Kollwig* for great coffe breaks, their patience and metal support.

*Stefan Ferscha* for never letting me down and always backing me up.

*Our co-opreation partners Andreas Hartig and Ceclie Brocard, and espescially to their group members Anja Huber, Johannes Koch and Sophie Merich for their support and always interresting discussions.*

The biggest thank you, goes to my parents Marija and Petar Pranjic who enabled me to study in the first place and supported me during my whole studies.

*And finally to all my friends who helped to get me through this!*

